Dissertation

submitted to the

Combined Faculties for the Natural Sciences and for Mathematics

of the Ruperto-Carola University of Heidelberg, Germany

for the degree of

Doctor of Natural Sciences

Presented by

M.Sc. Ying Wang

born in: Leshan, Sichuan, China

Oral-examination: October 10th, 2013

Spatiotemporal regulation of formin-like 2 by protein kinase C in invasive motility

Referees: **Prof. Dr. Herbert Steinbeisser**

Prof. Dr. med. Robert Grosse

This thesis was conducted at the Institute of Pharmacology, University of Heidelberg and the Institute of Pharmacology, University of Marburg under the supervision of Prof. Dr. Robert Grosse.

Part of this work that has been published is:

Kitzing, T.M., ***Wang, Y.***, Pertz, O., Copeland, J.W., and Grosse, R. (2010). Formin-like 2 drives amoeboid invasive cell motility downstream of RhoC. Oncogene 29, 2441–2448.

This thesis is the presentation of my original research work and every effort has been taken to specifically indicate the work done in collaboration with others, and is referenced with names for the contributions of collaborators. I hereby declare that the following thesis is my own work and has been written by the undersigned and without any assistance from third parties. Furthermore, I confirm that no sources have been used in the preparation of this thesis other than those indicated.

Heidelberg,

Table of Contents

Summary

Tumor metastasis requires cell motility driven by actin cytoskeleton dynamics, cell adhesion turnover and actomyosin contractility. Regulation of the actin cytoskeleton plays a pivotal role in protrusion formation, membrane internalization, force generation and intracellular trafficking. Many proteins which affect actin dynamics are found to be involved in tumorigenesis and metastasis. Among them, formin proteins as the largest group of actin nucleators are emerging to be candidates of drug targets for cancer therapy. However, the knowledge of formins in cancer cell invasion is limited. One member of the formin family, FMNL2 (formin-like 2), is mutated or upregulated in various cancer types.

In this work, FMNL2 is shown to be phosphorylated by PKCα at the residue Ser 1072. Phosphorylation of FMNL2 partially releases autoinhibition leading to higher activity. FMNL2-driven cancer cell invasion into 3D matrix is further enhanced by phosphorylation of the Ser 1072 residue. In addition, phosphorylation of FMNL2 by PKCα results in the internalization of FMNL2 from the plasma membrane through endocytic routes. Internalization of FMNL2 is reversible. Mutation of Ser 1072 into Ala impedes the rate of internalization. Internalized FMNL2 appears to colocalize with the α5 integrin positive vesicles, which is consistent with the fact that FMNL2 interacts with the cytoplasmic tail of α5 integrin. Furthermore, FMNL2 is required for β1 integrin internalization. Together with the fact that actomyosin contractility is reduced when FMNL2 is silenced, it is proposed here that FMNL2 drives cancer cell invasion through the regulation of integrin trafficking and actomyosin contractility.

Zusammenfassung

Die Metastasierung maligner Tumore erfordert zelluläre Motilität. Diese wiederum beruht im Wesentlichen auf einem dynamischen Umbau des Aktin-Zytoskeletts, einer gezielten Modulation adhäsiver Zelleigenschaften sowie der Kontraktilität von Aktin-Myosin-Filamenten. Eine kontrollierte Umgestaltung des Aktin-Zytoskeletts gilt hierbei als Grundvoraussetzung für die Ausbildung zellulärer Protrusionen, dient der Generierung von Kraft, ermöglicht eine Internalisierung definierter Bereiche der Plasmamembran und besitzt Bedeutung für eine Vielzahl zellulärer Transportprozesse. Entsprechend häufig zeigt sich eine Beteiligung Aktin-regulierender Proteine am Prozess der Kanzerogenese und Metastasierung. Die Proteinfamilie der Formine bildet die bislang größte Gruppe Aktin-regulierender Faktoren und gilt als aussichtsreiche Zielstruktur einer pharmakologisch orientierten Tumortherapie. Entsprechend bildet die funktionelle Charakterisierung einzelner Formine im Invasionsgeschehen entarteter Zellen einen interessanten Gegenstand derzeitiger Forschungsbemühungen, wobei für das Formin FMNL2 (formin-like 2) sowohl genetische Mutationen als auch eine gehäuft verstärkte Expression in verschiedenen Tumorentitäten nachgewiesen werden konnten.

Vor diesem Hintergrund gelang im Rahmen der vorliegenden Arbeit der Nachweis einer FMNL2-abhängigen Kontraktiliät und Invasivität von Tumorzellen. Als neuartiger Mechanismus einer regulierten FMNL2-Aktivität wurde eine PKCα-vermittelte Serin-Phosphorylierung an Position 1072 charakterisiert. Phosphorylierung von FMNL2 unterstützt die aktive, nicht/autoinhibierte Konformation des Proteins. Die Expression von FMNL2 in Tumorzellen erhöht deren Invasivität in einer dreidimensionalen Matrix. Diese Fähigkeit wird durch die Phosphorylierung von Serin 1072 weiter verstärkt. Aktivierung von PKCα bedingt eine reversible endozytotische Internalisierung von Plasmamembran-gebundenem FMNL2. Interessanterweise zeigt sich derart internalisiertes FMNL2 in vesikulären Strukturen, welche ebenfalls den Adäsionsrezeptor α5-Integrin beinhalten. Entsprechend kohärent gestaltet sich der Nachweis einer physikalischen Assoziation zwischen FMNL2 und dem zytoplasmatischen Proteinanteil von α5-Integrin. Darüber hinaus verdeutlicht eine verminderte Internalisierung von β1-

Integrin in Abwesenheit von FMNL2 die Bedeutung dieses Formins im intrazellulären Transportprozess dieser Adhäsionsmoleküle.

Entsprechend gelang mit der Untersuchung von FMNL2 der erste Nachweis einer regulatorischen Phosphorylierung eines Formins durch PKCα. Desweiteren offenbarte die Charakterisierung von FMNL2 erstmals die Beteiligung eines Formins an einem regulierten intrazellulären Transport des α5β1-Integrin Heterodimers. Somit ergeben sich entscheidende Faktoren einer globalen Beeinflussung invasiver Zelleigenschaften durch FMNL2 in Form einer ebenso zeitlich wie auch räumlich kontrollierten Beeinflussung des Aktin-Zytoskeletts, einer Modulation zellulärer Kontraktilität, ebenso wie einer intrazellulären Redirektion von Integrinen.

1 Introduction

Tumorigenesis requires the interplay of diverse functions in cells including cell survival and proliferation, cell motility, cell-cell communication and cell adaptation to the microenvironment. Therefore, it is crucial to understand the signal transduction and molecular mechanisms of tumor cell motility which enables invasion into surrounding tissue, intravasation, transit in the blood or lymph vessels, extravasation and formation of colonies at new sites. The motility of eukaryotic cells is regulated by the dynamic actin cytoskeleton turnover involved in force generation in membrane protrusion and contraction, membrane internalization and intracellular trafficking (Olson and Sahai, 2008; Pollard and Cooper, 2009).

1.1 The actin cytoskeleton

In eukaryotic cells, monomeric actin or globular actin (G-actin) binds ATP/ADP (Figure 1). G-actin polymerizes into long filaments (F-actin) made of two chains that turn gradually around each other to form a right-handed, two-chained long helix (Dominguez and Holmes, 2011). ATP hydrolyzes soon after monomers are assembled into the filaments but the phosphate dissociation is slow. G-actin always joins the filaments with a conformation pointing to the same direction that gives actin filaments an active and dynamic barbed end and a less active pointed end (Figure 1). The high amount of actin molecules in the cytoplasm is modulated by more than 100 additional proteins to maintain an equilibrium at steady state and to initiate reactions in response to signaling events. These additional proteins include thymosin-β4 which sequesters actin monomers by binding, profilin which inhibits actin nucleation but promotes barbed end elongation, capping proteins which block barbed end elongation, crosslinking proteins which make networks or bundles and severing proteins which destroy the network or generate free barbed ends rapidly available for polymerization (Figure 1) (Pollard, 2007).

The actin network is responsible for the formation of membrane protrusions at the leading edge by pushing the cell membrane. The protrusions, or the so-called pseudopods

include the fan-like lamellipodia and finger-like filopodia. These structures of a motile cell are important for the directional movement of cells growing on 2D substrates. However, for cells cultured in 3D environment or cells growing in the tissue environment of a multi-cell organism, the actin network is arranged to support and regulate more complicated morphologies including invadopodia and membrane blebs (Nürnberg et al., 2011).

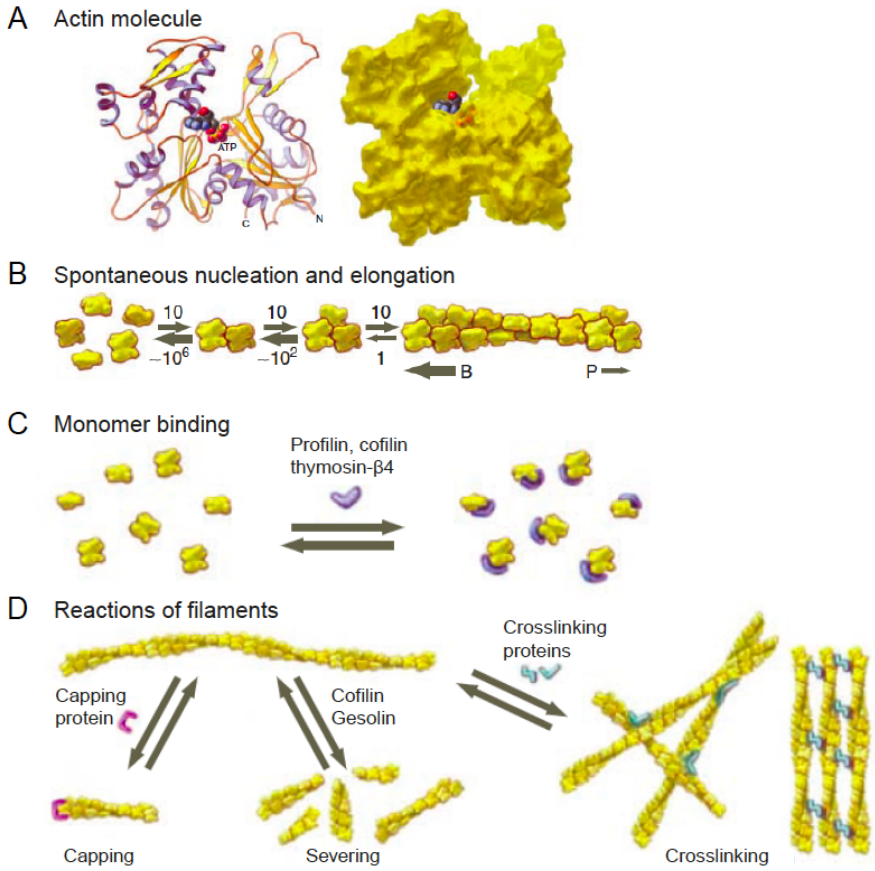

Figure 1. Actin structure and regulation of polymerization. A. Molecular structure model of actin monomer bound to ATP. **B.** Spontaneous nucleation and elongation. Dimers and trimers are unstable. Longer polymers grow rapidly at the barbed end (B) and slowly at the pointed end (P). **C.** Proteins binding to actin monomers. Profilin promotes nucleotide exchange and inhibits pointed end elongation. Cofilin inhibits nucleotide exchange and promotes nucleation. Thymosin-β4 blocks polymerization. **D.** Reaction of filaments. Capping protein blocks barbed end. Cofilin and gesolin sever filaments. Crosslinking proteins crosslink or bundle filaments to generate network. Adapted from Pollard and Cooper, 2009.

Actin polymerization also contributes to endocytosis (Kaksonen et al., 2006). This function of actin is comprehensively studied in budding yeast. Internalization regulates the lipid and protein composition of the plasma membrane, which enables cells to adapt to changes of the environment. This process depends on the dynamic actin cytoskeleton. In addition, the interaction of actin and myosin provides tracks for macromolecules or cell organelles trafficking along the actin filaments over short distances (Valdembri et al., 2009). The generation of contractile forces between actin filaments and myosin is the source for cytokinesis in both yeast and mammalian cells.

1.2 Regulation of actin nucleation

However, nucleation of actin filaments from monomer actin is unfavorable due to the extreme instability of small actin oligomers. To overcome this obstacle, cells use nucleating factors for *de novo* actin filament assembly, including the Arp2/3 complex, formins, Spire, Cordon-bleu and Leiomodin. The kinetic barrier of spontaneous actin assembly and the existence of different nucleating factors provide a platform for spatial and temporal control of actin dynamics. Regulation of the nucleators by Rho GTPase signaling, second messengers such as phospholipids and posttranslational modifications results in coordinated actin nucleation and elongation.

1.2.1 Arp2/3 complex and branching nucleation

The first nucleating factor discovered is the Arp2/3 complex (actin-related protein 2/3 complex) which is composed of seven subunits: Arp2, Arp3 and ARPC1-5. It is conserved in almost all eukaryotes (Machesky et al., 1994; Rotty et al., 2013). The Arp2/3 complex binds to the side of an existing "mother" actin filament and initiates the nucleation and elongation of a new "daughter" filament, resulting in a ~70° branch (Figure 2). The binding of Arp2/3 complex to the mother filament involves a conformational change that enables Arp2 and Arp3 as a dimer to function as the first two subunits of the daughter filament.

Arp2/3 complex by itself is not an efficient nucleator. Regulatory proteins called nucleation promoting factors (NPFs), actin filaments and an actin monomer are required for rapid branching nucleation by Arp2/3 complex (Pollard, 2007). It is also reported that phosphorylation of Thr and Tyr residues on Arp2 promotes potent nucleation (LeClaire et al., 2008). NPFs are activators of Arp2/3 complex that usually contain three short motifs: WH2 (WASP homology 2), connector region and acidic motif. In total it is termed as WCA domain. W and C motifs can bind actin monomer while C and A motifs can bind Arp2/3. By binding to Arp2/3 complex through WCA domain, NPFs cause a conformational change of Arp2/3. The further binding of the large complex to the mother filament primes the Arp2/3 complex for nucleation (Figure 2). WCA domain recruits actin monomers to Arp2/3 and nucleation continues, after which WCA domain dissociates (Goley and Welch, 2006). NPFs include WASP and N-WASP, WAVE/SCAR, WASH, WHAMM, JMY and cortactin. Branching nucleation by Arp2/3 complex plays crucial roles in membrane protrusion and cell motility, bacteria pathogen movement inside the host cell (the formation of the comet tail), and endocytosis (Campellone and Welch, 2010; Rotty et al., 2013).

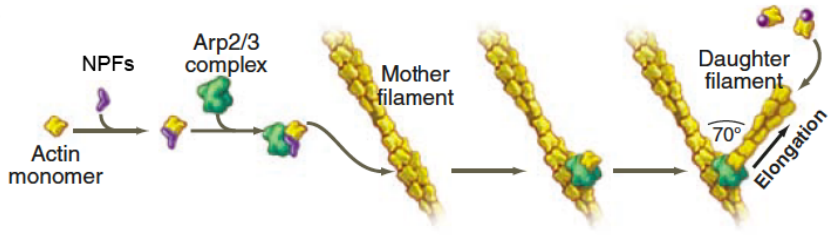

Figure 2. Branching nucleation by Arp2/3 complex. Nucleation promoting factors (NPFs) such as WASP bind an actin monomer and Arp2/3 complex. Binding to the side of a filament completes activation, and the barbed end of the daughter filament grows from Arp2/3 complex. Taken from Pollard and Cooper, 2009.

1.2.2 Formins and the WH2 domain containing nucleators

Formins are homodimers that catalyze the assembly of linear/unbranched actin filaments. FH2 (fomin homology 2) domains form donut-shaped head-to-tail dimers that stabilize spontaneously formed actin dimers/trimers, thus nucleate actin polymerization (Otomo et

al., 2005; Pring et al., 2003). FH2 dimers remain associated with the F-actin barbed end. After nucleation, the FH2 dimers move processively along the growing barbed end allowing for new actin monomer insertion (see details below).

The WH2 domain containing proteins, including Spire, Cordon-bleu (Cobl) and Leiomodin (Lmod), are recently identified actin nucleators. They employ the WH2 domain to recruit actin monomers to form polymerization seeds (Chesarone and Goode, 2009). Spire was found in Drosophila as a factor required for egg and embryonic development and was shown to have actin nucleation activity (Quinlan et al., 2005). It is suggested later that the Drosophila Spire and the formin protein Cappuccino interact and cooperate in actin assembly (Quinlan et al., 2007). The human homologues Spire1 and Spire2 also bind FMN1 and FMN2 (Figure 3).

Cobl nucleates actin into unbranched filaments similar to Spire but with a special characteristic that the lengths of the linker between the WH2 domains are crucial (Ahuja et al., 2007). Lmod is a muscle specific actin nucleator. It has three actin-binding motifs which stabilize actin trimer into a conformation that allows elongation along the barbed end (Chereau et al., 2008). Little is known about how Cobl and Lmod are regulated (Figure 3).

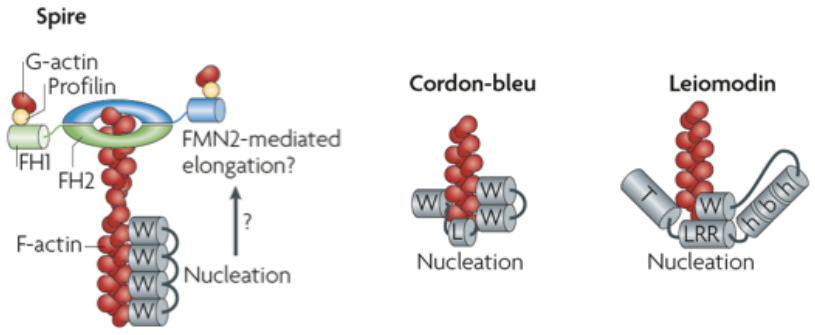

Figure 3. WH2 domain containing actin nucleators and models for polymerization. Spire cooperates with FMN2 to assemble actin filaments. Cobl and Lmod utilize multi actin monomer binding motifs to form actin nuclei. W: WH2; L: linker; LRR: Leu-rich repeat; T: tropomyosin and actin binding motif; h-b-h: helix-basic-helix. Taken from Campellone and Welch, 2010.

1.3 The formin family proteins as actin nucleators

Formins form the largest family of actin nucleators and elongators that assemble unbranched actin filaments. They are present in virtually all eukaryotes (Higgs, 2005). The first member identified in this family is mouse Formin-1. It was named on the hypothesis that a transgene insertion in the limb deformity locus resulted in limb formation defects in mice (Woychik et al., 1990). Although later it was found that the adjacent gene Gremlin is responsible for limb defects, the name of "formin" remains (Faix and Grosse, 2006). There are 15 formin proteins found in human, which are usually large polypeptides of more than 1000 amino acids. Phylogenetic analysis of the conserved FH2 (formin homology 2) domain reveals that metazoan formins are classified into seven subfamilies: Dia (diaphanous), DAAM (dishevelled-associated activator of morphogenesis), FMNL (formin-like protein) or FRL (formin-related gene in leukocytes), FHOD (formin homology domain-containing protein), INF (inverted formin), FMN (formin) and Delphilin (Table 1) (Higgs, 2005).

Table 1. List of mammalian formins

Subfamily	Members
Dia	mDia1 (DIAPH1) mDia2 (DIAPH3) mDia3 (DIAPH2)
DAAM	DAAM1 DAAM2
FMNL	FMNL1 (FRL1) FMNL2 (FRL3, FHOD2) FMNL3 (FRL2)
FHOD	FHOD1 FHOD2 (FMNL2) FHOD3
INF	INF1 INF2
FMN	FMN1 FMN2
Delphilin	Delphilin

1.3.1 Actin assembly by formins

Formins utilize the FH2 dimers to nucleate and elongate the actin filaments. Exactly how formins assemble actin nucleus is unknown. A co-crystal structure of yeast formin Bni1

with tetramethylrhodamine-actin shows that each FH2 dimer binds two actin subunits resembling the short-pitch actin dimer of a filament, suggesting that formins stabilize the spontaneously assembled actin dimers and trimmers to overcome the kinetic barrier of forming tetramers, thus stimulate the polymerization reaction (Figure 4) (Otomo et al., 2005). Recent studies reveal that in some formins, the region C-terminal to the FH2 domain might recruit actin monomers to promote nucleation (Chhabra and Higgs, 2006; Gould et al., 2011; Heimsath and Higgs, 2012; Moseley et al., 2004; Thompson et al., 2013).

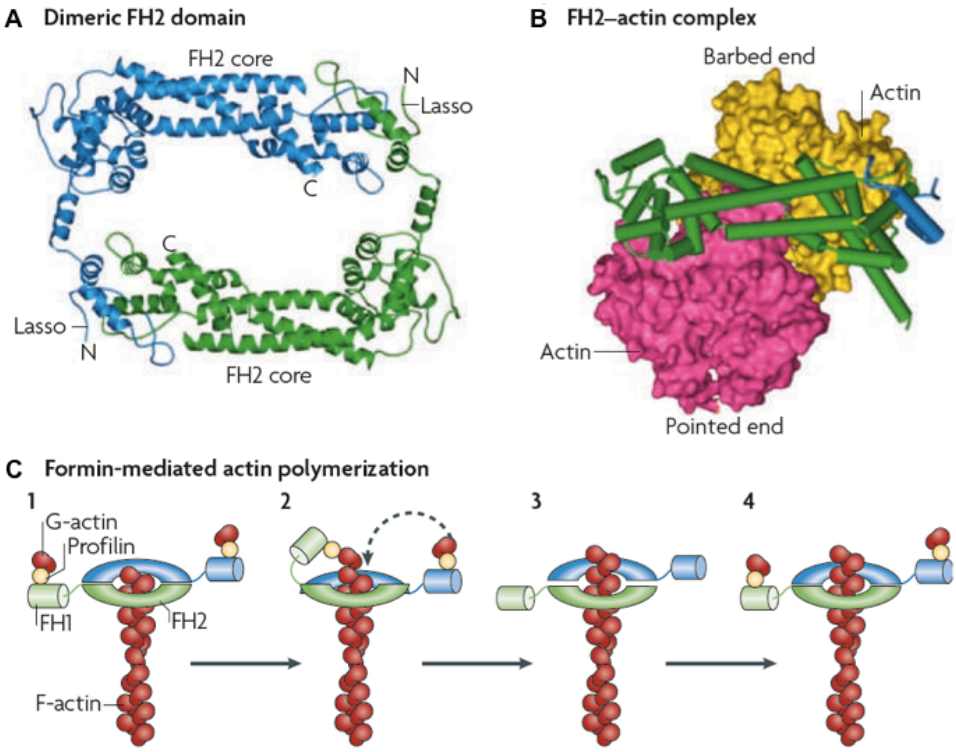

Figure 4. FH2 dimer structure, FH2-actin complex structure and the elongation model. A. FH2 dimer crystal structure of budding yeast formin Bni1. "Lasso" of one FH2 domain extends and wraps around the "Post" of the other FH2 domain forming a head-to-tail dimer in a donut shape. **B.** The co-crystal structure of Bni1 FH2 and actin. Space filling model is the actin dimer, with FH2 domains wrapped around. **C.** An elongation model where FH2 dimer adopts a closed (1, 4) and an open (2, 3) conformation. FH2 dimer associates with the barbed end and FH1 binds and recruits profilin-actin to the close vicinity to elongate the filaments. Taken from Campellone and Welch, 2010.

The donut shaped FH2 dimers then act as processive caps on elongating filaments preventing other capping proteins from terminating the elongation (Zigmond et al., 2003). The FH2 dimer has two states on the barbed end: a closed conformation where both FH2 domains bind the two actin subunits on the end allowing for no insertion of new subunits; an open conformation where actin insertion is enabled (Figure 4) (Otomo et al., 2005). The rate of elongation is greatly enhanced by the interaction of the adjacent FH1 (formin homology 1) domain and the profilin-actin (Kovar et al., 2006; Paul and Pollard, 2008; Romero et al., 2004). FH1 domain is rich in proline residues which can bind several profilin. The possible mechanism might be that by binding to multiple profilin-actin complexes using the "proline-rich track", FH1 domains increase the local concentration of G-actin which can be transferred to the barbed end directly (Vavylonis et al., 2006). Although diverse formins share a common mechanism, there exist substantial quantitative differences by orders of magnitude in some of the reaction parameters (Kovar, 2006; Pollard, 2007).

1.3.2 Regulation of formins on actin assembly

1.3.2.1 Autoinhibition

Mammalian formins, especially diaphanous-related formins (DRFs), share a conserved domain architecture. A prototypical DRF contains an N terminal regulatory region and a C terminal activity region. The N terminus interacts with the C terminus leading to an autoinhibition status of the molecule (Figure 5). The N and C termini interaction is mediated through DID (diaphanous inhibitory domain) in the N terminus and DAD (diaphanous autoregulatory domain) in the C terminus. Two motifs in the DAD region play important roles in the autoinhibition: an amphipathic helix (MDXLLXL, where X stands for any amino acids) which is the hydrophobic region contacting a conserved surface on DID (Alberts, 2001; Li and Higgs, 2003, 2005), followed by a 3-15 amino acid sequence rich in Lys and Arg basic residues which also contributes to the DID-DAD interaction (Schönichen et al., 2006; Wallar et al., 2006). The DID-DAD interaction inhibits the ability of FH2 domain activity on actin assembly *in vitro* and *in vivo* (Seth et

al., 2006). It is proposed that the autoinhibition interaction of DID and DAD sterically prevents FH2 to contact actin although there is no structural evidence so far.

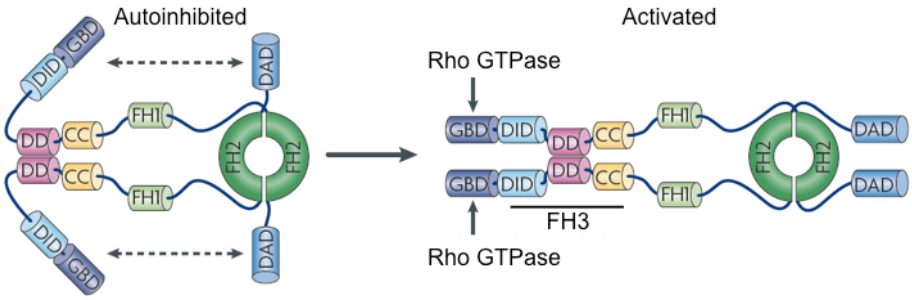

Figure 5. Diaphanous-related formins are autoregulated by N and C termini interaction. GBD: GTPase binding domain; DID: diaphanous inhibitory domain; DD: dimerization domain; CC: coiled-coil; FH1: formin homology 1; FH2: formin homology 2; FH3: formin homology 3; DAD: diaphanous autoregulatory domain. Adapted from Campellone and Welch, 2010.

In addition to autoinhibition between the N and C termini, there is a possible inter-FH2 autoinhibition. Unlike in Bni1 or FMNL3, structural analysis of DAAM1 FH2 dimer shows that the FH2 domains are packed together not allowing actin binding thus not being able to nucleate actin *in vitro* (Lu et al., 2007; Yamashita et al., 2007). The novel β-strand in FH2 linker region leads to the autoinhibition within the FH2 dimer. In fact, there are also several formins which are not autoregulated, for example mammalian delphilin, FMNL3 and INFs (Chhabra et al., 2009; Miyagi et al., 2002; Vaillant et al., 2008). How the activities of these formins are controlled is not clear. However it is probable that there are binding partners modulating formin activity. One example is Dia-interating protein DIP. DIP interacts with mDia1 and mDia2, and is required for the formation of cortical actin (Eisenmann et al., 2007).

1.3.2.2 Activation and localization by Rho GTPases

An enormous amount of research has provided evidences that formin activity and localization in cells are modulated by Rho GTPases. Rho GTPases have been demonstrated to induce actin stress fiber formation (Rho), lamellipodia formation (Rac, Cdc42) and filapodia formation (Cdc42) (Jaffe and Hall, 2005). The function of Rho

GTPases on actin remodeling is partially through the largest Rho effector protein family, the formins. Extracellular signals stimulate the activation of cell surface receptors and signaling factors which recruit and locally activate Rho GTPases. Activated Rho proteins bind the GBD domains of the formins thus disrupting the autoregulatory interaction of DID and DAD (Rose et al., 2005). In yeast, Rho1 and Cdc42 regulate Bni1 activity. Among mammalian formins, Dia, FMNL and DAAM subfamilies are known to interact with and be activated by certain Rho GTPases (Young and Copeland, 2010). The active Rho proteins also play important roles in plasma membrane localization of formins (Block et al., 2012; Chesarone et al., 2010; Seth et al., 2006).

A consistent effect of Rho activation of mammalian formins is the stimulation of F-actin assembly, whereas under different cellular context, the biological functions vary among the different formins and Rho GTPases. RhoB localizes to the endosome membranes and is associated with both early and late endosome motility. Either mDia1 or mDia2 acts downstream of RhoB activation on endosomes. The activated mDia1 or mDia2 stimulates actin assembly that impedes or enhances the endosome motility (Fernandez-Borja et al., 2005; Wallar et al., 2007). FMNL1 is a Cdc42 effector required for phagocytic cup formation in macrophages (Seth et al., 2006), while mDia1 acts downstream of RhoA or RhoC to induce stress fiber formation (Watanabe et al., 1999). In addition, the FH2 of mDia1 is found to be able to activate RhoA through binding to the Rho-GEF LARG, which suggests a positive feedback loop between formins and Rho GTPases (Kitzing et al., 2007; Shi et al., 2009).

However, *in vitro* pyrenyl-actin assays show that to disrupt the DID-DAD interaction between the N and C termini of formin mDia1 or FMNL1 requires much higher concentration of RhoA or Cdc42 protein than the N or C terminus proteins (Brandt et al., 2007; Seth et al., 2006). This indicates that additional factors other than active Rho GTPases are involved in the activation process in the cells. One possibility is the involvement of another interacting protein. Indeed, the DAD of DAAM1 binds Dishevelled (DVL) and this interaction either acts independently or together with Rho protein to fully activate DAAM1 in response to non canonical Wnt signaling (Liu et al., 2008).

1.3.2.3 Activation and localization by post-/co-translational modification and other factors

Release of autoinhibition can also be accomplished by post-translational modifications. During budding yeast mating, a pheromone-activated MAP kinase Fus3 phosphorylates Bni1 *in vitro*, and phosphorylation of Bni1 *in vivo* during the pheromone response is dependent on Fus3. Activated Fus3 is recruited to the cortex, where it activates Bni1 to assemble cortical actin cable and promote polarization and cell fusion (Matheos et al., 2004). Prk1 (p53-regulating kinase 1) also phosphorylates Bni1 and releases the autoinhibition thus mediating actin assembly involved in exocytosis and endocytosis of budding yeast (Wang et al., 2009). Mammalian FHOD1 is phosphorylated by ROCK (Rho associated coiled coil containing protein kinase) at three conserved residues in the polybasic region after DAD domain which is sufficient to disrupt the autoinhibition of FHOD1 to form stress fibers (Takeya et al., 2008). FHOD1 was also shown to physically interact with ROCK and induce plasma membrane blebs depending on Src and ROCK activity (Hannemann et al., 2008). Moreover, INF2 is farnesylated, which targets it to endoplasmic reticulum membranes possibly independent of Rho and enables INF2 to assemble actin locally needed for mitochondria fission (Chhabra et al., 2009; Korobova et al., 2013).

The FMNL formin subfamily is found to be co-translationally N-terminally myristoylated which regulates the localization of FMNL formins to the plasma membrane (Block et al., 2012; Han et al., 2009; Moriya et al., 2012). FMNL1γ, an isoform of FMNL1, is located at the cell membrane and cortex in diverse cell lines depending on myristoylation of Gly at the second position of the polypeptide. This isoform induces non-apoptotic membrane blebs independent of Src or ROCK activity (Han et al., 2009). Another study has reported that FMNL1γ regulates cellular F-actin levels required for maintaining structural integrity of the Golgi complex and lysosomes (Colón-Franco et al., 2011). FMNL2 and FMNL3 localization to the plasma membrane is also abolished if the second Gly is mutated into Ala. Block et al. have reported that FMNL2 localization depends on both N-myristoylation and Rho GTPases (Block et al., 2012). A previous report has pointed out

that FMNL2 drives rounded cell invasion in 3D downstream of RhoC (Kitzing et al., 2010).

As mentioned above, proper formin localization is not always completely disturbed by inhibition of Rho GTPases. The dimerization and coiled-coil domains of mDia1 can help direct the localization (Copeland et al., 2007). IQGAP binds to the FH3 of mDia1 and is required for mDia1 localization to the phagocytic cup (Brandt et al., 2007). The spatially controlled localization and activation of formins guarantee that they regulate actin assembly locally.

1.3.3 Cellular functions of formins

Formins mediate actin polymerization in the formation of a substantial variety of cell structures. In fission yeast cytokinesis, Rho activity is accumulated around the equator of the cell (Miller and Bement, 2009). Myosins capture actin filaments assembled by formins around the equator and pull the actin filaments into a contractile ring (Vavylonis et al., 2008). mDia2 is also found to induce F-actin forming a scaffold for the contractile ring and maintain its position in the middle of a dividing cell (Watanabe et al., 2008). Multiple DRFs also nucleate actin at filopodia or lammelipodia tips where they contribute to cell motility (Harris et al., 2010; Pellegrin and Mellor, 2005; Peng et al., 2003; Yang et al., 2007).

Actin polymerization triggered by the FH2 domains of formins is linked to the serum response factor (SRF) controlled transcription. G-actin can bind the myocardin-related SRF cofactor (MAL) in the N-terminal RPEL motifs, which inhibits MAL translocation from the cytoplasm into the nucleus. Formins, such as Dia, DAAM, FMNL and INF, employ large amount of G-actin to assemble F-actin so that MAL is released and able to enter the nucleus (Copeland and Treisman, 2002; Copeland et al., 2007; Grosse et al., 2003; Hill et al., 1995; Kitzing et al., 2010; Miralles et al., 2003; Sotiropoulos et al., 1999). As the transcriptional coactivator, MAL together with SRF starts an array of gene expression including 29 genes encoding cytoskeletal or contractile proteins (Baarlink et al., 2010; Faix and Grosse, 2006; Young and Copeland, 2010). Therefore, formins

contribute to the gene expression involved in cell migration, contractility and morphogenesis through serum response factor (Figure 6). Apart from that, G-actin is known to shuttle between the cytoplasm and the nucleus (Pederson and Aebi, 2002) while a number of formins have been shown to have nuclear localization signals (Chan and Leder, 1996; Copeland et al., 2007; Johnston et al., 2006). A very recent study has indeed identified that serum stimulation induces nuclear actin assembly depending on activated mDia1 and mDia2 in the nucleus. Formins polymerizing actin inside the nucleus drives serum-dependent MAL/SRF activity, suggesting a role of formins in the formation of the nucleoskeleton and a regulatory mechanism in transcription (Baarlink et al., 2013).

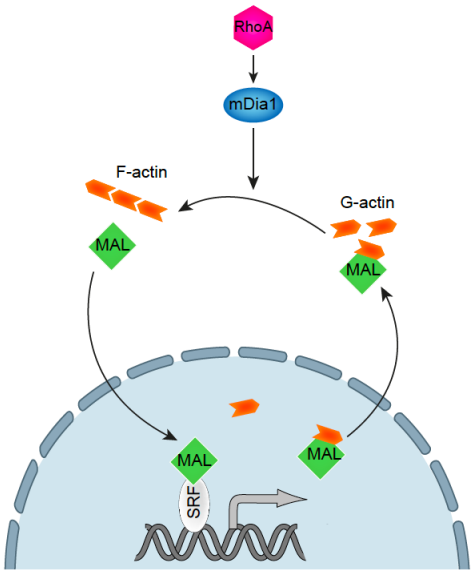

Figure 6. Representative scheme of MAL/SRF transcriptional activation by the formin mDia1. A pool of cytoplasmic G-actin binds to MAL which prevents MAL translocation into nucleus. Upon mDia1 activation by RhoA, G-actin molecules are utilized by the formin to polymerize F-actin. The conformational change of G-actin during assembly into F-actin releases MAL. MAL accumulates rapidly into nucleus, which in turn drives MAL/SRF-dependent gene transcription including genes involved in cytoskeletal dynamics, adhesion and cell shape. This is likely to form a feedback loop in response to the actin turnover in the cytoplasm.

1.4 Cancer cell invasion

Cancer cells spreading from the original tumor and the subsequent growth in new sites of the body is the most life-threatening disease which is called metastasis. This complicated process requires cancer cells responding to signaling cascades to survive, proliferate, move through the tissues surrounding the tumor, penetrate the basement membranes and endothelial walls into vasculature and disseminate to finally colonize in distant organs

(Figure 7) (Friedl and Alexander, 2011; Sahai, 2007). One of the crucial steps of acquiring invasive ability is the deregulation of signaling pathways leading to changes of gene expression and function that modulate the actin cytoskeleton dynamics. Alteration of actin cytoskeleton affects cell-cell contacts, cell adhesion and membrane protrusion which are all fundamental structures controlling cell motility. The pathways regulating actin dynamics may also affect growth control and cell survival (Olson and Sahai, 2008).

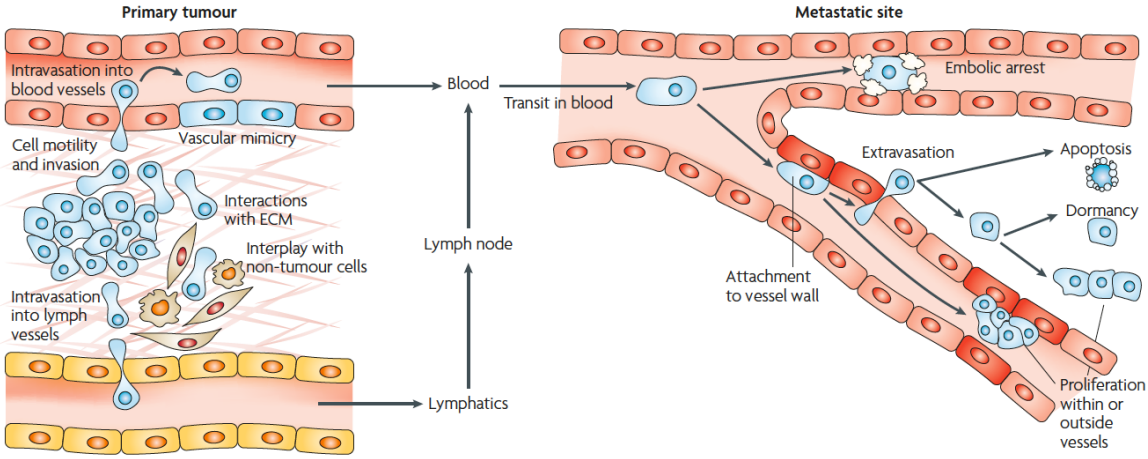

Figure 7. The metastatic process. Primary tumor cells invade in the tissue environment, disseminate and intravasate into blood or lymph vessels. These cells transit in blood stream, attach, extravasate and colonize in a new site. Taken from Sahai, 2007.

1.4.1 Modes of cancer cell invasion

To understand how cancer cells move, an enormous amount of researches have been performed using 2D or 3D *in vitro* models, consisting of random or directed cell movement on 2D substrate and cell invasion towards chemo-attractants through a barrier into 3D matrix, both in combination with time-lapse or conventional microscopy methods. The development of two-photon or multi-photon intravital imaging has provided insights into the tumor cell motility in living mouse models (Friedl and Wolf, 2003; Sahai, 2007). The combination of *in vivo* and *in vitro* research models reveals that cancer cells use different invasion patterns which can be roughly classified into mesenchymal motility, amoeboid/rounded motility and collective motility (Figure 8).

The mesenchymal mode of cell motility is so far the best understood mechanism of cell migration in either 2D or 3D environment. Cancer cells undergo epithelial to mesenchymal transition (EMT) due to the sustained change of oncogenic gene expression (Thiery, 2002). Mesenchymal motility is characterized by an elongated cell morphology with an established polarity and is dependent on focal adhesion turnover, actomyosin contractility and proteolysis of the extracellular matrix (ECM). Cells using the mesenchymal mode of motility move relatively slow (0.1-1 μm/min) (Friedl and Wolf, 2003). The signal transduction through cell surface receptors initiates the activation of Rac and production of phosphatidylinositol-3, 4, 5-triphosphate (PIP_3) which are known to activate WAVE and subsequently the Arp2/3 complex. The Arp2/3 complex regulates spatiotemporal actin assembly that drives the protrusion of pseudopods at the leading edge of the cell. Cdc42 and PI3K (phosphatidylinositol-4, 5-bisphosphate 3-kinase) are also activated to promote actin polymerization (Pollard and Borisy, 2003; Ridley et al., 2003). As the new protrusion of cells gets into contact with the ECM, cell starts the formation of small dynamic focal contacts through integrins and other receptors on the membrane. The adhesion molecules lead to the accumulation of surface proteases, such as membrane-type matrix metalloproteinases (MT-MMPs), which degrade the ECM providing space for the cells to crawl (Wolf et al., 2007). Some focal contacts develop into large focal adhesions that enable the actomyosin contractility regulated by Rho and ROCK activity to be transmitted to the ECM, facilitating cell body to follow the leading edge and retract the cell rear (Figure 8) (Sahai and Marshall, 2003). Mesechymal tumor cells usually come from tumors of connective tissue (Friedl and Alexander, 2011).

Intravital imaging approaches have demonstrated that some cancer cells in the tumor body can move like the single-cell amoeba Dictyostelium in an amorphous or round shape and at a relatively high speed (0.1-20 μm/min). This kind of cell movement is named as amoeboid or rounded motility (Friedl and Wolf, 2003). Amoeboid movement may employ Rac-dependent filopodia and has small or loosely organized adhesion sites. Cells have weak adhesion forces, no stress fibers, and lack proteolysis of the ECM (Lämmermann and Sixt, 2009). The second form of amoeboid movement uses Rho-ROCK dependent cortical actomyosin contractile forces to remodel the cell shape (Olson

and Sahai, 2008). Chemoattractant activates the membrane receptors triggering actin polymerization leading to the formation of a pseudopod. Rho-ROCK dependent contractile force in cortical actin generates hydrostatic pressure that reshapes the membrane. Amoeboid tumor cells exhibit low levels of β1 and β3 integrins, forming low levels of adhesion with collagen substrates (Friedl and Wolf, 2003; Hegerfeldt et al., 2002). Under the guidance of the chemoattractant, cells squeeze forward through the ECM with little or no focal contacts and cells move independently of extracellular proteolysis (Figure 8) (Sabeh et al., 2009). Amoeboid tumor cells usually originate from leukemia, lymphoma and small cell lung carcinoma (Friedl and Alexander, 2011). The rounded movement is also detected in other tumor cell types such as melanoma cells (Sanz-Moreno et al., 2008).

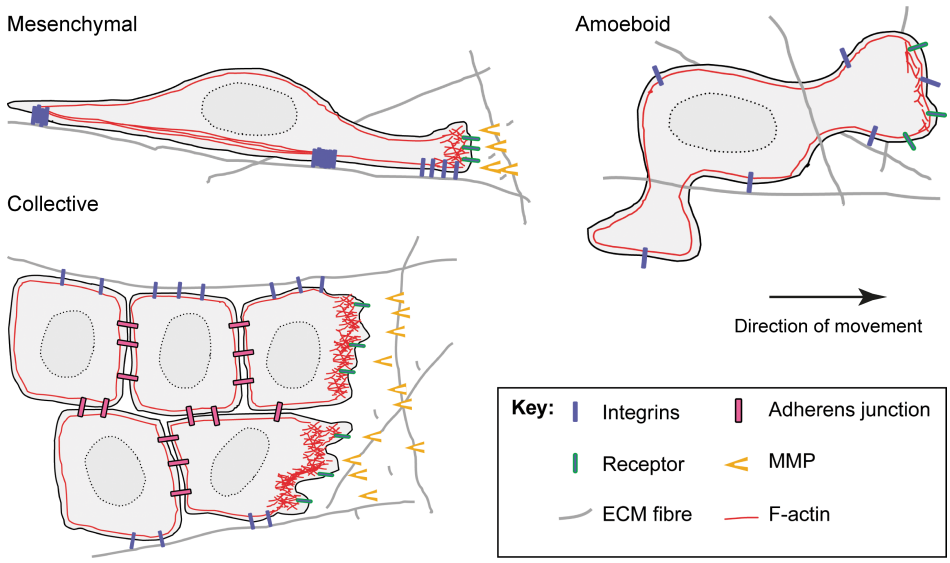

Figure 8. Mechanisms of cancer cell motility. Mesenchymal motility is characterized by an elongated morphology and ECM degradation. Amoeboid motility is defined by an amorphous morphology and dependent on actomyosin contractile force to reshape the cells while squeezing through the ECM. Collective motility retains cell-cell junctions and is characterized by the movement of a collection of cells. Adapted from Sahai, 2005.

Collective motility requires intact cell-cell junction, proteolytic activity and multicellular coordination during simultaneous migration. In most cases of collective invasion, cells move simultaneously with a mechanism similar to a collective form of mesenchymal

motility. Leading cells in the front respond to the chemoattractants, form protrusions, and degrade the ECM generating a "path" for the following cells to move through (Figure 8) (Gaggioli et al., 2007; Sahai, 2005). Collective motility resembles the cell movement of morphogenesis during development. Collective migrating tumor cells are found in most epithelial and mesenchymal tumor types (Friedl and Gilmour, 2009). However, collective invasion is poorly studied due to the difficulties in setting up a model system *in vitro*.

1.4.2 Switching between the modes of invasion and the plasticity of tumor invasion

Inhibition of the proteases required for mesenchymal motility fails to stop cancer cell invasion but leads to the switch to amoeboid motility (Wolf et al., 2003). Blocking β1 integrin with antibody results in the switch from collective invasion into amoeboid invasion that does not require adhesion to the ECM (Hegerfeldt et al., 2002). Constriction of the cortical actomyosin enables cells not only to squeeze themselves through the ECM but to remodel the ECM to create invading tracts (Sanz-Moreno et al., 2011; Wyckoff et al., 2006). All the evidences imply that there exists a high degree of plasticity in cancer cell invasion. In particular, it has been reported that Rac activation and inactivation control the plasticity of melanoma cells to adopt mesenchymal or amoeboid motility (Sanz-Moreno et al., 2008). In mesenchymal movement, activation of Rac through a complex containing NEDD9 and the Rac-GEF DOCK3 leads to the actin assembly via WAVE2-Arp2/3 pathway directing the elongated movement. Amoeboid motility is decreased via decreasing actomyosin contractility. Whereas in amoeboid movement, ROCK signaling inactivates Rac through activating the Rac-GAP ARHGAP22, thus suppressing the elongated motility. This study reveals the molecular mechanism of how cancer cells switch between modes of motility. Furthermore, tumor cells moving through all the obstacles to invade require various actin cytoskeleton organizations. The versatile nucleating, elongating, capping, severing, crosslinking factors that regulate the actin assembly also provide a flexible platform of cytoskeleton reorganization favorable during migration and invasion. In N-WASP and WAVE2 depleted cells, mDia1 acts downstream of RhoA to form jagged protrusions with lamellar properties and to increase filopodia

formation, indicating a crosstalk and compensatory mechanism between the two groups of actin nucleators in membrane protrusion formation required for cell motility (Sarmiento et al., 2008). Therefore, the plasticity of switching the tumor invasion modes and the diverse actin cytoskeleton regulation are challenges for researchers to develop cancer therapies.

1.4.3 Formin proteins in invasive diseases

The expression and activation of Rho family proteins have been extensively studied in cancer cell migration and invasion (Ellenbroek and Collard, 2007). As Rho effectors, formins are gradually recognized as potential candidates for anti-invasive drug targets.

Among all the formin proteins, mDia1 has been implicated in a variety of processes promoting cell adhesion and migration. The Rho-mDia1 pathway is implicated in Src-mediated remodeling of focal adhesions and migration of glioma cells (DeWard et al., 2010; Narumiya et al., 2009). In 3D invasion model studies, mDia1 is required for invasive cancer cell migration as well as invadopodia formation (Kitzing et al., 2007; Lizárraga et al., 2009). Another evidence for mDia1 in invadopodia formation and invasion is that mDia1 targets v-Src to the cell periphery and facilitates v-Src induced transformation. Depletion of mDia1 in v-Src transduced cells leads to the failure of these cells invading or forming tumors in nude mice (Tanji et al., 2010). Like mDia1, mDia2 is also implicated in invadopodia formation and invasion (Lizárraga et al., 2009). Moreover, depletion of mDia2 in prostate cancer cells enhanced plasma membrane blebbing upon EGF stimulation and increased metastasis, suggesting an interesting suppressive role of mDia2 in tumor progression (Hager et al., 2012; Vizio et al., 2009). Other formin proteins also play a role in bleb-associated cancer cell invasion such as FHOD1 and FMNL1 (Han et al., 2009; Hannemann et al., 2008) although the precise underlying mechanisms remain unclear.

Sequence analysis of cancer genomes from glioblastoma or pancreatic cancer patients has identified missense mutations in FMNL2 and FMNL3 (Jones et al., 2008; Parsons et al., 2008), while the functions of these mutations are not yet defined. However, FMNL2 was

found to be upregulated in colorectal cancer and in cell lines derived from colorectal cancer metastasis (Zhu et al., 2008). Studies from the same group later found that FMNL2 enhanced TGFβ-induced EMT and promoted colorectal carcinoma cell invasion and metastasis (Li et al., 2010; Zhu et al., 2011). They also identified that FMNL2 was targeted by micro RNA inhibiting signaling of PI3K, PKB/Akt (protein kinase B) and MAPK (mitogen-actiavted protein kinase) to reduce colorectal cancer invasion (Liang et al., 2013). Additionally, in a systematic screen of effects of human formins on cancer cell invasion, FMNL2 was identified as an important factor driving the amoeboid/rounded mode of invasion downstream of RhoC (Kitzing et al., 2010). Whether RhoC and FMNL2 or other factors play a role in invasion and metastasis *in vivo* would be interesting to investigate.

1.5 Protein kinase C and its role in invasion and metastasis

Protein kinase C (PKC) was identified by Nishizuka and colleagues as kinases that are activated by proteolysis (Takai et al., 1977). Diacylglycerol (DAG) was soon found to be the natural activator of the intact enzyme (Takai et al., 1979). PKC caught the attention of cancer researchers in the early 1980s after it had been identified as the target of the phorbol esters which have tumor promoting activity (Castagna et al., 1982; Kikkawa et al., 1983; Leach et al., 1983; Mochly-Rosen et al., 2012). This important discovery attracted researchers over years to develop drugs targeting PKC in cancer and other diseases. The identification of nine PKC genes encoding at least ten PKC isozymes complicates this research field. These isozymes are highly homologous and can be classified into three groups according to different activation mechanism: classical PKCs (cPKCs: PKCα, PKCβI, PKCβII, PKCγ), novel PKCs (nPKCs: PKCδ, PKCε, PKCη, PKCθ) and atypical PKCs (aPKCs: PKCζ, PKCλ/ι). cPKCs are activated by calcium and DAG. nPKCs are activated only by DAG, whereas aPKCs are not responsive to either calcium or DAG (Griner and Kazanietz, 2007). PKCα, PKCδ and PKCε are ubiquitously expressed while other PKCs are more cell-type specific. PKC is able to phosphorylate large number of substrates at their Ser/Thr residues. Therefore, PKC regulates a broad range of cellular events.

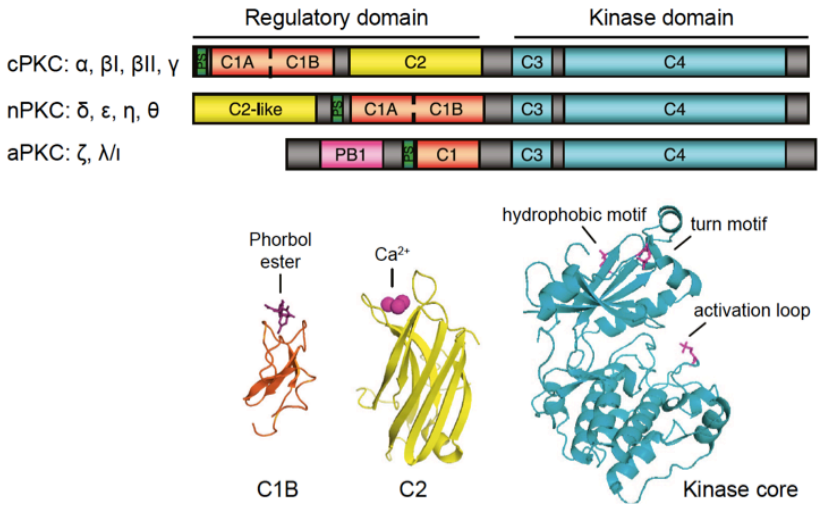

Figure 9. Domain structure of PKCs. Upper: all PKCs have a regulatory domain containing C1, C2 regions and a pseudosubstrate (PS) region (in green). C1 binds phorbol esters or DAG. C2 binds calcium. C2 of nPKCs does not bind calcium. C1 of aPKCs does not bind DAG. Kinase domains are more conserved among PKCs than regulatory domains. PKC isoform variable regions are shown in gray. PB1 (Phox and Bem 1) of aPKCs interacts with other proteins. Lower: structures of C1, C2 and kinase core. Adapted from Steinberg, 2008.

1.5.1 Structure and activation of protein kinase C

PKC contains a regulatory domain in the N terminus and a kinase domain in the C terminus (Figure 9) (Steinberg, 2008). In the inactive state, the regulatory domain binds to the kinase domain inhibiting the catalytic activity of the kinase. Upon stimulation of the receptor tyrosine kinase or the G-protein coupled receptor, phospholipase C (PLC) cleaves phosphatidylinositol-4, 5-biphosphate (PIP_2) into soluble second messenger inositol triphosphate (IP_3) and the membrane lipid DAG. IP_3 releases calcium from the endoplasmic reticulum. Calcium binds to the C2 region of the regulatory domain which pre-targets the cPKCs to membranes. DAG binding to the C1 region of the regulatory domain further promotes the membrane-binding affinity of PKC. Subsequently a massive conformational change happens to release the pseudosubstrate domain from the substrate-binding site allowing for substrate binding and phosphorylation of the downstream effectors. In the activation process, receptor of activated C-kinase (RACK) acts as the anchoring protein for PKCs (Figure 10). nPKCs lack calcium binding sites but have an

increased affinity for DAG as a compensation (Griner and Kazanietz, 2007; Parekh et al., 2000). In addition, to undergo trans- and auto-phosphorylation on themselves is a pre-requisition for the maturation, activation and stability of PKCs. Of note, in response to the stimulation of receptors or phorbol esters, PKCs can translocate from cytosol to the plasma membrane, nuclear membrane, Golgi apparatus, mitochondria or other organelles, implying a specific mechanism of local activation of downstream events (Garcia-Bermejo et al., 2002; Wang et al., 1999). The redistribution to different organelles might relate to PKC binding to specific lipids or proteins (Jaken and Parker, 2000).

1.5.2 Protein kinase C in invasion and metastasis

Much of the work on PKC function was performed with phorbol esters which are irreversible. DAG stimulation in cells is only transient. It is also known that there exist far more DAG effectors than only PKCs. Nevertheless, PKCs have been implicated to play important roles in cell proliferation and cell death, gene transcription and translation, cell motility, cell-cell contacts, regulation of receptors and channels, endocytosis and so on. More efforts are required to identify the functions of each isozymes in disease progression using isozyme specific pharmacological drugs or other approaches.

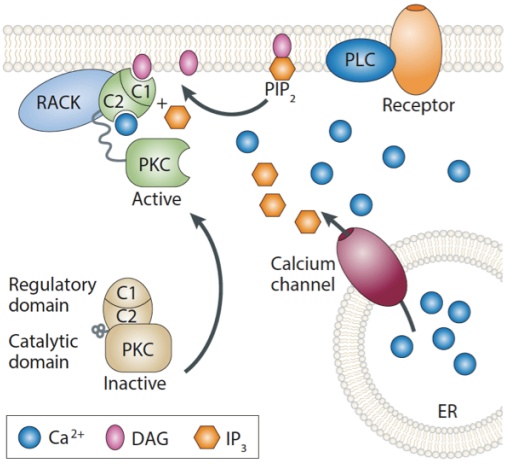

Figure 10. Activation of classical PKCs. Upon stimulation, PLC cleaves PIP_2 into DAG and IP_3. IP_3 releases calcium from ER. cPKCs bind calcium, DAG and RACK undergoing a significant conformational change which leads to the full activation of the kinase. Adapted from Mochly-Rosen et al., 2012.

Being involved in cell proliferation, cell death and cell motility, it is not surprising that PKCs play crucial roles in invasion and metastasis. It is known that PKCε is upregulated

in several cancer types, whereas PKCα and PKCδ are downregulated (Griner and Kazanietz, 2007). A single mutation was identified in PKCα (D294G) in the invasive pituitary tumor as well as in the thyroid follicular adenomas and carcinomas (Alvaro et al., 1993; Prévostel et al., 1997). This mutation affects the hinge region between the regulatory and the kinase domains which impairs the translocation of PKCα. Furthermore, overexpression of PKCα in MCF7 breast cancer cells increases the anchorage-independent growth, tumorigenesis and metastasis in mouse (Ways et al., 1995), while downregulation or inhibition of PKCα reduces cell migration in MDA-MB-231 breast carcinoma cells (Lønne et al., 2010). Similarly, overexpression of PKCβII in rat intestinal epithelial cells increases invasiveness via Ras/MEK pathway (Zhang et al., 2004). PKCε seems to play a role in invasive motility through the activation of RhoA and RhoC in head and neck squamous carcinoma (Pan et al., 2006), while depletion of PKCε in MDA-MB-231 cells significantly decreases tumor growth and metastasis (Pan et al., 2005). It has also been realized that PKC might influence cancer cell motility through regulating integrins or MMPs (Liu et al., 2002; Ng et al., 1999; Parsons et al., 2002; Urtreger et al., 2005). Although evidences exist to show that the link between PKC and invasive motility is strong, the underlying mechanisms of specific isozymes remain largely unknown. Moreover, some PKC isozymes, such as PKCα and PKCε, promote invasion and metastasis while some (like PKCδ) have a contradictory role. Therefore, phorbol ester induced tumor promotion needs to be revisited and further characterized.

1.6 Integrin and its role in cell invasion

Integrins are the major extracellular cell matrix receptors in metazoa without any homologues in prokaryotes, fungi, or plants (Hynes, 2002). Integrins are transmembrane heterodimers composed of α and β subunits, which couple extracellular matrix to actin cytoskeleton inside the cells enabling mechanosensing. Activated integrin dimers mediate downstream signaling through Rho GTPases, Src, PKB/Akt, MAPK and so on, playing key roles in development, immune responses, intracellular trafficking, cell proliferation and migration (Caswell and Norman, 2008). In mammals, there are 18 α subunits and 8 β subunits forming 24 different integrins (Figure 11) which appear to have distinct,

nonredundant functions. The 24 integrins have ligand binding specificities (Figure 11) and they show specific phenotypes in specific integrin knockout mice (Hynes, 2002).

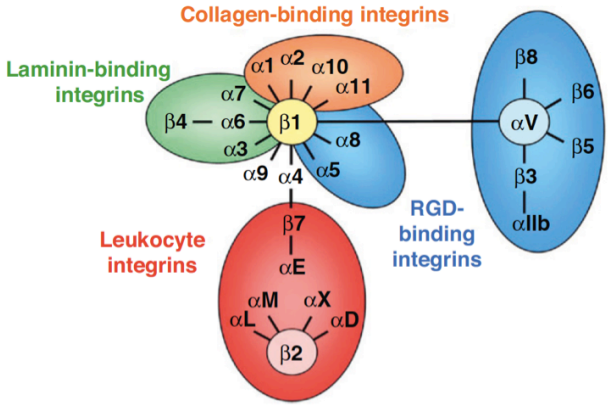

Figure 11. Mammalian integrins and their ligands. RGD (Arg-Gly-Asp) peptide containing ligands include fibronectin, vitronectin, thrombospondin, osteopontin, etc. Leukocyte integrin ligands include E-cadherin, figrinogen, factor X, von Willebrand Factor, intracellular adhesion molecule, vascular cell adhesion molecule, and so on. Taken from Margadant et al., 2011.

1.6.1 Integrin activation and endocytic trafficking

The heterodimeric transmembrane protein complex has a remarkable ability to transmit signals "bidirectionally", from outside into the inside of the cell ("outside-in") or on the contrary ("inside-out"). Integrins adopt low affinity, intermediate affinity or high affinity conformations on the plasma membrane (Figure 12). Activated integrins (high affinity) are recognized by the separation of the cytoplasmic tails of the α and β subunits and an extended open conformation of the extracelluar heads which can bind the ligands. Extracellular stimuli activate G-protein coupled receptors or receptor tyrosine kinases which in turn transduce signals leading to an allosteric conformational change of the heterodimer. Adaptor proteins talin and kindlin binding to the cytoplasmic tail of β subunit fully activates the integrins (inside-out). Active integrins subsequently bind their extracellular ligands, reinforce the α and β interaction and initiate "outside-in" signaling by recruiting adaptor proteins forming the links with actin filaments and other protein structures (Hynes, 2002; Margadant et al., 2011; Moser et al., 2009; Wickström and Fässler, 2011).

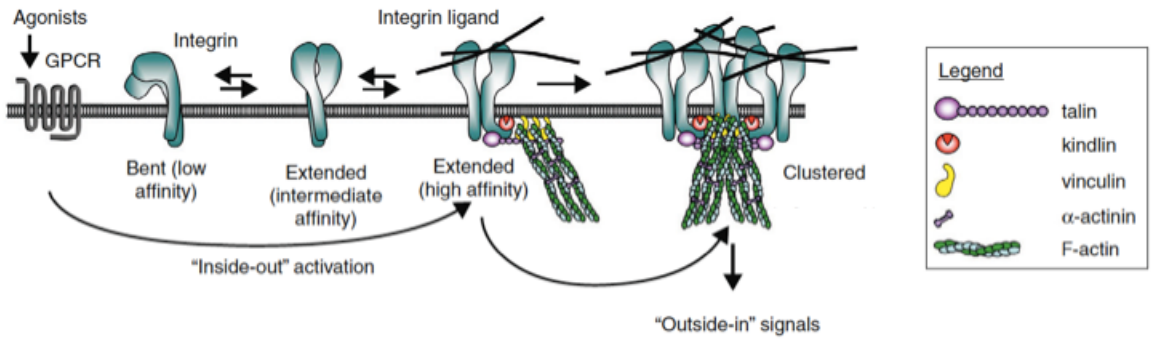

Figure 12. Activation of integrins. Extracellular stimuli transmit signals through receptors to change the integrin conformation from inactive to active through binding of talin and kindlin (inside-out). Active integrins bind extracellular ligands, and initiate outside-in signaling by further recruiting adaptor proteins such as talin and kindlin to connect to actin cytoskeleton, integrin clustering and a plethora of signaling cascades. Taken from Margadant et al., 2011.

It is well established that integrins undergo endocytic transport contributing to the regulation of integrin surface levels upon signaling events (Bretscher, 1992; Caswell and Norman, 2006). The dynamic vesicular trafficking internalizes and recycles integrins of the cell thus exerting a pivotal role in focal adhesion assembly, matrix turnover and the dynamic redistribution of integrins to new adhesion sites in a moving cell (Caswell et al., 2009). Integrins can follow either clathrin-dependent or clathrin-independent endocytic pathway to be internalized. Some integrins utilize more than one route.

The cytoplasmic tail of β subunit contains a conserved NXXY motif (in which X represents any amino acid), which is found to recruit proteins to clathrin coated pits usually via interaction with endocytic adaptor proteins. Some clathrin adaptor proteins which contain phosphotyrosine binding domains, such as Numb, can interact with the NXXY motif. Numb localizes to the clathrin coated pits at the leading edge and interacts with β1 or β3 tails. Numb acting downstream of aPKC and PAR3 (proteinase-activated receptor 3) signaling regulates α5β1 and αvβ3 integrin internalization and directional cell migration (Nishimura and Kaibuchi, 2007). Another study has shown that albeit α5β1 integrin internalization normally depends on the NXXY motif and clathrin, it can also be clathrin-independent by overexpressing the small GTPase Rab21 (Pellinen et al., 2008). It is possible that Rab21 induces α5β1 integrin endocytosis through caveolin-dependent

route. It has also been reported that α2β1 integrin internalizing through caveola is dependent on PKCα (Upla et al., 2004). Moreover, a direct association is found between β1 integrin cytoplasmic tail and PKCα (Ng et al., 1999).

The internalized integrins may be returned to the plasma membrane or transported to the lysosomes for degradation. A portion of fibronectin bound α5β1 integrin is ubiquitinated on the α5 tail and transported to the lysosomes, which is required for proper fibroblast migration (Lobert et al., 2010). Most of the integrins are recycled either via Rab4-dependent short route or Rab11/ADF-ribosylation factor 6 (Arf6)-dependent long recycling route. Recycling of integrins through either path depends on protein kinases such as PKB/Akt, PKC and PKD (Di Blasio et al., 2010; Ivaska et al., 2002, 2005; Li et al., 2005). Different routes of recycling affect integrin signaling on Rho GTPases and thus directional migration (Pankov et al., 2005; Vial et al., 2003; White et al., 2007).

1.6.2 Integrin in tumor cell migration and invasion

Most integrins activate focal adhesions and are required for proliferation and migration of cells in response to extracellular stimuli such as growth factors and cytokines. In spite of the fact that cancer cells have undergone transformation so that they require much less extracellular matrix cues and adhesions for their growth and proliferation, they still utilize integrin signals, especially in tumor initiation and progression (Guo and Giancotti, 2004). Enhanced integrin signaling can promote EMT and extracellular matrix degradation, which in turn drives the migration of the cancer cell.

Evidences implicate that loss of E-cadherin which plays a key role in cell-cell adhesion is required for EMT (Friedl and Alexander, 2011; Perl et al., 1998; Vleminckx et al., 1991; Yang et al., 2004). Overexpression of β1 integrin in normal epithelial cells disrupts adherens junctions (Gimond et al., 1999). In v-Src transformed cells, integrin signaling is enhanced to promote E-cadherin internalization and surpress E-cadherin expression (Avizienyte et al., 2002; Tan et al., 2001). Furthermore, integrins αvβ6 and αvβ8 might promote EMT through activating TGFβ (Mu et al., 2002; Munger et al., 1999; Wipff et al., 2007). It is also reported that αvβ3 integrin is upregulated in glioblastoma and

melanoma (Albelda et al., 1990; Gladson and Cheresh, 1991), where it possibly recruits and activates MMP2 to degrade extracellular matrix in the tumor microenvironment facilitating tumor invasion and metastasis (Brooks et al., 1996, 1998).

By activating focal adhesion kinase (FAK) and thereby Src, integrins initiate a signaling cascade which can promote cell migration and invasion (Geiger et al., 2009; Hynes, 2002). This signaling activates c-Jun N-terminal kinase (JNK) which may phosphorylate paxillin, a component of the focal adhesions. The phosphorylation of paxillin might regulate migration by promoting focal adhesion turnover (Huang et al., 2003; Miranti and Brugge, 2002). Downstream signaling also activates Rac and Rho which are key players in cell protrusion and contraction through regulating the actin cytoskeleton (Caswell et al., 2009; Ridley et al., 2003). Furthermore, through integrins β1, β2, αvβ3 and α4β7, tumor cells develop cell-cell interactions with endothelial cells and platelets to mediate intravascular migration and adhesion arrest, thus facilitating extravasation. (Friedl and Alexander, 2011; Stoletov et al., 2010).

During all the migration and invasion steps, integrin trafficking plays a pivotal role since it regulates the quantity and activity of integrin heterodimers on the plasma membrane as well as different membrane compartments so that integrins are able to exert their functions through signaling cascades. It was shown that mutant p53 significantly enhanced random cell motility and cell invasiveness into 3D matrix through promoting α5β1 recycling (Muller et al., 2009). Moreover, Rab11 trafficking of α6β4 integrin regulates hypoxia stimulated carcinoma invasion (Yoon et al., 2005). Rab25, a member of the Rab11 family, is reported to be strongly related to the aggressiveness of epithelial cancer (Cheng et al., 2004; Wang et al., 2004). Rab25 specifically regulates α5β1 integrin recycling by interacting directly with the β1 integrin cytoplasmic tail. Rab25 driving ovarian cancer cell invasion into 3D matrix depends on the interaction with β1 tail and the fibronectin ligand binding of α5β1 integrin. Rab25 promotes the delivery of α5β1 integrin to the pseudopodial tips of the invading cell and keeps a pool of α5β1 integrin at the cell front. Therefore, directing integrin recycling and the vesicle localization facilitates the tumor cell invasion into 3D matrix (Caswell et al., 2007).

Because of the multi-faceted roles in tumor cell migration and invasion, integrins have become targets for cancer therapy, especially αvβ3 and α5β1 integrins (Cox et al., 2010). However, blocking one type of integrin might affect the trafficking of other integrins or growth factor receptors that are necessary for other functions (Caswell et al., 2009), which should be considered during the research and development of anti-integrin drugs.

2 Aims of the project

FMNL2 was identified to have a role important for driving rounded mode of invasion downstream of RhoC (Kitzing et al., 2010). Genetic analysis discovered mutations of FMNL2 in cancer patients (Jones et al., 2008; Parsons et al., 2008). It was also reported that FMNL2 was upregulated in colorectal cancer and related to metastasis (Zhu et al., 2008). RhoC, one of the regulatory factors of FMNL2 activity, was described in promoting invasion and metastasis in various cancer types (Clark et al., 2000; Hakem et al., 2005; Iiizumi et al., 2008; Pillé et al., 2005). It is worth further investigating the underlying mechanism of FMNL2 regulation and its role in cancer cell migration. Although the autoinhibition could be regulated by RhoC, there are evidences that indicate additional factors in the regulation of FMNL2 (Kitzing et al., 2010). Besides, the actin polymerization activity of FMNL2 remains elusive. Little is known about its subcellular localization. Hence it would be intriguing to broaden the views on the properties and functions of FMNL2. The major aim of my thesis was to investigate the molecular mechanism of the regulation of FMNL2 and its biological functions. Biochemical studies are to be performed in order to understand FMNL2 activity on actin assembly, and to identify new regulatory factors in FMNL2 autoinhibition. Investigation on the subcellular localization of FMNL2 in cells is important to understand the relationship of FMNL2 with intracellular structures and the possible cellular functions. Functional analysis of FMNL2 and its new regulatory factors that direct FMNL2 localization and activity is aimed to uncover novel signaling regulation and to better understand the role of FMNL2 in cancer cell invasion. This will provide insights for the formin research field and might be useful for the development of formins as anti-invasive cancer drug targets.

3 Materials and Methods

3.1 Materials

Table 2. Reagents used in this work.

Reagent	Manufacturer
A23187	Sigma-Aldrich, Taufkirchen
Acetic acid	Roth, Karlsruhe
Ampicillin	AppliChem, Darmstadt
Acrylamide (30%) – bisacrylamide (0.8%) mixture	Roth, Karlsruhe
Agar	Roth, Karlsruhe
ATP	Sigma-Aldrich, Taufkirchen
BES	Sigma-Aldrich, Taufkirchen
Bisindolylmaleimide I	Calbiochem/Merck, Darmstadt
Bovine serum albumin	Roth, Karlsruhe
Bromophenol blue	Roth, Karlsruhe
Coomassie Brilliant Blue G250	Roth, Karlsruhe
DAPI	Sigma-Aldrich, Taufkirchen
DNA 1 kb plus marker	Fermentas/Thermo Scientific, St. Leon-Rot
DPBS (Ca^{2+} and Mg^{2+} free)	PAA/GE Healthcare, Cölbe
DMEM	PAA/GE Healthcare, Cölbe
Doxycycline hyclate	Sigma-Aldrich, Taufkirchen
Dry milk, fat free	Roth, Karlsruhe
DTT (1,4-dithiothreitol)	Roth, Karlsruhe
EDTA (ethylendiamine tetraacetic acid)	Roth, Karlsruhe
EGTA, molecular biology grade (ethylene glycol-bis-(β-aminoethyl ether)-	Sigma-Aldrich, Taufkirchen

Reagent	Manufacturer
N,N,N´,N´-tetraacetic acid)	
Ethanol, absolute	Roth, Karlsruhe
Ethidium bromide	Sigma-Aldrich, Taufkirchen
Enzymes for cloning	Fermentas/Thermo Scientific, St. Leon-Rot
FBS (fetal bovine serum)	Invitrogen, Karlsruhe
Flag (M2) -conjugated agarose	Sigma-Aldrich, Taufkirchen
Formaldehyde	Roth, Karlsruhe
Fugene HD	Promega, Mannheim
G418 sulfate	PAA/GE Healthcare, Cölbe
Glutaraldehyde	Sigma-Aldrich, Taufkirchen
Glycerol anhydrous	Roth, Karlsruhe
β-glycerolphosphate	Calbiochem/Merck, Darmstadt
Glycine	Roth, Karlsruhe
Glutathione, reduced	Sigma-Aldrich, Taufkirchen
Glutathione Sepharose 4B	GE Healthcare, München
Gö6976	Sigma-Aldrich, Taufkirchen
H_2O_2	Sigma-Aldrich, Taufkirchen
HEPES (N-(2-Hydroxyethyl)piperazine-N´-2-ethane-sulfonic acid)	Roth, Karlsruhe
HiperFect	Qiagen, Hilden
Hydrochloric acid	Roth, Karlsruhe
Imidazole	Merck, Darmstadt
IPTG (Isopropyl β-D-1-thiogalactopyranoside)	AppliChem, Darmstadt
Kanamycin	Roth, Karlsruhe
Luminol	Sigma-Aldrich, Taufkirchen
Magnesium chloride hexahydrate	Roth, Karlsruhe
2-mercaptoethanol	Merck, Darmstadt
Methanol	Roth, Karlsruhe
myc-conjugated agarose	Sigma-Aldrich, Taufkirchen

Reagent	Manufacturer
Ni-NTA agarose	Qiagen, Hilden
NP-40	Merck, Darmstadt
dNTP set (2'-deoxynucleosides 5'-triphosphates)	Fermentas/Thermo Scientific, St. Leon-Rot
Optiprep	Invitrogen, Karlsruhe
^{32}P-γ-ATP	Hartmann Analytic, Braunschweig
p-Coumaric acid	Sigma-Aldrich, Taufkirchen
Penicillin/Streptomycin	PAA/GE Healthcare, Cölbe
Phalloidin, Rhodamine- /AlexaFluor 488-conjugated	Invitrogen (Molecular Probes), Karlsruhe
Phusion Hot Start II DNA Polymerase	Fermentas/Thermo Scientific, St. Leon-Rot
Polybrene	Sigma-Aldrich, Taufkirchen
Poly-L-Lysine	Sigma-Aldrich, Taufkirchen
Protease inhibitor cocktail tablets, complete, EDTA-free	Roche, Mannheim
Protein A/G beads	Santa Cruz, Heidelberg
Protein molecular weight standard, pre-stained	Fermentas/Thermo Scientific, St. Leon-Rot
SDS (sodium dodecylsulfate)	Roth, Karlsruhe
Sodium azide	Merck, Darmstadt
Sodium chloride	Roth, Karlsruhe
Sodium hydroxide	Roth, Karlsruhe
Sodium orthovanadate	AppliChem, Darmstadt
Sodium pyrophosphate	Roth, Karlsruhe
Sodium pyruvate	PAA/GE Healthcare, Cölbe
Streptavidin Sepharose High Performance	GE Healthcare, Munich
Sucrose	Roth, Karlsruhe
T4 DNA Ligase	Fermentas/Thermo Scientific, St.

Reagent	Manufacturer
	Leon-Rot
TEMED	Roth, Karlsruhe
(N,N,N',N'-tetramethyl-ethane-1,2-diamine)	
TPA (12-O-tetradecanoylphorbol-13-acetate)	Calbiochem/Merck, Darmstadt
Transferrin, AlexaFluor 488-conjugated	Invitrogen (Molecular Probes), Karlsruhe
Tris (tris-(hydroxymethyl)-aminomethane)	Roth, Karlsruhe
Triton X-100	Merck, Darmstadt
Trypsin-EDTA 0.05%	PAA/GE Healthcare, Cölbe
Tryptone	Roth, Karlsruhe
Tween-20	AppliChem, Darmstadt
Yeast extract	Roth, Karlsruhe

PCR primers were ordered from Sigma-Aldrich, Taufkirchen.

Ultra pure water was produced by water purification and deionization system OPTIPURE Analytic (membraPure GmbH, Bodenheim, Germany).

Table 3. Antibodies used in this work.

Antibody	**Manufacturer**
anti-CD29	Beckman Coulter, Krefeld
anti-CD49e	AbD Serotec, Düsseldorf
anti-CD49e	BD Transduction Laboratories, Pharmingen, Heidelberg
anti-Integrin α5β1	Merck/Millipore, Darmstadt
anti-EEA1	BD Transduction Laboratories, Pharmingen, Heidelberg
anti-Flag, horseradish peroxidase-conjugated	Sigma-Aldrich, Taufkirchen
anti-FMNL2	Atlas antibodies, Stockholm
anti-GM130	BD Transduction Laboratories, Pharmingen, Heidelberg
anti-GFP	Santa Cruz, Heidelberg
anti-HA, horseradish peroxidase-conjugated	Sigma-Aldrich, Taufkirchen
anti-MLC	Sigma-Aldrich, Taufkirchen
anti-myc, horseradish peroxidase-conjugated	Sigma-Aldrich, Taufkirchen
anti-phospho MLC	Cell Signaling, Danvers
anti-phospho-(Ser) PKC substrate	Cell Signaling, Danvers
anti-PKCα	Cell Signaling, Danvers
anti-PKCβ	Santa Cruz, Heidelberg
anti-PKCδ	Cell Signaling, Danvers
anti-PKCε	Cell Signaling, Danvers
anti-PKCζ	Cell Signaling, Danvers
anti-RhoC	Cell Signaling, Danvers
anti-TfR	Invitrogen, Karlsruhe
Goat anti-rabbit IgG horseradish peroxidase-conjugated	Bio-Rad, Munich
Sheep anti-mouse IgG horseradish peroxidase-conjugated	GE Healthcare, Munich

Table 4. Biochemical kits used in this work.

Kit	Manufacturer
Dual-Luciferase® Reporter Assay System	Promega, Mannheim
Nucleo Spin Extract II Kit	Macherey-Nagel, Düren
Nucleo Spin Plasmid Kit	Macherey-Nagel, Düren
PureLink™ HiPure Plasmid Maxiprep Kit	Invitrogen, Karlsruhe

Table 5. Composition of solutions used in this work.

Solution	Composition		Remarks
2× BBS transfection	BES	0.05 M	pH 6.92
buffer	NaCl	0.28 M	autoclaved
	Na_2HPO_4	0.0015 M	
	dissolved in deionized water		
ECL solution A	Tris-HCl	100 mM	pH 8.5
	Luminol	2.5 mM	
	p-Coumaric acid	0.4 mM	
ECL solution B	Tris-HCl	100 mM	pH 8.5
	H_2O_2	0.018% v/v	
4×Laemmli buffer	Glycerol	28%	pH 6.8
	EDTA	10 mM	
	SDS	5.7%	
	2-mercaptoethanol	4.7 mg/ml	
	Bromophenol blue	3.5 mg/ml	
	Tris-HCl	286 mM	
LB agar	NaCl	1%	autoclaved
	Yeast extract	0.5%	
	Tryptone	1%	
	Agar	1.5%	

Solution	Composition		Remarks
	dissolved in deionized water		
LB medium	NaCl	1%	autoclaved
	Yeast extract	0.5%	
	Tryptone	1%	
	dissolved in deionized water		
PBS	Na_2HPO_4	8 mM	pH 7.4
	KH_2PO_4	1.5 mM	
	NaCl	137 mM	
	KCl	2.7 mM	
	dissolved in deionised water		
PCR sample loading	Glycerol	30%	
buffer (6×)	Bromophenol blue	0.25%	
	dissolved in deionised water		
SDS-PAGE	Acrylamide	9.9%	pH 8.8
separating gel	Bisacrylamide	0.26%	
	TEMED	9.5 µM	
	SDS	0.1%	
	Tris-HCl	0.36 M	
	$(NH_4)_2S_2O_8$	0.1%	
SDS-PAGE	Glycine	192 mM	pH 8.3
running buffer	SDS	0.1%	
	Tris-HCl	25 mM	
SDS-PAGE	Acrylamide	5.9%	pH 6.8
stacking gel	Bisacrylamide	0.16%	
	TEMED	14.5 µM	
	SDS	0.1%	
	Tris-HCl	0.12 M	
	$(NH_4)_2S_2O_8$	0.15%	
TAE buffer	EDTA	2 mM	pH 8.0
	Tris	40 mM	

Solution	Composition		Remarks
	Acetic acid	20 mM	
	dissolved in deionized water		
TBS-DM buffer	Dry milk	5%	pH 7.5
	NaCl	500 mM	
	Tris-HCl	20 mM	
	Tween-20	1%	
	dissolved in deionized water		
TBST buffer	NaCl	500 mM	pH 7.5
	Tris-HCl	20 mM	
	Tween-20	1%	
	dissolved in deionized water		
Western blot	NaCl	500 mM	pH 7.5
blocking solution	Tris-HCl	20 mM	
	Bovine serum albumin	5%	
	NaN_3	0.1%	
	Tween-20	1%	
Western blot	Glycine	192 mM	pH 8.5
transfer buffer	Tris-HCl	25 mM	
	Methanol	20% v/v	
	dissolved in deionized water		

3.2 Constructs and cloning

Expression constructs were generated and sequence-verified following standard cloning procedures. Flag-FMNL2, Flag-/myc-FMNL2-FH1-CT, Flag-mDia1, Flag-mDia1-CT and HA-RhoCV14 were described previously (Kitzing et al., 2010; Vaillant et al., 2008). myc-FMNL2, FMNL2-myc, FMNL2-GFP-myc, Flag-/myc-FMNL2-FH1-1023, Flag-/myc-FMNL2-FH1-1045, and myc-FMNL2-FH3 (aa 262-484) were sub-cloned into EFpLink with N-terminal or C-terminal myc-tag as indicated. GST-FMNL2-959-CT for protein purification was cloned into pGEX-6P-1 (GE Healthcare). His-FMNL2-NT (23-484) and His-FMNL2-F1F2-CT were cloned into pET20b (Novagen). His-mDia1-FH2 (mDia1-CT) was described (Brandt et al., 2007). FMNL2-mCherry and FMNL2-GFP were cloned into pmCherryN1 or pEGFPN1 vectors (Clonetech). Point mutants FMNL2-S1072A, S1072E, and ILI3A were generated by site-directed point mutation. Plasmids for generating inducible stable cell lines were kind gifts from Guang Hu. FMNL2 point mutants fused with EGFP or EGFP alone were amplified and inserted into pENTR11 (Invitrogen) and shifted into pINDUCER20 (Meerbrey et al., 2011) by site-specific recombination with LR Clonase™ II (Invitrogen). Plasmids for FMNL2 overexpressing stable cell line were constructed by shifting FMNL-GFP, FMNL2-S1072A-GFP and FMNL2-S1072E-GFP from pEGFPN1 to pWPXL. Lentiviral pGIPZ-shFMNL2 was from Thermo Scientific. α5-integrin-GFP, GFP-PKCα and GFP-PKCα-T497A were described (Mostafavi-Pour et al., 2003; Tuomi et al., 2009). GFP-PKCα-CA was generated by deleting the first 30 amino acids and subcloned into pEGFPC1 vector (Clonetech). TGN38-YFP and mRFP-Lamp1 were gifts from Oliver Fackler (Uni Heidelberg). Human Rab4, Rab5 and Rab7 were kind gifts from Douglas Richardson (Harvard University). Primers used in this work are listed in Table 6.

3.2.1 Agarose gel electrophoresis

DNA samples were mixed with 6× PCR sample loading buffer and loaded to 1% agarose gels containing 10 μg/mL ethidium bromide. DNA fragments were separated on the gel in TAE buffer electrophoretically under constant voltage in a agarose gel chamber (Bio-

Rad). The gel was later illuminated under UV light and visualized using INFINITY gel documentation system (PEQLab).

Table 6. List of primers.

Name	**Sequence (5' -> 3')**
FMNL2-1ClaFw	GCGCGCATCGATGGCAACGCAGGGAGCATG
FMNL2-3279SpeRv	GCGCGCACTAGTTCACATTGTTATTTCGGCACC
FMNL2-1023SpeRv	GCGCGCACTAGTTCACTTTGATTTATGAGAAGG
FMNL2-1045SpeRv	GCGCGCACTAGTTCAATATACATGTCTGTTATC
FMNL2-1XhoFw	TACGATCTCGAGATGGGCAACGCAGGGAGCATGGATTC
FMNL2-1094KpnRv	GCGCGCGGTACCCCCATTGTTATTTCGGCACC
FMNL2-FH3ClaFw	GCGCGCATCGATACAAAAGCCCTTGTCTTA
FMNL2-FH3SpeRv	GCGCGCACTAGTTCACTGAATTTTAATGGTCCC
FMNL2-3216AFw	AGGAGAGCCGTCAGGCGG
FMNL2-3216ARv	CCTGACGGCTCTCCTCAC
FMNL2-3216EFw	AGGAGAGAGGTCAGGCGG
FMNL2-3216ERv	CCTGACCTCTCTCCTCAC
FMNL2-SalFw	TACGATGTCGACATGGGCAACGCAGGGAGCAT
FMNL2-3279NotRv	AGCTAAGCGGCCGCTCACATTGTTATTTCGGCACC
FMNL2-PmeI1Fw	TACGATGTTTAAACTAATGGGCAACGCAGGGAGCATGGA
FMNL2-SpeGFPRv	GCGCGCACTAGTTTACTTGTACAGCTCGTCCATGC
FMNL2-2110Fw	CTTGCCGCCACTTTAAGG
FMNL2-2110Rv	TAAAGTGGCGGCAAGATT
FMNL2-LIAAFw	CAAGAGGCCGCAGCAGAATTA
FMNL2-LIAARv	TTCTGCTGCGGCCTCTTGCTG

Name	Sequence (5' -> 3')
PKCα-30XhoFw	ACTATCCTCGAGCTAACGTGCACGAGGTGAAG
PKCα-672KpnRv	GCGCGCGGTACCTCATACTGCACTCTGTAAGAT

3.3 Cell culture, drug treatments, transfections and stable cell lines

HEK293, HEK293T, HeLa and A375M2 (kind gift from Erik Sahai, Cancer Research, London) cells were maintained in DMEM supplemented with 10% fetal bovine serum at 37°C in a 5% CO2 environment. Inducible stable A375M2 cells were cultured with the addition of 800 μg/mL G418. When needed, cells were treated with 5 nM to 200 nM 12-O-tetradecanoylphorbol-13-acetate (Calbiochem), 2 μM bisindolylmaleimide I (Calbiochem), 1 μM Gö6976 (Sigma) or 8 μM A23187 (Sigma).

3.3.1 Transfection of DNA

DNA plasmids were transfected with calcium phosphate method for HEK293 and HEK293T cells. Briefly, plasmids were mixed with autoclaved deionized distilled water. The same volume of 2×BBS buffer was added followed by adding 1/20 volume of 2.5 M $CaCl_2$ dropwise. The transfection mixtures were incubated at room temperature for 20 min before adding to the cells drop by drop. Cells were changed into fresh complete media after 3 hours. For transfection of HeLa cells, Fugene HD (Promega) was used according to manufacturer's instructions. For one 6-well, plasmids were mixed in 96 μL serum free medium. 4 μL of Fugene HD was added and mixed by vortex. After 5 min incubation at room temperature, transfection mixtures were added to the cells.

3.3.2 Transfection of siRNA

siRNAs were transfected using HiperFect (Qiagen) following manufacturer's instructions. For one 6-well, 20 μM siRNA in the volume of 2 μL was mixed with 186 μL serum free media and 12 μL HiperFect. After 5min incubation at room temperature, the transfection mixtures were added to cells in a total volume of 2 mL. All siRNAs were purchased from Qiagen. Transfection of both siRNA and DNA in one experiment was

achieved by transfecting siRNA on the day of splitting cells and transfecting DNA subsequently on the following day. siRNA targeting sequences are listed in Table 7.

Table 7. List of siRNA targeting sequences.

Name	Targeting sequence (5' -> 3')
human RhoC	CACCATGGCTGCAATCCGAAA
human FMNL2, targeting 3'-UTR, 3'-AlexaFluor 555 modified	CTGCGGGCACATTCCCATAAA
human PKCα	AACCATCCGCTCCACACTAAA
human PKCβ	CCGGATGAAACTGACCGATTT
human PKCδ	AACTCTACCGTGCCACGTTTT
human PKCε	CCCGACCATGGTAGTGTTCAA
human PKCζ	CGGAAGCATGACAGCATTAAA

3.3.3 Generating stable cell lines by virus transduction

A375M2 or HeLa stable cell lines were generated by lentiviral transduction. Viruses were produced by transfecting HEK293T cells with packaging plasmid psPAX2, envelope plasmid pMD2G and expressing plasmids pINDUCER20-/pWPXL-GFP, FMNL2-S1072A-GFP, FMNL2-S1072E-GFP, FMNL2-ILI3A-GFP, FMNL2-ILIS4A-GFP or FMNL2-ILI3ASE-GFP. Supernatants were harvested 48 h after transfection and filtered through 0.45 μm filter. A375M2 or HeLa cells were infected by the virus supernatant with the addition of 10 μg/mL Polybrene. 48 h after infection, cells were trypsinized and passaged. To induce the expression of the desired protein when needed, doxycycline was applied to the cells at 1 μg/mL.

3.4 Analysis of protein expression from cultured cells

3.4.1 Isolation of protein from cells

Cell culture media were removed from cultured cell. Cells were lysed by adding 1× Laemmli buffer at the ratio of 10 µL per 1×10^5 cells. The lysates were scraped from the cell culture dish into Eppendorf tubes and incubated at 95°C for 10 to 15 min. Extracted cell lysates were subjected to SDS-PAGE immediately or stored at -20°C.

3.4.2 SDS-PAGE

Proteins were separated by sodium dodecyl sulfate polyacrylamide gel electrophoresis (SDS-PAGE) using Mini-PROTEAN Tetra Cell gel system (Bio-rad). From 8% to 13% separating gel and 6% stacking gel (Table 5) were used according to the different sizes of the proteins which were to be separated. Gels were casted and polymerized in a vertical glass space and assembled into the vertical Tetra Cell chamber following manufacturer's instructions. The chamber was filled with SDS running buffer (Table 5). Cell lysates and standard pre-stained protein marker were loaded into the wells. Proteins were electrophoretically separated at constant voltage (80 V for stacking gel and 120 V for separating gel). The gels were subjected to coomassie blue staining or transfer.

3.4.3 Transfer, blocking and detection of the proteins by antibodies

SDS-PAGE gels and 0.22 or 0.45 µm nitrocellulose membranes (Whatman) were assembled into a Mini Trans-Blot module and then into the Mini Trans-Blot Electrophoretic Transfer Cell (Bio-rad) following manufacturer's instructions. The transfer cell chamber was filled with Western blotting transfer buffer (Table 5) and proteins were transferred from the gel to the membrane at constant voltage of 100 V for 45 min to 1.5 h.

After transfer, membranes were placed into blocking buffer (Table 5) and incubated for 1 h at room temperature. Different primary antibodies were diluted in the blocking buffer and incubated with the membranes on a shaker for 1 to 2 h at room temperature or

overnight at 4°C subsequently. Membranes were washed 10 min each for three times with TBST (Table 5) and incubated with secondary antibodies in blocking buffer for 1 h at room temperature when necessary. Membranes were washed again 10 min each for three times with TBST before developing. Enhanced chemiluminescence (ECL, Table 5) was used to detect the horseradish peroxidase-conjugated antibodies. Films (Fuji) were exposed on top of the membrane with ECL at different time points in a dark room and developed with the developing machine. The primary and secondary antibody dilutions are listed in Table 8.

Table 8. List of antibody dilutions used in this work.

Antibody	**Dilutions**
anti-CD29	1:1000
anti-CD49e	1:1000
anti-Flag, horseradish peroxidase-conjugated	1:5000
anti-FMNL2	1:2000
anti-GFP	1:3000
anti-HA, horseradish peroxidase-conjugated	1:2000
anti-MLC	1:500
anti-myc, horseradish peroxidase-conjugated	1:2000
anti-phospho MLC	1:1000
anti-phospho-(Ser) PKC substrate	1:1000
anti-PKCα	1:1000
anti-PKCβ	1:200
anti-PKCδ	1:1000
anti-PKCε	1:1000
anti-PKCζ	1:500
anti-RhoC	1:1000
anti-TfR	1:500
Goat anti-rabbit IgG horseradish peroxidase-conjugated	1:5000

Antibody	Dilutions
Sheep anti-mouse IgG horseradish peroxidase-conjugated	1:3000

3.5 Protein purification

The expression plasmid was transformed into E. coli BL21 (DE3). Bacteria were cultured in LB medium at 37°C until OD=0.6 and induced with 200 μM IPTG at 22°C for 16 h. GST fusion protein was purified using Glutathione Sepharose 4B beads (GE Healthcare) as described before (Brandt et al., 2007). Briefly, bacteria were harvested by centrifugation and lysed by sonication in lysis buffer (50 mM Tris-HCl pH 8.0, 150 mM NaCl, complete protease inhibitors). After centrifugation at 13,000 rpm at 4°C for 45 min, supernatant was collected and loaded to pre-equilibrated Glutathione Sepharose 4B beads. Beads were washed three times with high-salt washing buffer (50 mM Tris-HCl pH 8.0, 500 mM NaCl) and three times with non-salt washing buffer (50 mM Tris-HCl pH 8.0) subsequently before eluting with elution buffer (50 mM Tris-HCl pH 8.0, 10 mM Glutathione reduced).

6×His fusion protein was purified using Ni-NTA agarose beads (Qiagen). Bacteria were lysed in 1×PBS pH 7.4, 30 mM Imidazole and 1% NP-40 with complete protease inhibitors. After centrifugation, supernatant was collected and loaded to pre-equilibrated Ni-NTA beads followed by three times high salt washing (1×PBS pH 7.4, 20 mM Imidazole, 350 mM NaCl) and three times low salt washing (1×PBS pH 7.4, 20 mM Imidazole). 6×His fusion proteins were eluted in fractions with elution buffer (1×PBS pH 7.4, 350 mM Imidazole).

Fractions were loaded to SDS-PAGE gels and subjected to coomassie blue staining to visualize the proteins of interests. Fractions with desired protein were pooled and dialyzed in 20 mM Hepes (pH 7.4), 25 mM $MgCl_2$, 5 mM EDTA and 5 mM DTT. For

formin FH2 containing proteins, dialyzing buffer contained 2 mM Na_3PO_4, pH 7.4, 50 mM NaCl, 0.1 mM $MgCl_2$, 0.1 mM EGTA and 0.5 mM DTT (Chhabra and Higgs, 2006).

3.6 In vitro kinase assay

Purified recombinant GST fusion Protein kinase C protein isoforms were purchased from ProQinase GmbH. 20 ng of each PKC isoform and 1 μg substrate protein were incubated in 50 mM Hepes (pH 7.4), 150 mM NaCl, 5 mM EDTA, 5 mM DTT, 25 mM $MgCl_2$, 0.02% Triton X-100, 1 mM ATP and 5 μCi ^{32}P-γ-ATP at 30°C for 15 min. Kinase reaction was stopped by adding the 1×Laemmli buffer (Table 5). After running SDS-PAGE and fixation of the gel, films were exposed on top of the gel in the dark room or at -80°C and developed at different time points.

3.7 Biotin-strepdavidin pull-down assay

24 hours after transfection, HEK293 cells were scraped and lysed using lysis buffer containing 20 mM Tris-HCl (pH 7.4), 150 mM NaCl, 2 mM EDTA, 0.1% Triton X-100, 1 mM DTT, 2.5 mM sodium pyrophosphate, 1 mM β-glycerophosphate, 1 mM sodium orthovanadate, and complete protease inhibitors (Roche). Cell lysates were centrifuged (13,000 rpm, 10 min at 4°C) and the supernatants were collected. 10 μL of biotinylated α5/β1 integrin cytoplasmic tail peptides (5 μg/μL each) were pre-incubated with cell lysates respectively for 4 h (Pellinen et al., 2008; Tuomi et al., 2009). The peptide sequences were: β1 integrin cytoplasmic tail: Biotin-HDRREFAKFEKEKMNAKWDTGENPIYKSAVTTVVNPKYEGK; α5 integrin cytoplasmic tail: Biotin-YKLGFFKRSLPYGTAMEKAQLKPPATSDA. Strepdavidin sepharose beads (GE Healthcare) were washed with lysis buffer and added to the pre-incubated mixture after the 4 h pre-incubation. Another 1 h incubation was conducted before washing the beads three times with lysis buffer. 1×Laemmli buffer (Table 5) was added and samples were subjected to SDS-PAGE gel and Western blotting.

3.8 Immunoprecipitation

Cells were harvested 24 or 48 h after transfection by scraping and lysed in lysis buffer containing 20 mM Tris-HCl (pH 7.4), 150 mM NaCl, 2 mM EDTA, 0.1% Triton X-100, 2.5 mM sodium pyrophosphate, 1 mM β-glycerophosphate, 1 mM sodium orthovanadate, and complete protease inhibitors (Roche). Supernatants were collected after centrifugation (13,000 rpm, 10 min at 4°C) and incubated with Flag/myc-conjugated agarose beads (Sigma) or Protein A/G beads (Santa Cruz) together with antibodies for 1 to 5 h at 4°C. Beads were centrifuged and washed three times with lysis buffer. 1×Laemmli buffer （Table 5）was added and samples were subjected to SDS-PAGE gel and Western blotting.

3.9 MAL/SRF luciferase reporter assay

MAL/SRF luciferase assays were performed as described previously (Brandt et al., 2009). Briefly, HEK293 cells were transfected with plasmids of genes of interests, p3DA.luc and pRL-TK reporter plasmids. 24 h after transfection, cell media were removed and cells were washed once with PBS. 200 µL 1× Passive lysis buffer (Promega) was added per 6-well. Cells were lysed on ice for 20 min, scraped and centrifuged at 13,000 rpm for 15 min at 4°C. From 5 to 20 µL cell lysates were used for each assay. Firefly and Renilla luciferase signals were recorded sequentially by Luminoscan Ascent Microplate Luminometer (Thermo Scientific) using the Ascent software (Thermo Scientific) with 900 ms integration time. Firefly signal was normalized to Renilla signal for each sample.

3.10 Membrane flotation

HeLa cells were seeded 48 h or HEK293 cells were transfected 24 h before analysis. Membrane flotation assays were performed as described (Pan et al., 2012). 200nM TPA or DMSO were applied to the cells for 30 min at 37°C. Cells were washed once with ice cold PBS and lysed in TNE buffer (50 mM Tris-HCl pH 7.4, 150 mM NaCl, 5 mM EDTA, protease inhibitors and phosphatase inhibitors) for 20 min. The cell lysates were

passed through 25G syringe needle 20 times. After brief centrifugation, supernatants were mixed with 67% Optiprep (Invitrogen) and loaded to SW60 centrifuge tubes. Each sample was overlaid with 2.5 mL 28% Optiprep and 600 µL TNE buffer carefully without disturbance. Ultracentrifugation was performed with SW60 rotor at 35,000 rpm for 3 h at 4°C (Beckman Coulter). 500 µL fractions were collected with the 2nd and 8th as the membrane and soluble fractions respectively. 30 µL of each fraction was subjected to Western blotting analysis.

3.11 Subcellular fractionation with discontinuous sucrose density gradient

HeLa cells were seeded 48 h or HEK293 cells were transfected 24 h before analysis. Sucrose gradient analysis was performed as described (Pan et al., 2012). In short, discontinuous sucrose gradient was poured 16 h before use at 4°C, which was composed of 700 µL of each 0.5 M, 0.8 M, 1.0 M, 1.2 M and 1.5 M sucrose in TE buffer (50 mM Tris-HCl pH 7.4, 5 mM EDTA) from top to bottom in a centrifuge tube suitable for SW60 rotor. 200nM TPA or DMSO were applied to the cells for 30 min at 37°C when necessary. Cells were washed once with ice cold PBS and lysed in 1 mL TNE buffer (50 mM Tris-HCl pH 7.4, 150 mM NaCl, 5 mM EDTA, protease inhibitors and phosphatase inhibitors) for 20 min. The cell lysates were passed through 25G syringe needle 20 times and subjected to centrifugation at 4,000 rpm for 6 min. 750 µL of the supernatant was loaded to the top of the sucrose gradient. Ultracentrifugation was performed with SW60 rotor at 35,000 rpm for 1.5 h at 4°C (Beckman Coulter). 420 µL fractions were collected from the top of the tube and fractions were subjected to Western blotting analysis.

3.12 Immunocytochemistry

HeLa cells were seeded on cover slips in 6-well plates. 24 h or 48 h after transfection, cells were washed with PBS and fixed with 8% formaldehyde for 10 min at room temperature. After washing with PBS, 0.02% Triton-X 100 in PBS was used to permeablize cells for 10 min. Cells were blocked with 5% BSA in PBS for 1 h at room temperature. Primary and secondary antibodies were diluted in the blocking solution and incubated with the coverslips for 1 h each with three times PBS washing between the two

steps. DAPI staining was performed for 10 min when indicated. Coverslips were then mounted on the glass slides using fluorescent mounting media (Dako).

3.13 Live cell imaging

HeLa cells were seeded on cover slips in 6-well plates. 24 h or 48 h after transfection, cover slips seeded with cells were inserted into a customized imaging dish and mounted to the microscope objective. Live cell imaging was performed at 37°C, in a CO_2 chamber. Images were acquired every 5 to 10 s with a LSM 700 confocal microscope (Zeiss) and the Zen software (Zeiss), using the 63×/1.4 oil objective. Drugs were applied to the cells directly at the microscope while scanning. EGFP and mCherry or AlexaFuor 555 channels were scanned sequentially by line within 1.94 s. Images were later processed with Image J software.

3.14 Invasion assays and image analysis

Inverted transwell invasion assays were performed as described (Kitzing et al., 2010). Cells were seeded 24 h before the assay. Doxycycline (1 µg/mL) was applied to the inducible stable cell lines in all the solutions. Upper chambers of the Transwell inserts (Greiner Bio-one) were coated with 50 µL growth factor reduced Matrigel (BD Biosciences) and polymerized for 60 min at 37°C. The inserts were inverted allowing cell seeding (6,000 cells per inserts for A375M2 cells) and adhering on the outer bottom. After 3 h, the Transwell inserts were reverted. The upper chambers were filled with medium containing 20% fetal bovine serum and the lower chamber with medium containing 0.5% fetal bovine serum. Cells were invading for 48 h before fixation, permeabilization and subsequent staining with DAPI and rhodamine phalloidin. Confocal z-stacks of 100 µm were acquired every 5 µm for five random imaging fields of each insert with LSM 700 confocal microscope (Zeiss), using the 20×/0.75 objective and the ZEN software (Zeiss). Quantification of the invaded (more than 15 µm) and non-invaded cell number was achieved using the Image J Analyze Particle function counting the number of the nucleus.

3.15 Analysis of fluorescence intensity changes on the plasma membrane

The analysis was performed by Haisen Ta (Max Planck Institute for Biophysical Chemistry, Göttingen). In brief, 2D fluorescence intensity images with time stamps were segmented by Sobel edge detection with building function in MATLAB to identify the plasma membrane region. The fluorescence intensity was summed up in membrane region for each cell, and normalized by their maximum intensity. Photo bleaching was corrected by the overall intensity of the whole cell. Statistics was given on the normalized fluorescence intensity at each time point.

3.16 Actin polymerization assay with fluorescence microscopy

Unlabeled actin monomers (2.4 μM, Hypermol) were added to 50 μL polymerization buffer (2 mM Tris-HCl, pH 8.0, 0.5 mM DTT, 0.2 mM ATP, 1.1 mM $MgCl_2$, 50 mM KCl, 1 mM EGTA, 10 mM imidazole, pH 7.0 and 0.01% NaN_3) containing formin FH2 domain proteins. At different time points, take 1 μL of the reaction and dilute it in 80 μL 0.4×KMEI buffer (20 mM KCl, 4 mM $MgCl_2$, 4 mM EGTA, and 40 mM imidazole, pH 7.0) (Chhabra and Higgs, 2006) with 0.5 μL Alexa 488-phalloidin (6.6 μM, Invitrogen). From each dilutions, take 20 μL mixing with fluorescent mounting medium (Dako) and drop onto poly-L-Lysine coated coverslips, then mount on glass slides before going to microscope. Images of actin filaments were taken with Nikon Eclipse Ti epifluorescence microscope using the 100×/1.4 objective and NIS-Element AR software (Nikon).

3.17 Pyrenyl-actin assembly assay

Pyrenyl-actin assembly assays were adapted from previously described protocols (Kitzing et al., 2007). For the assays using cell lysates, HEK293 cells were transfected with formin proteins. 24 h after transfection, cells were lysed in lysis buffer containing 20 mM Tris-HCl (pH 7.4), 150 mM NaCl, 2 mM EDTA, 0.1% Triton X-100, 2.5 mM sodium pyrophosphate, 1 mM β-glycerophosphate, 1 mM sodium orthovanadate, and complete protease inhibitors (Roche). After brief centrifugation at 13,000 rpm for 10 min, 500 μL supernatant of each sample were collected and dialyzed against dialysis buffer (2

mM Na_3PO_4, pH 7.4, 50 mM NaCl, 0.1 mM $MgCl_2$, 0.1 mM EGTA, 0.5 mM DTT) for 1 h. All samples were diluted to a total protein concentration of 20 mg/mL. For the assays using eluted Flag tag proteins, immunoprecipitation was performed as described in the section 3.7. After final washing, Flag beads were eluted three times with 40 µL Flag peptide (Sigma) elution buffer (20 mM Tris-HCl pH 7.4, 150 mM NaCl, 1 mM EDTA, 200 µg/mL Flag peptide). Fractions were pooled and dialyzed with dialysis buffer for 1 h. To start the pyrenyl-actin assemply assay, 5 to 10 µL protein was diluted in 80 µL dialysis buffer, followed by sequentially adding 10 µL of energy buffer (150 mM creatine phosphate, 20 mM ATP, 2 mM EGTA, 20 mM $MgCl_2$) and 10 µL of pyrenyl-actin (final concentration 2 µM, 10% labeled, Hypermol). Fluorescence was immediately monitored for 5 to 10 min at 407 nm with an excitation at 365 nm using a SHIMADZU RF-5301PC spectrofluorophotometer.

4 Results

FMNL2, along with FMNL1 and FMNL3, belong to the formin-like subfamily of mammalian formins (Figure 13A). FMNL3 was reported to be a formin lacking autoinhibition mediated by N- and C-termini interaction, while FMNL1, FMNL2 and FMNL3 all have the capacity to bundle actin filaments (Harris, 2006; Vaillant et al., 2008). FMNL2 is widely expressed in human tissues, especially in central and peripheral nervous system (Gardberg et al., 2010). It has been reported that FMNL2 is required for amoeboid mode of invasion downstream of RhoC (Kitzing et al., 2010). Other properties of FMNL2 remain elusive.

4.1 The role of FMNL2 in actin polymerization

4.1.1 FMNL2 is a poor actin nucleator

Formin proteins are the largest group of actin nucleators. Unlike FMNL1 and FMNL3, the actin nucleation activity of FMNL2 was poorly studied. In order to understand the actin assembly properties of FMNL2, plasmids expressing 6×His tagged FMNL2 N-terminus (FMNL2-NT, aa 1-484), FH1 domain to C-terminus (FMNL2-FH1-CT, aa 504-1092) and FH2 domain to C-terminus (FMNL2-FH2-CT, aa 599-1092) were constructed (Figure 13A) and proteins were purified (Kitzing et al., 2010; Moseley et al., 2006; Vaillant et al., 2008). Pyrenyl-actin polymerization assays showed that FMNL2 inhibited actin polymerization. The more FMNL2-FH1-CT added to the reaction, the rate became slower (Figure 13B), indicating that purified FMNL2-FH1-CT might strongly bind actin monomers or the barbed ends of the filaments sequestering nucleation and/or elongation. Additionally, FMNL2-NT exhibited no activity on actin assembly in pyrenyl-actin assay while FMNL2-FH2-CT seemed to inhibit actin assembly (Figure 13B).

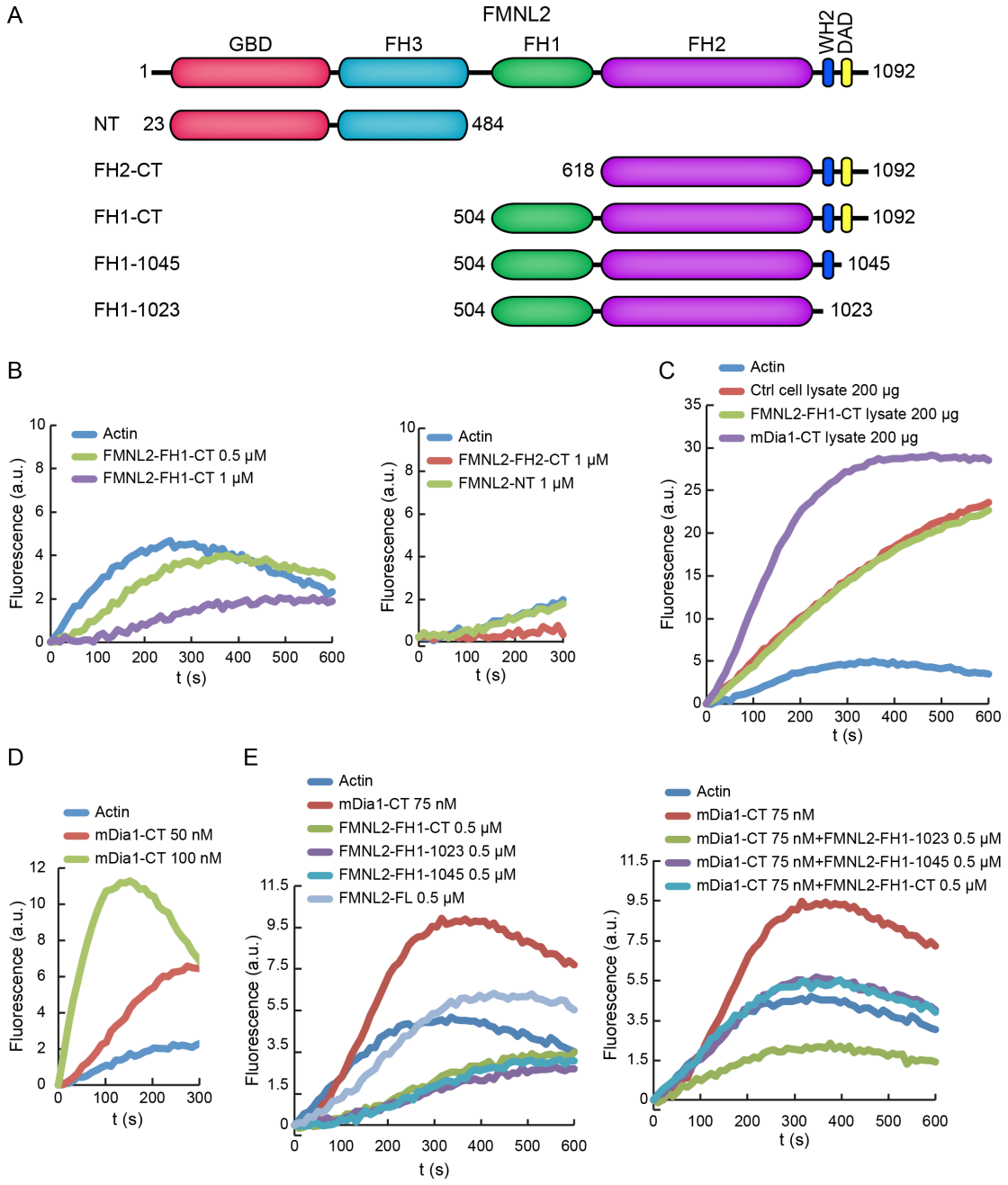

Figure 13. Pyrenyl-actin polymerization assays implicate that FMNL2 is a poor actin nucleator. A. Schemes of FMNL2 proteins described in the experiments. GBD: GTPase binding domain; FH1/2/3: formin homology 1/2/3; WH2: WASP homology 2; DAD: diaphanous autoregulatory domain. Numbers indicate boundaries of amino acids. **B.** Pyrenyl-actin assays using purified proteins from bacteria. **C.** Pyrenyl-actin assays using HEK293 cells lysates expressing different proteins. **D.** Pyrenyl-actin assays using Flag tagged mDia1-CT purified from

HEK293 lysates. **E.** Pyrenyl-actin assays using Flag tagged proteins purified from HEK293 lysates.

However, purified protein from bacteria might exhibit different properties due to lack of the co-/post-translational modification system and regulating partners of eukaryotes. Thus, pyrenyl-actin assays were subsequently conducted using HEK293 cell lysates expressing mDia1 C-terminus containing the FH2 domain (mDia1-CT) or FMNL2-FH1-CT. mDia1 is known to be a potent actin nucleator and the cell lysate expressing mDia1-CT showed significant activity on actin assembly comparing to the control cell lysate or the actin alone. Cell lysate expressing FMNL2-FH1-CT exhibited almost the same basal activity as the control cell lysate, showing that expression of FMNL2-FH1-CT in cells could not additionally increase actin assembly more than control lysate (Figure 13C). Moreover, efforts were made to purify proteins from HEK293 cell lysates. Flag-tagged proteins were overexpressed in HEK293 cells and immunoprecipitated. Flag peptides were used to elute the proteins from the Flag antibody-conjugated agarose beads. The eluted proteins were also applied to pyrenyl-actin polymerization assay. mDia1-CT showed potent activity on actin assembly as shown in Figure 13D. There was no obvious activity from FMNL2 full length (FMNL2-FL), while FMNL2-FH1-CT, FMNL2-FH1-1023 (without WH2 and DAD domains) and FMNL2-FH1-1045 (without DAD domain) inhibited actin assembly to the same extent (Figure 13E). Interestingly, when FMNL2-FH1-CT, FMNL2-FH1-1023 or FMNL2-FH1-1045 was pre-incubated with mDia1-CT and applied to the pyrenyl assay, the polymerization activity of mDia1-CT was inhibited (Figure 13E). Hence, it is possible that the FH2 domain of FMNL2 strongly bind the barbed ends. In the closely related FMNL3, it was reported that both FH2 and WH2 bound actin monomers and barbed ends (Heimsath and Higgs, 2012; Thompson et al., 2013). In fact, in the Flag-IP elution, an actin band was detected together with FMNL2-FH1-CT indicating that FMNL2 FH2 or WH2 domain strongly interact with actin (data not shown).

Since FMNL2 did not show obvious actin assembly activity in pyrenyl-actin assays with proteins from three different sources, it was necessary to visualize the effects of FMNL2 on actin assembly. After 30 or 60 s reaction of actin monomers and formin proteins in

polymerization buffer, samples were collected and AlexaFluor 488-phalloidin was used to stain and stabilize the polymerized actin seeds (Figure 14). In control reaction, nucleation happened at a quite slow rate, showing few differences between 30 s and 60 s reactions. mDia1-CT as a potent nucleator gave prominent actin filaments within 30 s and more within 60 s. FMNL2-FH1-CT and FMNL2-FH2-CT showed no differences in comparison to control condition (Figure 14). Therefore, both pyrenyl-actin assembly assay and actin assembly assay with phalloidin staining indicate that FMNL2 is a poor actin nucleator *in vitro*.

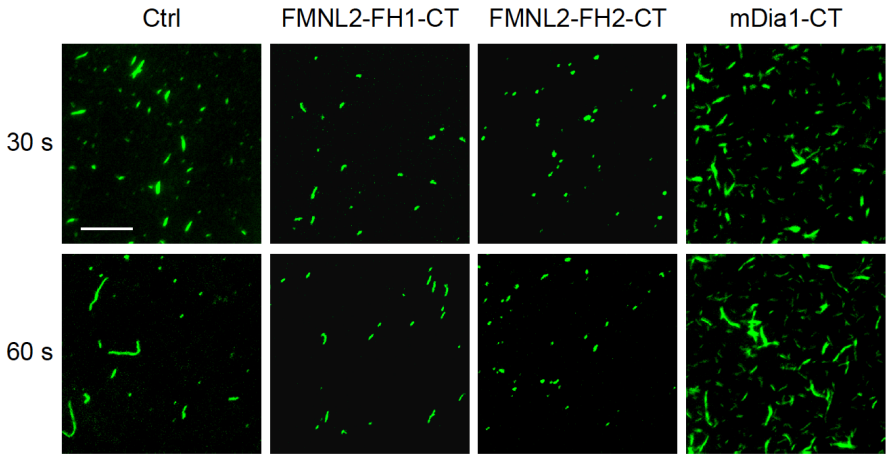

Figure 14. Visualizing actin filaments assembled under various conditions by microscopy. Actin assembly reactions were conducted in polymerization buffer. Reactions were stabilized and stained with AlexaFluor 488-phalloidin at different time points and visualized by epi-fluorescence microscope. Amounts of the proteins used were: 0.5 µM FMNL2-FH1-CT, 0.5 µM FMNL2-FH2-CT and 75 nM mDia1-CT. Scale bar: 5 µm.

To further understand the cellular context of FMNL2 and actin filaments, FMNL2-FH1-CT, FMNL2-FH1-1023 or FMNL2-FH1-1045 was expressed in HeLa cells. The expression of all three proteins induced robust formation of stress fibers (Figure 15). Interestingly, FMNL2-FH1-CT and FMNL2-FH1-1045 exhibited a prominent accumulation in the nucleus of the cells which resembles the case of mDia1-FH1-CT. mDia1-FH1-CT localization in the nucleus is dependent on a C-terminal cryptic nuclear localization sequence (NLS) after the FH2 domain (Copeland et al., 2007). FMNL2-FH1-1023 lost the nuclear localization and distributed in the cytoplasm, implicating that the

possible NLS in FMNL2 lies between amino acid 1023 and 1045. Given the fact that there are several lysine and arginine residues within this region, the NLS might reside within the WH2 domain (Figure 28A). The reason why FMNL2 harbors such a signal and how it is regulated needs further investigation. As shown in Figures 13 and 14, how FMNL2 as a poor nucleator *in vitro* regulates stress fiber formation also needs further study.

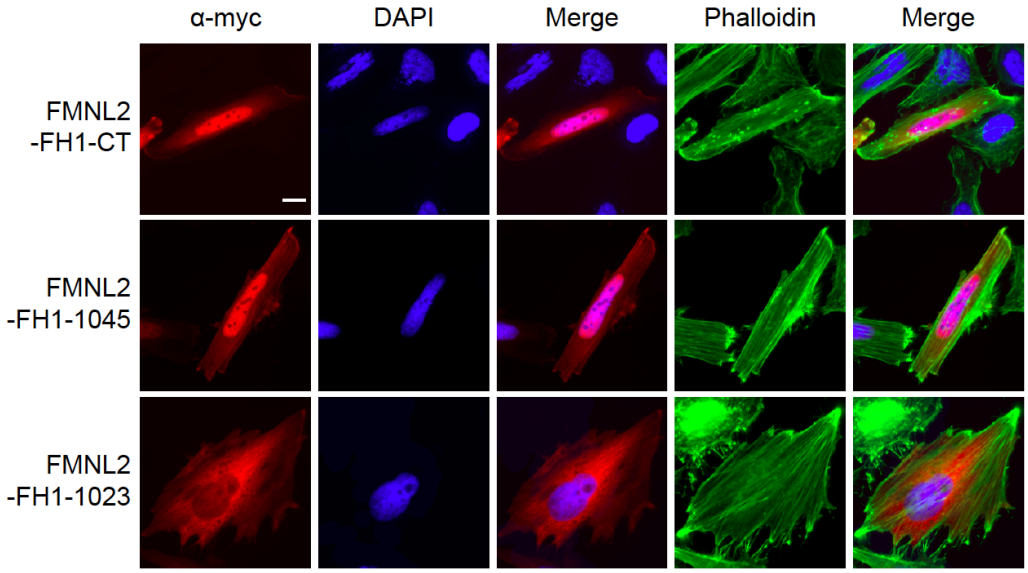

Figure 15. FMNL2 derivatives induce stress fibers and accumulate in nucleus. myc-FMNL2-FH1-CT, myc-FMNL2-FH1-1045 and myc-FMNL2-FH1-1023 (red) were expressed in HeLa cells. Nucleus was visualized with DAPI (blue) and F-actin was visualized with phalloidin (green). All three induced stress fiber while only myc-FMNL2-FH1-CT and myc-FMNL2-FH1-1045 accumulated in nucleus. Scale bar: 10 μm.

4.1.2 The actin polymerization activity and the plasma membrane localization of FMNL2 are regulated by RhoC

Previously, it was shown that the constitutively active Rho GTPase, RhoC V14, interacted with the GBD of FMNL2, while the closely related RhoA or RhoB did not (Kitzing et al., 2010). However, it was not shown where FMNL2 localized or how the actin assembly activity of FMNL2 was regulated in cells. In order to verify the cellular role that RhoC plays on FMNL2, FMNL2-mCherry was transiently expressed in HeLa

cells (Figure 16A). Under control condition, around 90% cells showed that FMNL2 predominantly localized on the plasma membrane and also distributed in the cytoplasm but not homogeneously. When RhoC was silenced with siRNA or inhibited by C3 transferase, only about 30% of cells showed proper plasma membrane localization of FMNL2. Western blot was shown to verify the knockdown efficiency of RhoC (Figure 16A). To functionally explore the role of RhoC on FMNL2 actin assembly activity, MAL/SRF luciferase reporter assay was performed (Copeland and Treisman, 2002; Grosse et al., 2003). Expression of autoinhibited FMNL2 or mDia1 full length proteins showed no activity as control (Figure 16B). Autoinhibition was released when constitutively active RhoC V14 was co-expressed with FMNL2, while constitutively active RhoA V14 did not induce FMNL2 activity. This implicates that active RhoC regulates FMNL2 activity on actin dynamics. In contrast, mDia1 was activated to the same extend by both RhoC V14 and RhoA V14, suggesting that mDia1 is modulated by both Rho GTPases as previously reported (Rose et al., 2005; Watanabe et al., 1999).

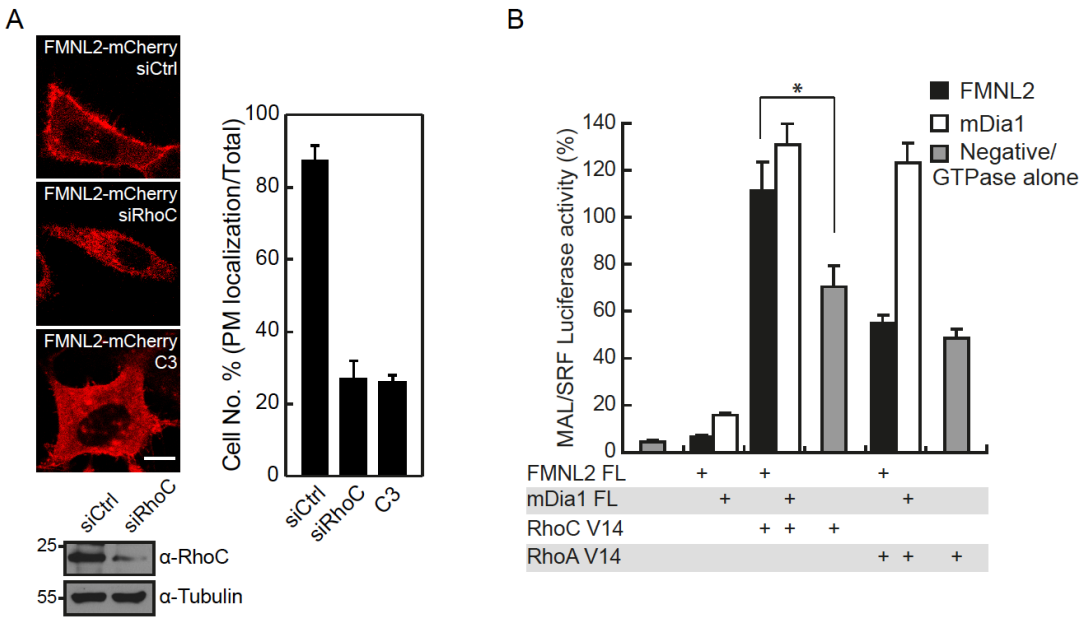

Figure 16. RhoC regulates the localization and activity of FMNL2. A. FMNL2-mCherry and siCtrl, siRhoC or C3 were co-expressed in HeLa cells. Knockdown of RhoC is shown. Cells expressing FMNL2-mCherry with plasma membrane localization were quantified over the total cell number counted. Scale bar, 10 µm. Error bar, + s.e.m. (n=3). **B.** HEK293 cells expressing full length FMNL2 or mDia1 together with RhoC V14 or RhoA V14 as indicated, MAL/SRF reporter

3DA.Luc and Renilla luciferase pRLTK. SRF activity was measured 24 h after transfection. Error bar: + s.e.m. (n=3), $p<0.05$.

4.2 FMNL2 is phosphorylated by PKC and the phosphorylation is enhanced by RhoC

4.2.1 FMNL2 is phosphorylated by PKC

Although autoinhibition of FMNL2 depends on the DID-DAD interaction (Vaillant et al., 2008), a previous study showed that inhibition of C-terminal activity of FMNL2 required higher concentration of N-terminus (Kitzing et al., 2010). It was reported that the formin FHOD1 could be activated through phosphorylation by ROCK (Hannemann et al., 2008; Takeya et al., 2008). The DAD domain of FHOD1 is composed of the core motif and its C-terminal flanking region is abundant in basic residues (Takeya et al., 2008). Similarly the flanking sequence of FMNL2 DAD core region is also abundant in basic residues. There is a conserved Ser residue (S1072) which resides in the basic region indicating that it might be a target of kinases (Figure 17A). However, the R/KR/KXS/THydR/K (X stands for any residue, Hyd stands for hydrophobic residue, R: Arg, K: Lys, S: Ser, T: Thr) motif is the substrate sequence motif of classical PKC (Nishikawa et al., 1997). In the flanking polybasic region of FMNL2 DAD core, the RRSVR motif resembles the sequence motif of cPKC substrate (Figure 17A). Therefore, FMNL2 or mDia1 was overexpressed in cells and treated with either DMSO, the PKC activator 12-O-tetradecanoylphorbol-13-acetate (TPA) or the PKC inhibitor bisindolylmaleimide I (BIM I). MAL/SRF reporter assay showed that both FMNL2 and mDia1 under control conditions were autoinhibited formins that showed low activity on actin assembly. In contrast, under TPA treatment, FMNL2 exhibited a robust activity while mDia1 did not. When PKC activity was inhibited by BIM I, both FMNL2 and mDia1 kept inactive in spite of the presence of TPA (Figure 17B). Albeit phoborl esters were known to be unspecific, the reporter assay implicated that PKC might play a role in regulating FMNL2 but not mDia1 activity through phosphorylation. To further investigate the possible phosphorylation of FMNL2 by PKC, a point mutation of the Ser residue into Ala (S1072A) to destroy the phosphorylation was introduced to full length FMNL2. FMNL2

and the S1072A mutant were transiently expressed in cells and immunoprecipitated. A commercially available antibody, which identifies phospho-Ser PKC substrates, was used to detect whether FMNL2 was phosphorylated by PKC. Wild type FMNL2 could be phosphorylated with a strong increase under TPA treatment. Importantly, phosphorylation was diminished under BIM I treatment. The mutant S1072A could not be detected by the phospho-Ser PKC substrate antibody in all treatments, while mDia1 as a control showed no phosphorylation (Figure 17C).

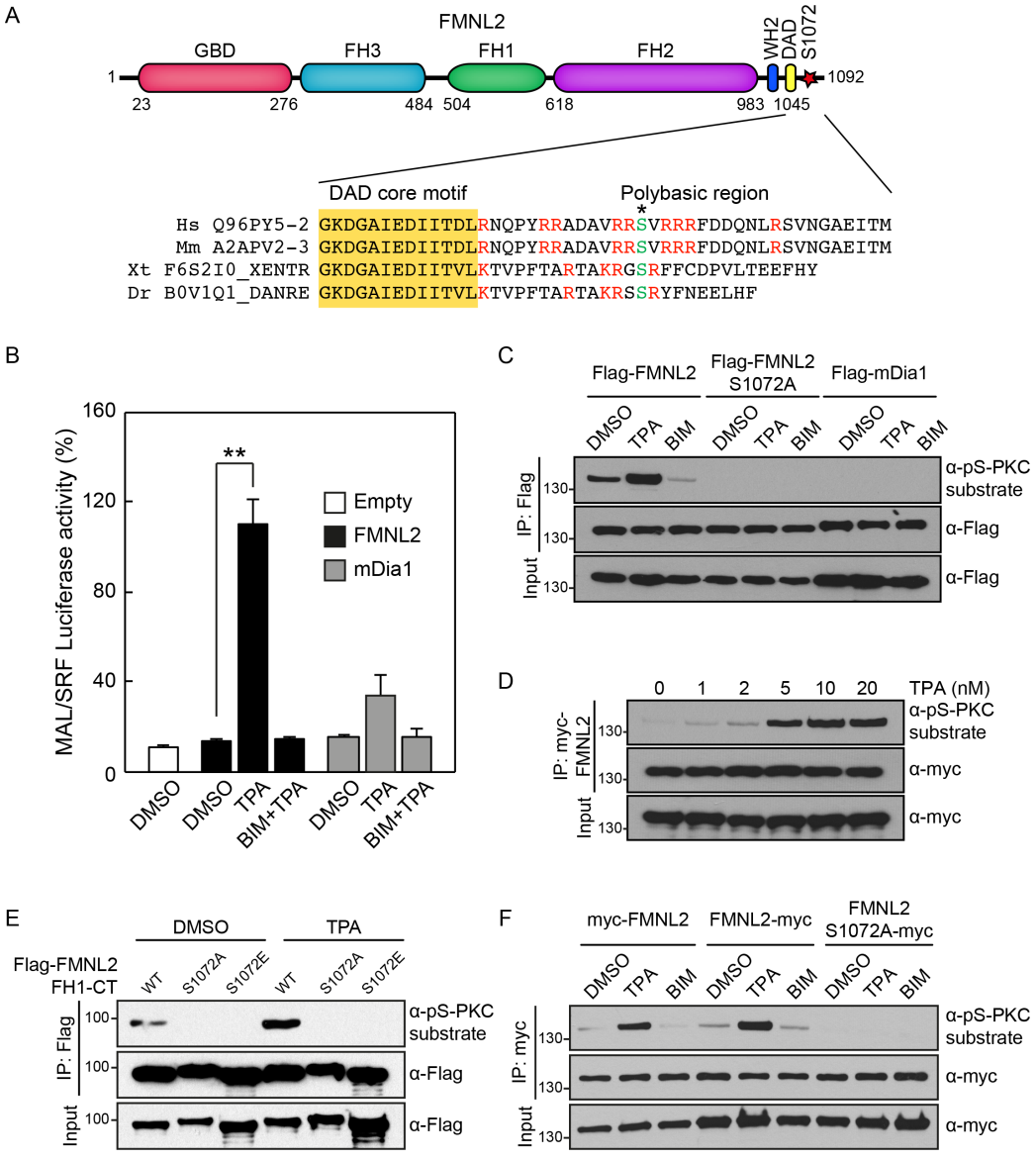

Figure 17. FMNL2 is phosphorylated by PKC at the residue Ser 1072. A. Schematic representation of FMNL2 protein and the amino acid sequences from different species are shown

for the DAD to C terminus regions. Hs: *Homo sapiens*; Mm: *Mus musculus*; Xt: *Xenopus tropicalis*; Dr: *Danio rerio*. Protein IDs from UniProt are listed. Yellow shadow shows the DAD domain. Basic residues are shown in red. The conserved Ser (S1072 in human) is labeled with asterisk and shown in green. Numbers indicate the residue boundaries of the domains. **B.** HEK293 cells expressing full length FMNL2 or mDia1 as indicated, together with MAL/SRF reporter 3DA.Luc and Renilla luciferase pRLTK. DMSO, 20 nM TPA or 2 μM BIM I + 200 nM TPA was incubated with the cells for 6 h. SRF activity was measured 24 h after transfection. Error bar: + s.e.m. (n=3), $p<0.001$. **C.** Flag-FMNL2, the phospho-deficient mutant Flag-FMNL2-S1072A or Flag-mDia1 was expressed in HEK293 cells and immunoprecipitated after DMSO, TPA (20 nM) or BIM I (2 μM) treatments for 30 min. An antibody specifically recognizing phospho-Ser PKC substrate (α-pS-PKC substrate) was used to detect the phosphorylated proteins. **D.** Titration of TPA stimulated FMNL2 phosphorylation by PKC. The amount of TPA (nM) used in cell treatments is indicated. myc-FMNL2 was immunoprecipitated after 0 - 20 nM TPA treatments for 30 min. Phosphorylated FMNL2 was detected by α-pS-PKC substrate. **E.** Flag-FMNL2-FH1-CT (WT), Flag-FMNL2-FH1-CT-S1072A (S1072A) or Flag-FMNL2-FH1-CT-S1072E (S1072E) was immunoprecipitated after DMSO or TPA (20 nM) treatments for 30 min. Phosphorylated FMNL2 was detected by α-pS-PKC substrate. **F.** myc-FMNL2, FMNL2-myc or FMNL2-S1072A-myc was immunoprecipitated after DMSO, TPA (20 nM) or BIM I treatments for 30 min. Phosphorylated FMNL2 was detected by α-pS-PKC substrate. Numbers indicate molecular weight (kD).

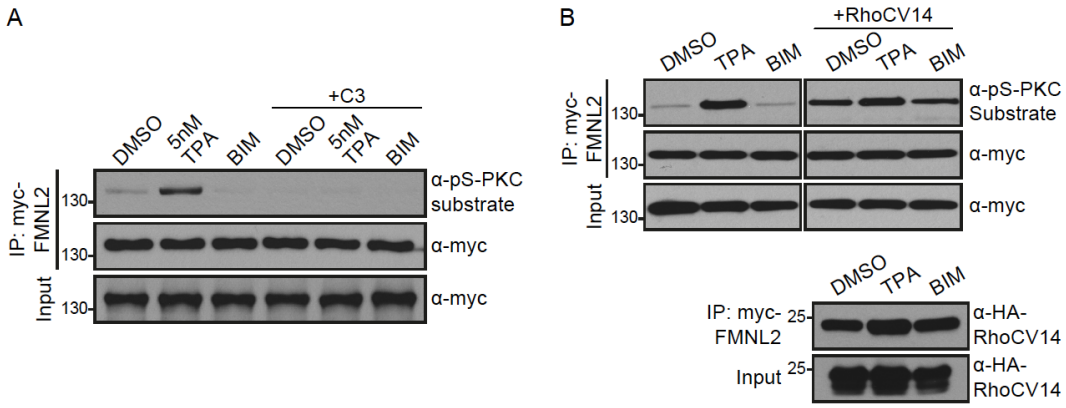

Figure 18. Phosphorylation of FMNL2 by PKC is enhanced by RhoC. A. FMNL2 was co-expressed with or without C3 co-enzyme in HEK293 cells. myc-FMNL2 was immunoprecipitated after DMSO, TPA (5 nM) or BIM I (2 μM) treatments for 30 min. Phosphorylated FMNL2 was detected by phospho-Ser PKC substrate antibody. **B.** FMNL2 and HA-RhoCV14 were expressed.

myc-FMNL2 was immunoprecipitated after DMSO, TPA (20 nM) or BIM I (2 μM) treatments for 30 min. Phosphorylated FMNL2 and bound HA-RhoCV14 were detected. Numbers indicate molecular weight (kD).

Moreover, FMNL2 phosphorylation could be induced in a dosage-dependent manner by TPA, and 5 nM was sufficient to show a distinguishing band in the immunoprecipitation (Figure 17D). A phospho-mimetic mutation was also introduced into FMNL2-FH1-CT (Ser 1072 mutated into Glu, S1072E) apart from the phospho-deficient mutantion S1072A. The wild type C-terminal half of FMNL2 was also phosphorylated while both S1072A and S1072E mutations in the C-terminal half were not (Figure 17E). It was reported that FMNL2 was N-myristoylated and this modification could localize FMNL2 to the lamellipodia protrusions. N-terminal fusion of an epitope to FMNL2 would disrupt the co-translational myristoylation and the subcellular localization (Block et al., 2012). However, both N- and C- terminal tagged FMNL2 could be phosphorylated as shown in Figure 17F, suggesting that the epitope fusion did not affect the detection of phosphorylation.

4.2.2 Phosphorylation of FMNL2 by PKC is enhanced by RhoC

Since FMNL2 was previously shown to be a RhoC effector (Figure 16), I assessed whether RhoC influences FMNL2 phosphorylation by PKC. First, C3 transferase was co-expressed with FMNL2 and treated with DMSO, TPA or BIM I. Although 5 nM TPA was sufficient to induce phosphorylation of FMNL2 by PKC, no phosphorylation could be detected in the presence of C3 (Figure 18A) implying a role of Rho GTPase in the proper phosphorylation of FMNL2 by PKC. When constitutively active RhoC V14 was co-expressed with FMNL2, it was intriguing to see that phosphorylation was significantly enhanced even under an inhibitory condition of BIM I treatment (Figure 18B). Interestingly, in the immunoprecipitation, RhoC V14 was shown to interact with full length FMNL2 (Figure 18B), recapitulating the previous finding that FMNL2 specifically interacts with RhoC (Kitzing et al., 2010). In conlusion, FMNL2 harbors a phosphorylation site, Ser 1072, which can be phosphorylated by PKC but not ROCK. This phosphorylation is enhanced in the presence of RhoC probably due to the roles of

RhoC in releasing the autoinhibitory conformation of FMNL2 and localizing FMNL2 to the plasma membrane or possibly other membrane structures of the cells.

4.3 FMNL2 is specifically phosphorylated by PKCα in cells

The protein kinase C family is composed of ten highly homologous isozymes, which can be classified into three groups: classical PKCs (cPKCs: PKCα, PKCβI, PKCβII, PKCγ), novel PKCs (nPKCs: PKCδ, PKCε, PKCη, PKCθ) and atypical PKCs (aPKCs: PKCζ, PKCλ/ι). Individual PKC isozymes have distinct roles in proliferation, apoptosis, cell survival and migration in a cell-type dependent manner (Griner and Kazanietz, 2007). In order to find out which isozyme is able to phosphorylate FMNL2, *in vitro* kinase assays were performed. Both wild type and S1072A mutant peptides ranging from the DAD domain to the C-terminus of FMNL2 (aa 959-1092) were subjected to the kinase reactions. Among the ten human PKC isozymes, PKCα, PKCβI, PKCβII, PKCδ and PKCε could phosphorylate FMNL2 *in vitro* whereas none of the PKCs could phosphorylate the S1072A mutant (Figure 19A). When incubated with the kinase inhibitor staurosporine, wild type peptide was not phosphorylated by PKCα (Figure 19A). It is known that PKC substrate specificity is less specific *in vitro* than *in vivo*. Therefore immunoprecipitations were conducted to uncover the specificity between the kinase and the substrate. PKCα, PKCβ, PKCδ and PKCε which showed activity toward FMNL2 peptide *in vitro*, along with PKCζ as a control, were silenced respectively in cells overexpressing FMNL2. Only when PKCα was silenced in cells, the phosphorylation level of FMNL2 was dramatically reduced (Figure 19B) implicating that FMNL2 is specifically a substrate of PKCα.

Gö6976, which specifically inhibits PKCα and PKCβI, was then used. Gö6976 reduced the phosphorylation of FMNL2 to the same extent as BIM I (Figure 20A). To test whether FMNL2 associates with PKCα, immunoprecipitations were performed under DMSO, TPA or BIM I treatments. When cells were treated with BIM I, a stronger interaction between FMNL2 and PKCα was detected (Figure 20B). Importantly, the dominant-negative form of PKCα inhibited FMNL2 phosphorylation as well as BIM I, while the wild type and constitutively active form of PKCα could increase the

phosphorylation the same as the TPA treatment (Figure 20C). Moreover, endogenous FMNL2 was immunoprecipitated from cells treated with BIM I or TPA. Phosphorylation of the endogenous FMNL2 could be detected when induced by TPA, suggesting that phosphorylation of FMNL2 by PKCα happens under physiological conditions (Figure 20D). Taken together, FMNL2 is phosphorylated by PKCα, both *in vitro* and *in vivo*. PKCα associates with FMNL2 and the phosphorylation of FMNL2 is inhibited when PKCα is inactive.

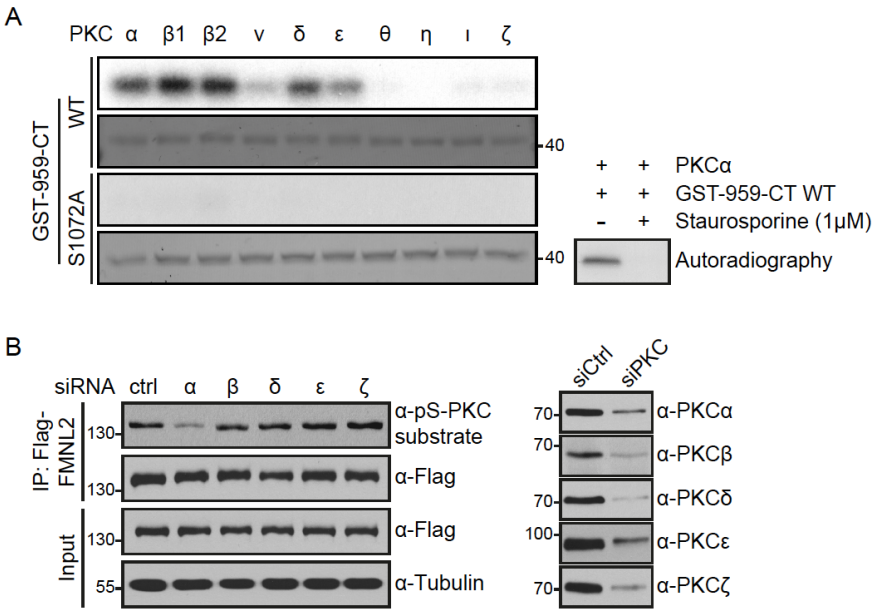

Figure 19. FMNL2 is specifically phosphorylated by PKCα in cells. A. *In vitro* kinase assays were performed using purified PKC isozymes and wild type (WT) or S1072A mutant FMNL2 C terminal fragments (GST-959-CT) as indicated. Autoradiography and coomassie blue stained gels are shown. 1 μM kinase inhibitor staurosporine was used when indicated. **B.** HEK293 cells were transfected with Flag-FMNL2 and siRNA against different PKC isoforms respectively. siPKCβ recognizes both PKCβI and PKCβII. Left: Flag-FMNL2 was immunoprecipitated and phosphorylated FMNL2 was detected by phospho-Ser PKC substrate antibody. Right: knockdown of different PKC isoforms are shown. Numbers indicate molecular weight (kD).

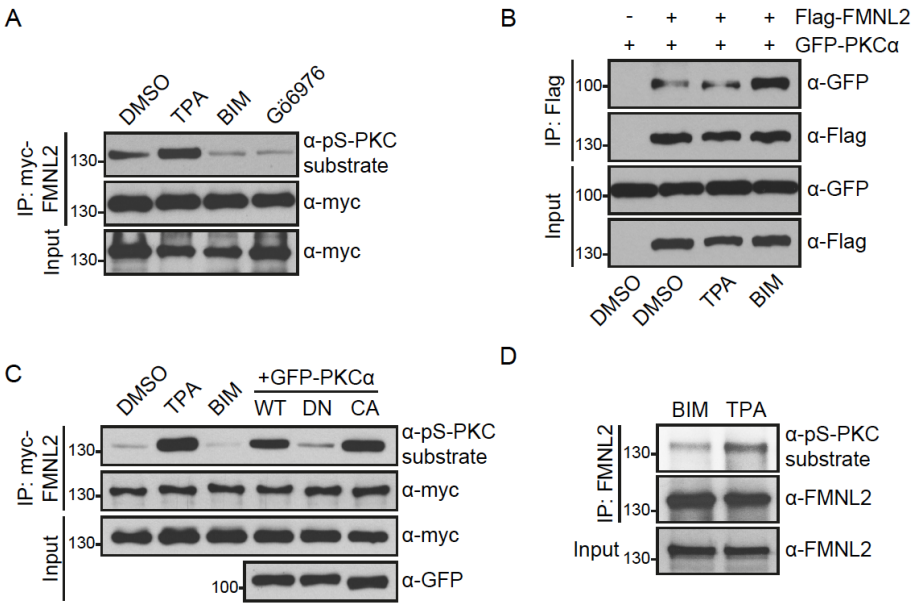

Figure 20. FMNL2 phosphorylation depends on PKCα activity. A. HEK293 cells expressing myc-FMNL2 were immunoprecipitated after DMSO, 20 nM TPA, 2 µM BIM treatment or 1 µM Gö6976 treatment. Phosphorylation was detected by phospho-Ser PKC substrate antibody. **B.** Immunoprecipitations of HEK293 cells expressing Flag-FMNL2 and GFP-PKCα after DMSO, 20 nM TPA or 2 µM BIM treatments. Bound GFP-PKCα was detected by Western blotting. **C.** myc-FMNL2 was immunoprecipitated in the presence or absence of GFP-PKCα wild type (WT), dominant-negative (DN) or constitutively active (CA). DMSO, 20 nM TPA or 2 µM BIM was added when indicated. Phosphorylation was detected. **D.** HeLa cells were treated with 2 µM BIM or 20 nM TPA for 30 min and immunoprecipitated with FMNL2 antibody. Endogenously phosphorylated FMNL2 was detected by phospho-Ser PKC substrate antibody. Numbers indicate molecular weight (kD).

4.4 FMNL2 is internalized upon PKCα activation

4.4.1 FMNL2 is internalized upon PKCα activation by TPA

Classical PKCs and nPKCs, both containing a regulatory C1 domain with diacylglycerol (DAG) binding ability, are known to be translocated from the cytosol to membrane fractions when activated by DAG or phorbol esters (Kraft et al., 1982; Mochly-Rosen et al., 2012; Sakai et al., 1997). Only the fully translocated and activated PKCs have kinase activity towards the substrates. Since FMNL2 shows prominent plasma membrane

localization and is proved to be a substrate of PKCα, it is important to image the changes of FMNL2 and PKCα localization upon PKCα activation in living cells. Therefore, FMNL2-mCherry and GFP-PKCα were transiently expressed in HeLa cells. FMNL2 showed intense fluorescence on the plasma membrane and some vesicular structures in the cytoplasm, while PKCα was homogenously distributing in the cytoplasm when inactive. Upon addition of TPA, PKCα rapidly translocated from the cytoplasm to the plasma membrane within 300 s. FMNL2 gradually disappeared from the cortical plasma membrane and appeared in the intracellular vesicular structures (Figure 21A). Changes of fluorescence intensity on the plasma membrane were quantified for both FMNL2 and PKCα. The fluorescence intensity of PKCα on the plasma membrane increased upon activation by TPA until it reached a peak at around 300 s. Concomitantly, FMNL2 was internalized and the plasma membrane fluorescence intensity dropped (Figure 21A).

BIM I inhibitor was then used to test whether internalization of FMNL2 is a consequence of PKCα activation. Cells were pre-incubated with BIM I inhibitor for 30 min and imaging acquisition was started immediately after TPA was added. Translocation of PKCα happened similar to that of TPA treatment only (Figure 21B). BIM I is an ATP-competitive inhibitor which binds the kinase domain (Grodsky et al., 2006), while TPA binds the regulatory domain (Steinberg, 2008). Hence, although PKCα was translocated, it could not phosphorylate the substrates for its ATP binding site was occupied by BIM I. Thus FMNL2 was not phosphorylated. The observation that FMNL2 kept the plasma membrane localization throughout the experiment suggests that FMNL2 internalization depends on PKCα activity (Figure 21B). Quantification confirmed that although PKCα translocated, FMNL2 exhibited no change of fluorescence intensity on the plasma membrane (Figure 21B). Of note, the vesicular-like structures in cells treated with BIM I came from the fluorescent signals of the BIM I compound.

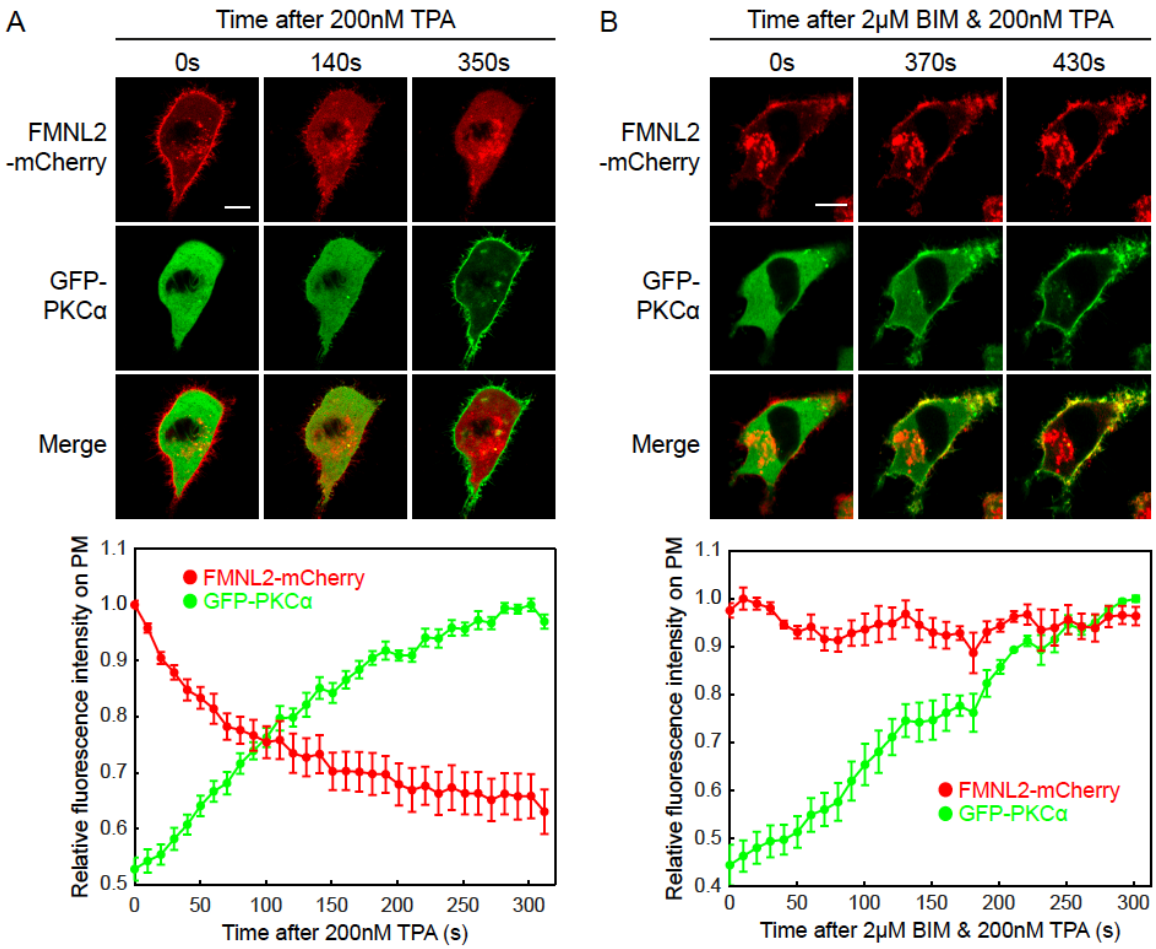

Figure 21. FMNL2 changes localization from the plasma membrane to intracellular membrane structures upon PKCα activation by TPA. A. Upper: HeLa cells expressing FMNL2-mCherry and GFP-PKCα were imaged immediately after applying 200 nM TPA. Representative frames are shown at indicated time points. Lower: Quantification of fluorescence intensity changes on the plasma membrane for both the red and the green channel. Photo bleaching was corrected. Red: mCherry; Green: GFP. Scale bar: 10 μm. Error bar, +/- s.e.m of 11 cells. **B.** Upper: HeLa cells expressing FMNL2-mCherry and GFP-PKCα were pre-treated with 2 μM BIM for 30min. Images were acquired immediately after applying 200 nM TPA. Representative frames are shown at indicated time points. Lower: Quantification of fluorescence intensity changes on the plasma membrane. Photo bleaching was corrected. Scale bar: 10 μm. Error bar, +/- s.e.m of 4 cells.

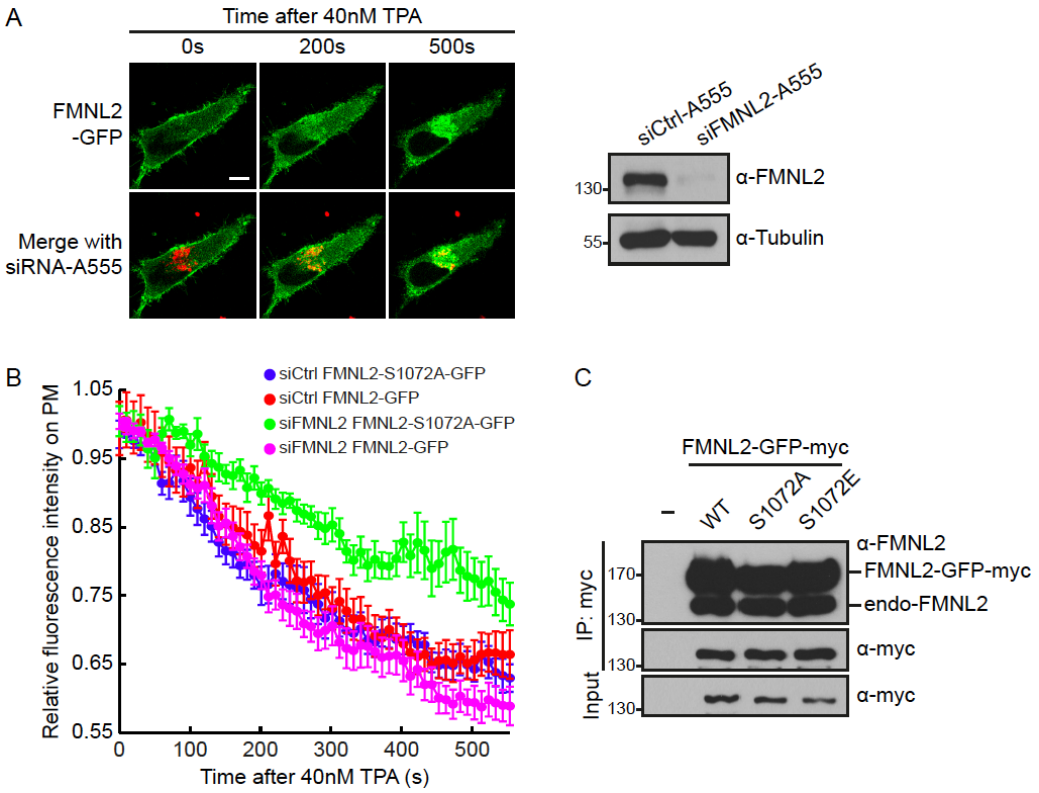

Figure 22. Ser 1072 affects FMNL2 internalization rate. A. HeLa cells were transfected with control siRNA or FMNL2 siRNA labeled with AlexaFluor 555. siFMNL2 targeting 3'-UTR allowed FMNL2 wild type (FMNL2-GFP) or mutant (FMNL2-S1072A-GFP) DNA expression in the same cell. Left: Representative frames upon addition of 40 nM TPA are shown at indicated time points. Green: GFP; Red: AlexaFuor 555. Scale bar: 10 µm. Right: Western blots show knockdown of FMNL2. **B.** Quantification of fluorescence intensity changes on the plasma membrane when FMNL2-GFP or FMNL2-S1072A-GFP was expressed in control siRNA or FMNL2 siRNA transfected cells upon addition of 40 nM TPA. Photo bleaching was corrected. Error bar, +/- s.e.m of 7 (blue), 11 (red), 8 (green) and 9 (purple) cells respectively. **C.** FMNL2-GFP-myc wild type, S1072A, or S1072E were expressed in HEK293 cells and immunoprecipitated. Endogenous and ectopic FMNL2 were detected by FMNL2 antibodies. Numbers indicate molecular weight (kD).

Next, I examined whether the phospho-deficient mutant of FMNL2 (S1072A) could be internalized upon TPA stimulation. FMNL2-S1072A-mCherry displayed the same internalization pattern as wild type FMNL2 (data not shown). Since formins function as dimers and FMNL2 was reported to form homodimers (Vaillant et al., 2008), endogenous

FMNL2 was silenced with fluorescently labeled siRNA (siFMNL2-AlexaFluor 555) targeting 3'-UTR of FMNL2 gene, allowing for expression of exogenous FMNL2 proteins. Upon TPA stimulation, both FMNL2-GFP and FMNL2-S1072A-GFP could be internalized in control siRNA transfected cells (Figure 22 A and B). FMNL2-GFP in FMNL2 siRNA transfected cells exhibited a decrease of fluorescence intensity on the plasma membrane the same as in the control siRNA condition. However, FMNL2-S1072A-GFP in FMNL2 siRNA transfected cells showed a significantly slower internalization rate (Figure 22B). The difficulty to capture the discrepancy between the wild type and mutant proteins might come from the fact that the ectopic FMNL2 dimerizes with the endogenous FMNL2. Indeed, when the overexpressed FMNL2 wild type or mutant was immunoprecipitated, endogenous FMNL2 could be detected (Figure 22C). Therefore, the Ser 1072 residue contributes to FMNL2 internalization upon PKCα activation.

4.4.2 FMNL2 internalization is reversible

PKC activation by DAG in cells is transient, while activation by TPA is permanent and irreversible (Griner and Kazanietz, 2007). Whether FMNL2 internalization is reversible like the PKC translocation is the next question to explore. The translocation of PKCγ induced by calcium was rapid and reversible when the cells were treated with the calcium ionophore A23187 (Sakai et al., 1997). Therefore, A23187 was tested with FMNL2 and PKCα. Upon addition of 8 μM A23187, PKCα translocated within 20 s and completed at 75 s, while FMNL2 internalization followed. After 75 s, PKCα gradually translocated back from the plasma membrane to the cytoplasm probably due to the decrease of the intracellular calcium concentration. At 150 s, PKCα was completely cytoplasmic again, indicating the deactivation of the kinase. As a consequence, at 150 s, FMNL2 started to return to the plasma membrane, further suggesting that FMNL2 internalization is reversible and dependent on PKC activity (Figure 23A).

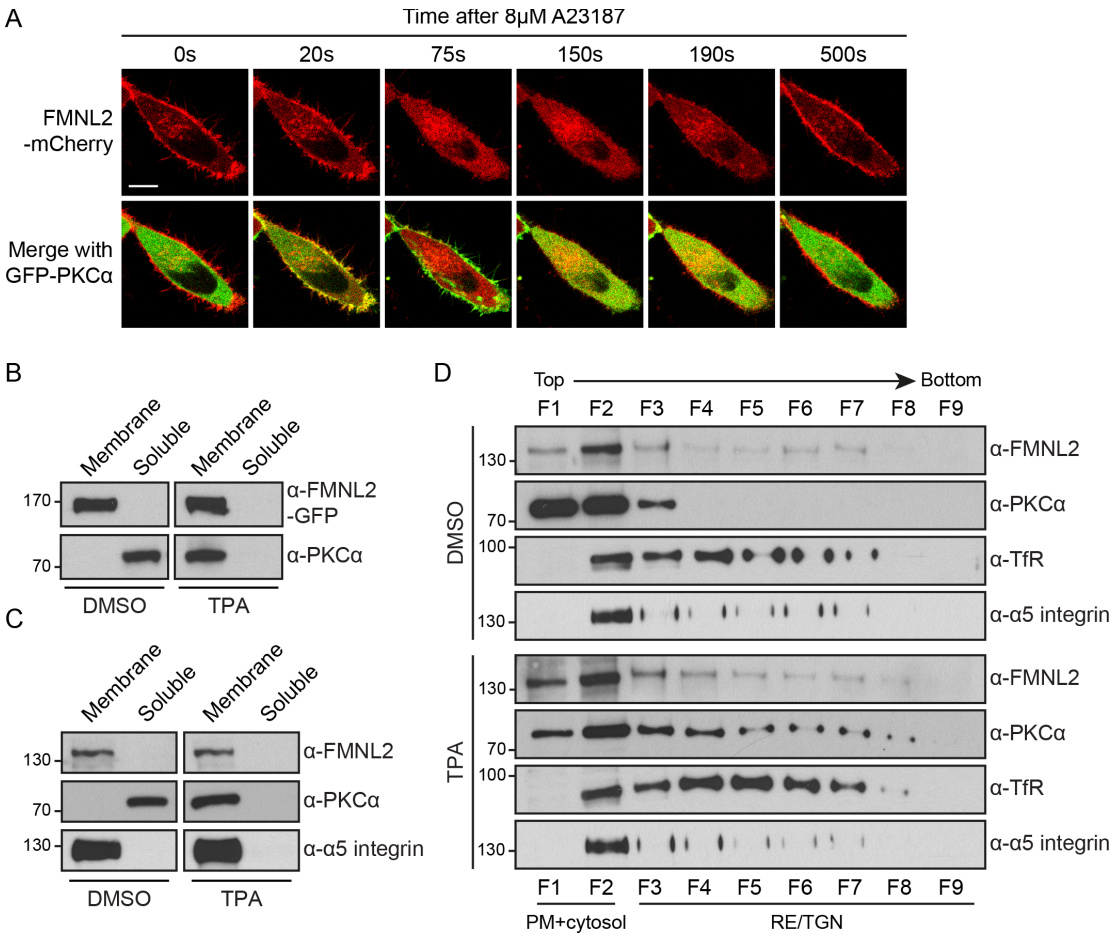

Figure 23. FMNL2 internalization is reversible and it localizes to the membrane structures throughout the process. A. HeLa cells expressing FMNL2-mCherry and GFP-PKCα were imaged immediately after applying 8 μM calcium ionophore A23187. Representative images are shown at indicated time points. Scale bar: 10 μm. **B.** HEK293 cells over expressing FMNL2-GFP were fractionated by membrane flotation assays with or without 200 nM TPA treatment for 30 min. Membrane and soluble fractions were analyzed by Western blotting using different antibodies as indicated. **C.** HeLa cells were fractionated by membrane flotation assay with or without 200 nM TPA treatment for 30 min. Membrane and soluble fractions were analyzed by Western blotting using different antibodies as indicated. Numbers indicate molecular weight (kD). **D.** HeLa cells were fractionated using discontinuous sucrose density gradient centrifugation with or without 200 nM TPA treatment for 30 min. All the fractions (F1 ~ F9) were analyzed by Western blotting using different antibodies as indicated. TfR: transferrin receptor; PM: plasma membrane; RE: recycling endosome; TGN: trans-Golgi network.

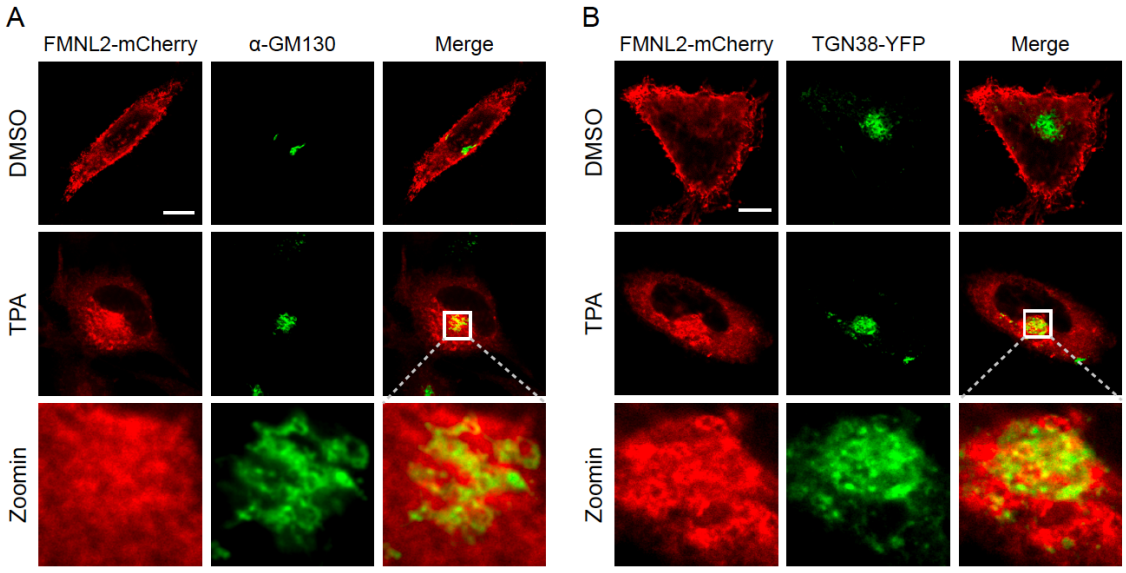

Figure 24. FMNL2 does not colocalize with Golgi network upon TPA. A. HeLa cells expressing FMNL2-mCherry (red) with or without 200 nM TPA for 10 min were stained for cis-Golgi marker GM130 (green). White square of the TPA treated cell is enlarged to show details. **B.** HeLa cells expressing FMNL2-mCherry (red) and TGN38-YFP (green) with or without 200 nM TPA are shown. TGN38 is trans-Golgi marker. White square of the TPA treated cell is enlarged to show details. Scale bar: 10 μm.

To further explore whether FMNL2 remains bound to the cellular membrane structures, membrane flotation assays were carried out. FMNL2-GFP was overexpressed and fractionated. As expected, PKCα as a soluble protein in the cytosol became membrane bound protein upon activation by TPA. However, FMNL2 remained as a membrane bound protein despite of the internalization observed, indicating that FMNL2 as a membrane bound protein is highly probably internalized via endocytic route. Endogenous FMNL2 behaved the same as overexpressed FMNL2 (Figure 23 B and C). To differentiate between individual cellular membrane systems, discontinuous sucrose density gradient was used to fractionate different membranes (Pan et al., 2012). Combining the membrane flotation results, FMNL2 primarily localized to the plasma membrane without TPA, while PKCα mainly localized in the cytoplasm. Transferrin receptor and α5 integrin distributed throughout the plasma membrane and recycling endosome membranes. When treated with TPA, PKCα translocated to membrane systems including the plasma membrane and Golgi membrane which was consistent with previous

reports (Goodnight et al., 1995; Griner and Kazanietz, 2007). However, FMNL2, transferrin receptor and α5 integrin did not show many changes upon TPA treatment, suggesting that within the time frame of the experiments FMNL2 did not go from the plasma membrane to the recycling endosomes or Golgi networks (Figure 23D). Meanwhile, immunostaining of FMNL2 and Golgi markers confirmed that FMNL2 did not colocalize with either cis- or trans-Golgi network before or after TPA treatment (Figure 24 A and B).

4.4.3 FMNL2 is internalized through endocytosis

To identify the dynamics of FMNL2 after TPA treatment, endogenous or overexpressing subcellular markers were used to test whether they colocalize with FMNL2. Early endosome marker EEA1 (early endosome antigen 1) did not colocalize with FMNL2 before or after TPA treatment (Figure 25A). When cells were loaded with fluorescently labeled transferrin showing the endocytic pathway from early endosomes to recycling endosomes, FMNL2 did not colocalize with transferrin (Figure 25B). However, in some of the cells, FMNL2 colocalized with the endosome markers Rab4, Rab5 and Rab7 to different extents after TPA treatment (Figure 25C). FMNL2 accumulated in the region where Lamp1 (lysosomal-associated membrane protein 1) localized after addition of TPA, but did not exhibit any distinct structure which resembled Lamp1 (Figure 25D). Finally, constitutively active RhoC V14 was co-expressed with FMNL2. Without TPA treatment, RhoC V14 localized to the plasma membrane and intracellular membrane compartments. FMNL2 colocalized with RhoC V14 at the plasma membrane. Upon TPA treatment, FMNL2 was internalized and it colocalized with RhoC V14 on the intracellular membrane compartments (Figure 25E) confirming the RhoC-FMNL2 interaction.

In summary, FMNL2 follows an internalization route when PKCα is translocated and activated. Due to the dimerization with endogenous FMNL2, phospho-deficient mutant FMNL2-S1072A is internalized at a slower rate only when endogenous FMNL2 level is reduced, suggesting that the Ser residue plays a role in the kinetic process. Moreover, FMNL2 internalization is reversible. Deactivation of PKCα leads to the returning of FMNL2 to the plasma membrane. FMNL2 always associates with cell membrane

structures, but not with Golgi network, EEA1 or transferrin. However, in some cells, FMNL2 partially colocalizes with the ectopically expressed endosome markers Rab4, Rab5 and Rab7 indicating that FMNL2 might follow the endocytic pathway to be internalized.

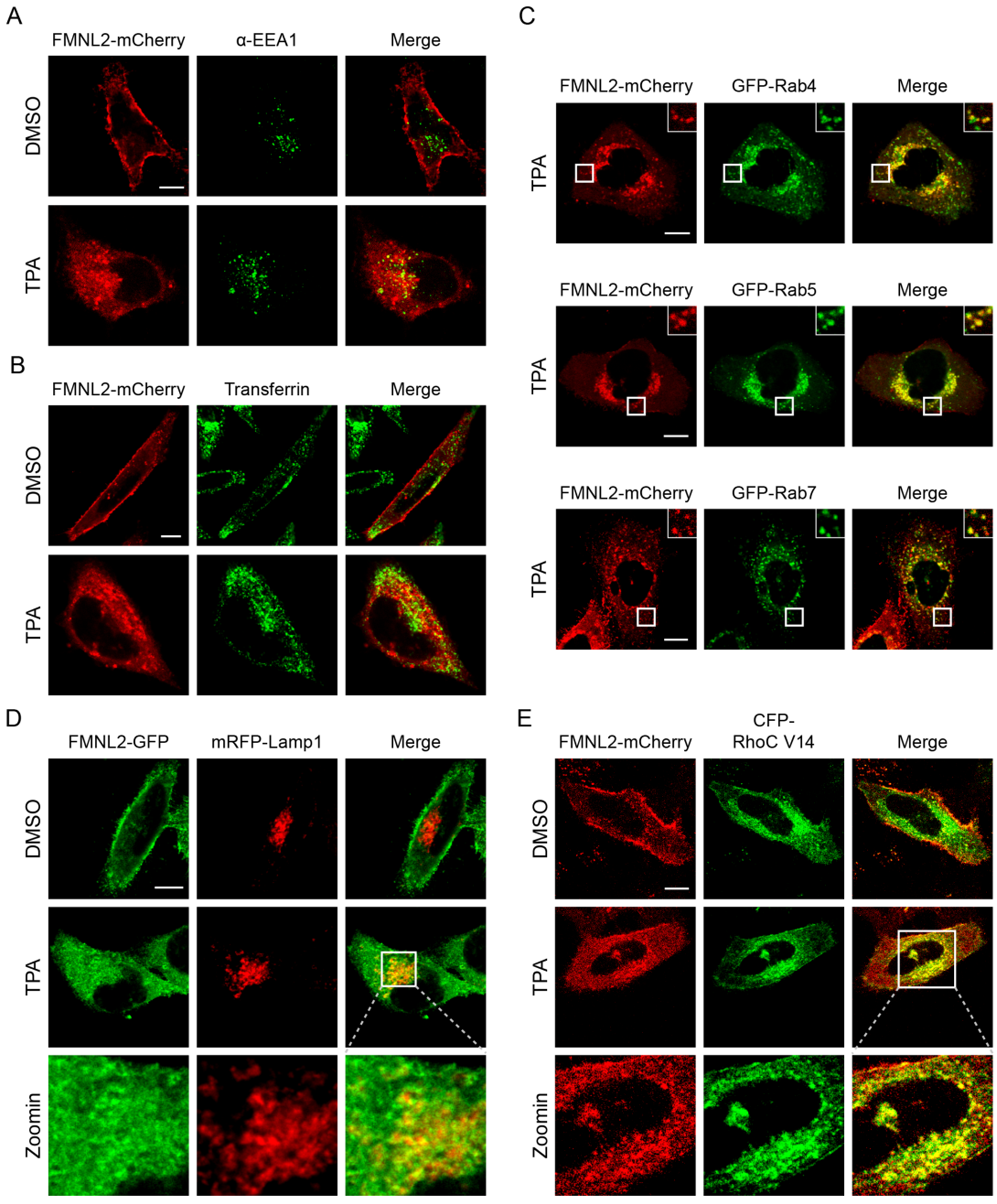

Figure 25. FMNL2 is internalized to intracellular membrane structures upon TPA. A. Representative images of FMNL2-mCherry (red) and EEA1 (green) in HeLa cells. **B.**

Representative images of FMNL2-mCherry (red) and transferrin (green) in HeLa cells. Fluorescently labeled transferrin were uptaken by HeLa cells for 10 min. **C.** Representative images of FMNL2-mCherry (red) and GFP-Rabs (green) in HeLa cells. Inserts show details of the colocalization. **D.** Representative images of FMNL2-GFP (green) and Lamp1 (red) in HeLa cells. White square of the TPA treated cell is enlarged to show details. **E.** Representative images of FMNL2-mCherry (red) and CFP-RhoC V14 (green) in HeLa cells. White square of the TPA treated cell is enlarged to show details. TPA treatment: 200 nM, 10min. Scale bars: 10 μm.

4.5 FMNL2 is required for α5β1 integrin internalization

4.5.1 Knockdown of FMNL2 reduces β1 integrin internalization

A cell spot microarray screen (Arjonen et al., 2012; Rantala et al., 2011) of genes regulating β1 integrin endocytosis was conducted by Arjonen et al. of Turku Centre for Biotechnology, Finland, which revealed that among all the formins except for INF1, silencing of FMNL2 led to a dramatic decrease in β1 integrin endocytosis in both HeLa and MDA-MB-231 cells (Arjonen et al., unpublished data). Thereby, HeLa cell lines stably expressing shFMNL2 or control shRNA were made with nice reduction of endogenous FMNL2 (Figure 26A). Pouwels et al. of Turku Centre for Biotechnology, performed biotin-IP based β1 integrin endocytosis assay with the stable cell line and validated that loss of FMNL2 in cells led to a significant decrease of β1 integrin endocytosis at 15, 20 or 30 min time points (Figure 26A). To test whether FMNL2 interacts with integrin cytoplasmic tail like other integrin interacting partners, biotin-strepdavidin pull down assays were performed. Biotinylated cytoplasmic tail of α5 but not β1 integrin could interact with FMNL2 (Figure 26B). Since α5β1 integrin was known to function as heterodimers, cell surface levels of α5 or α5β1 integrin were measured with silenced FMNL2 in cells. Corresponding to the β1 integrin endocytosis results, loss of FMNL2 in HeLa cells led to an increased level of cell surface α5 or α5β1 integrin (Figure 26C). Thus, FMNL2 interacts with the α5 integrin cytoplasmic tail and is required for α5β1 integrin internalization.

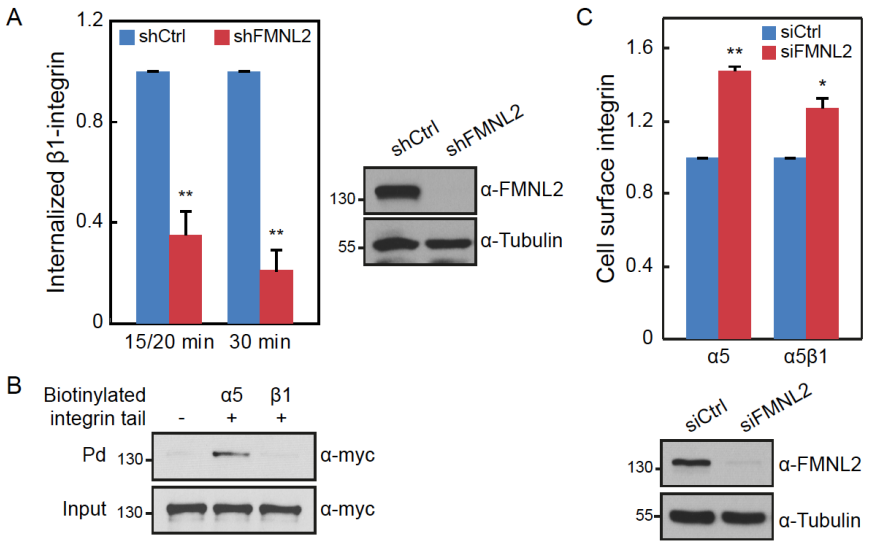

Figure 26. FMNL2 is required for α5β1 integrin internalization. A. Left: biotin-IP based β1 integrin internalization assays show silencing of FMNL2 leading to less internalized β1 integrin in HeLa cells stably expressing control or FMNL2 shRNA. Error bars: +s.e.m (n=3), $p<0.001$. Time points indicate the time of the internalization. Right: Western blotting showing the knockdown efficiency of the stable cell line. **B.** Biotin-strepdavidin pull down (Pd) of integrin cytoplasmic tails and FMNL2-myc from HEK293 cell extracts. **C.** Upper: Flow cytometry measurements of cell surface α5 or α5β1 integrin level while silencing FMNL2 in HeLa cells. Error bars: +s.e.m (n=3), two stars: $p<0.001$, one star: $p<0.05$. Lower: Western blotting showing the knockdown efficiency. Numbers next to Western blots indicate the molecular weight of molecules.

4.5.2 FMNL2 localizes to α5 integrin positive vesicles

To further confirm that FMNL2 and α5 integrin interact in cells, immunoprecipitation was carried out. Indeed, α5 integrin could be detected when FMNL2 was immunoprecipitated from HEK293 cells transiently expressing both proteins (Figure 27A). However, when α5 integrin and FMNL2 were co-expressed in HeLa cells, FMNL2 was found mainly on plasma membrane while α5 integrin localized on plasma membrane, intracellular membrane compartments and vesicular structures (Figure 27A). It was previously reported that stimulation of PKCα activity induced β1 integrin internalization (Ng et al., 1999). FMNL2 was found to be internalized and it interacted with α5 integrin. Thus, the effects of TPA on FMNL2 and α5 integrin were examined. Upon TPA

treatment, FMNL2 started to be internalized, co-trafficking with α5 integrin vesicles and finally accumulated in the perinuclear membrane compartments where α5 integrin was also present (Figure 27A). Moreover, FMNL2 also colocalized with endogenous α5 integrin (Figure 27B).

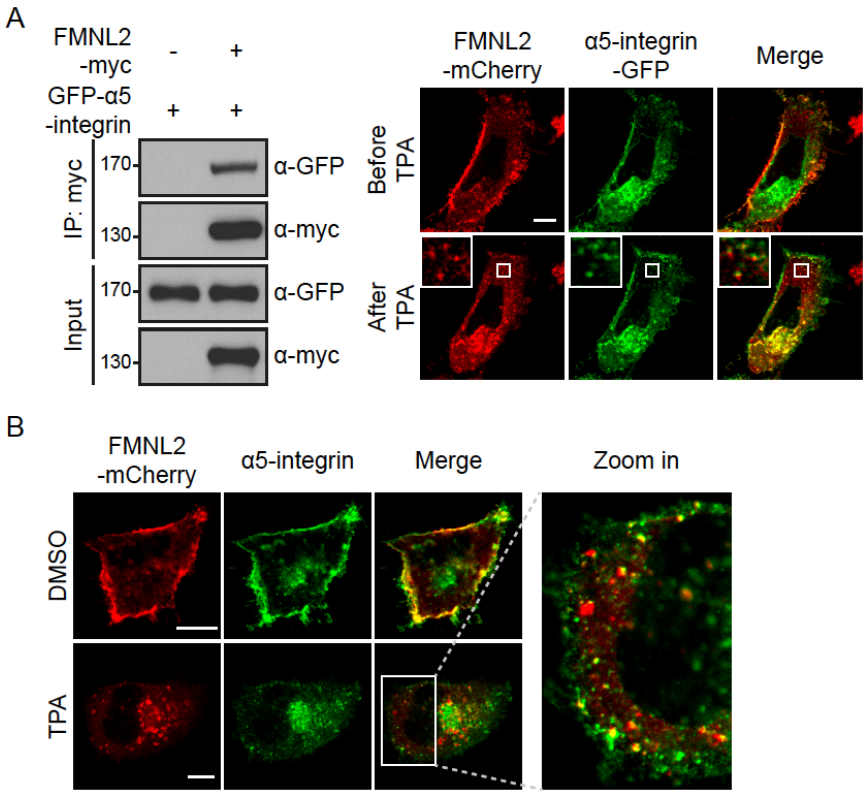

Figure 27. FMNL2 localizes on α5 integrin positive vesicles upon TPA treatment. A. Left: immunoprecipitation showing FMNL2 interacting with α5 integrin in cells. Numbers indicate the molecular weights. Right: FMNL2-mCherry and α5 integrin-GFP were expressed in HeLa cells and 200 nM TPA was applied to cells at timepoint zero. Representative images of the live cell imaging are shown here. White square of is zoomed in to show details. **B.** FMNL2-mCherry and endogenous α5 integrin localization with or without 200 nM TPA treatment for 10 min. White box of the TPA treated cell is enlarged to show details. Scale bars: 10 µm.

4.5.3 Effects of FMNL2 mutants on α5β1 integrin surface levels

To understand whether internalization of FMNL2 depends on its actin polymerization activity, mutations were made to disrupt FMNL2-actin interaction. It is known that an Ile residue in the FH2 domain is conserved among all formins and is essential for formins to bind barbed ends of actin filaments (Xu et al., 2004). In FMNL2, it is Ile 704 (I704). Thus I704 was mutated into Ala (I704A) in FMNL2. In addition, all the three FMNLs contain a WH2 domain between FH2 and DAD domains. In FMNL3, the C-terminal region containing the WH2 binds actin monomers and barbed ends (Heimsath and Higgs, 2012). Therefore, by comparing the WH2 domain sequences of FMNLs, INF2, WASP and WAVE2, the two conserved residues Leu 1028 and Ile 1029 which are important for actin binding were also mutated into Ala in FMNL2. In total, this actin binding-deficient FMNL2 mutant was named ILI3A (I704A, L1028A and I1029A. Figure 28 A and B). Indeed, ILI3A mutant showed no activity in MAL/SRF luciferase reporter assays and when co-expressed with wild type FMNL2, ILI3A behaved as a dominant-negative mutant that inhibited FMNL2 activity on actin assembly (Figure 28B).

To test whether the phospho-deficient, phospho-mimetic and actin binding-deficient mutants affect α5β1 integrin internalization, cell surface α5β1 integrin levels were measured in stable HeLa cell lines (Figure 28C). Silencing of FMNL2 led to a dramatic decrease in β1 integrin internalization and an increase in α5β1 integrin cell surface level (Figure 26 A and C). Expression of FMNL2 resulted in lower α5 or α5β1 integrin cell surface levels (Figure 28C). However, FMNL2-S1072A or FMNL2-S1072E expression in cells did not show any difference in comparison to the wild type. The actin binding-deficient mutant of FMNL2 (ILI3A) also led to lower α5 or α5β1 integrin levels on the cell surface the same as wild type. Moreover, combined mutations (ILIS4A or ILI3ASE) affecting FMNL2 phosphorylation (S1072A or S1072E) and actin binding (ILI3A) were generated. Their effects on the α5β1 integrin cell surface levels were also not altered (Figure 28C). The similar effects of wild type and mutant FMNL2 on α5β1 integrin surface levels could be due to the dimerization between the endogenous FMNL2 and the ectopic FMNL2.

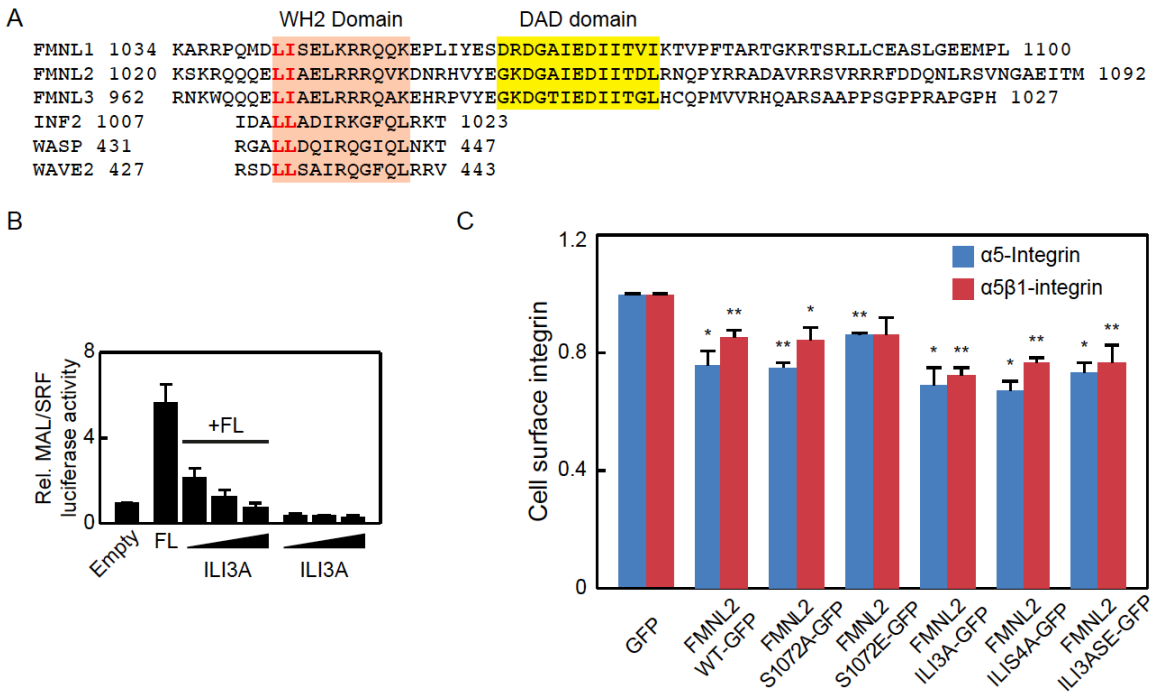

Figure 28. Effects of FMNL2 mutants on α5β1 integrin cell surface levels. A. The C-terminal sequences of FMNLs, INF2, WASP and WAVE2 showing the WH2 domains. Light orange shadow indicates the WH2 domain. Yellow shadow indicates the DAD domain. Numbers indicate the amino acids in the genes. Red letters show the conserved residues that are important for actin binding. Sequences are from UniProt. **B.** HEK293 cells expressing full length FMNL2-GFP (FL) or mutant as indicated, together with MAL/SRF reporter 3DA.Luc and Renilla luciferase pRLTK. Black triangle indicates the increasing amount of DNA transfected. SRF activity was measured 24 h after transfection. Error bar: + s.e.m. (n=3). **C.** Flow cytometry measurements of cell surface α5 or α5β1 integrin levels from stable HeLa cell lines as indicated. Error bars: +s.e.m (n=3), two stars: $p<0.001$, one star: $p<0.05$. Student t-tests were always performed between the control cells expressing GFP only and the cells expressing FMNL2 variants either for α5 or α5β1 integrin, respectively.

4.6. Release of FMNL2 autoinhibition by PKCα phosphorylation promotes rounded cell invasion in 3D

As shown in Figure 16B, autoinhibition of FMNL2 could be released by constitutively active RhoC V14. Whether phosphorylation of FMNL2 by PKCα plays a role in the autoregulation was then assessed with MAL/SRF luciferase reporter assay. N- or C-

terminal tagged FMNL2, FMNL2-S1072A and FMNL2-S1072E were expressed in cells. Wild type FMNL2 showed a bit higher activity compared to control, while FMNL2-S1072A behaved almost the same as the control. Interestingly, FMNL2-S1072E which mimics the phosphorylated version of FMNL2 exhibited a much higher activity compared to the other two (Figure 29 A and B). Moreover, FMNL2-FH3 which includes the DID domain interacted with FMNL2-FH1-CT which includes the DAD domain. The interaction was stronger in cells treated with DMSO or BIM I than in cells treated with TPA (Figure 29C). TPA induces FMNL2-FH1-CT phosphorylation on Ser 1072 by PKC (Figure 17E). The data suggest that phosphorylation of S1072 disrupts FMNL2 DID-DAD interaction and thus autoinhibition.

Knockdown of FMNL2 significantly reduced rounded cell invasion in transwell invasion assays using Matrigel (Kitzing et al., 2010). Amoeboid or rounded single cell invasion requires low integrin mediated adhesion and high Rho-mediated cortical actomyosin contractility (Hegerfeldt et al., 2002; Sanz-Moreno et al., 2008). As shown in Figure 26C, knockdown of FMNL2 led to an increased cell surface α5 or α5β1 integrin. To test the actomyosin contractility, phosphorylation of myosin II light chain (p-MLC) was examined (Olson and Sahai, 2008; Somlyo and Somlyo, 2000) in cells which FMNL2 was silenced. Reduced FMNL2 level led to reduced p-MLC, especially when cells were starved and stimulated with serum (Figure 29D), indicating a possible feedback loop among FMNL2-Rho GTPase-ROCK, similar to mDia1 (Kitzing et al., 2007). Similar phenomena were observed in both HeLa and MDA-MB-435 cells (data not shown for MDA-MB-435 cells). Furthermore, when FMNL2, FMNL2-S1072A or FMNL2-S1072E was stably expressed in A375M2 melanoma cells which employ round morphology during invasion (Sahai and Marshall, 2003), all induced cell invasion into 3D Matrigel but to different extents (Figure 29E). The phospho-mimetic mutant S1072E induced A375M2 invasion more than two folds compared to the control indicating that the partial release of the autoinhibition promotes actin turnover so that cells might invade faster. Wild type FMNL2 induced invasion better than the phospho-deficient mutant S1072A, suggesting that wild type FMNL2 can be phosphorylated so that it is more active than S1072A mutant. In conclusion, phosphorylation of FMNL2 by PKC partially releases its

autoinhibition. FMNL2 is required for cells to keep proper levels of cell surface integrin and actomyosin contractility, which is important for rounded cell invasion. The phospho-mimetic mutant S1072E driving A375M2 rounded cell invasion more than the wild type or the phospho-deficient mutant, is probably due to the higher actin assembly activity of this mutant.

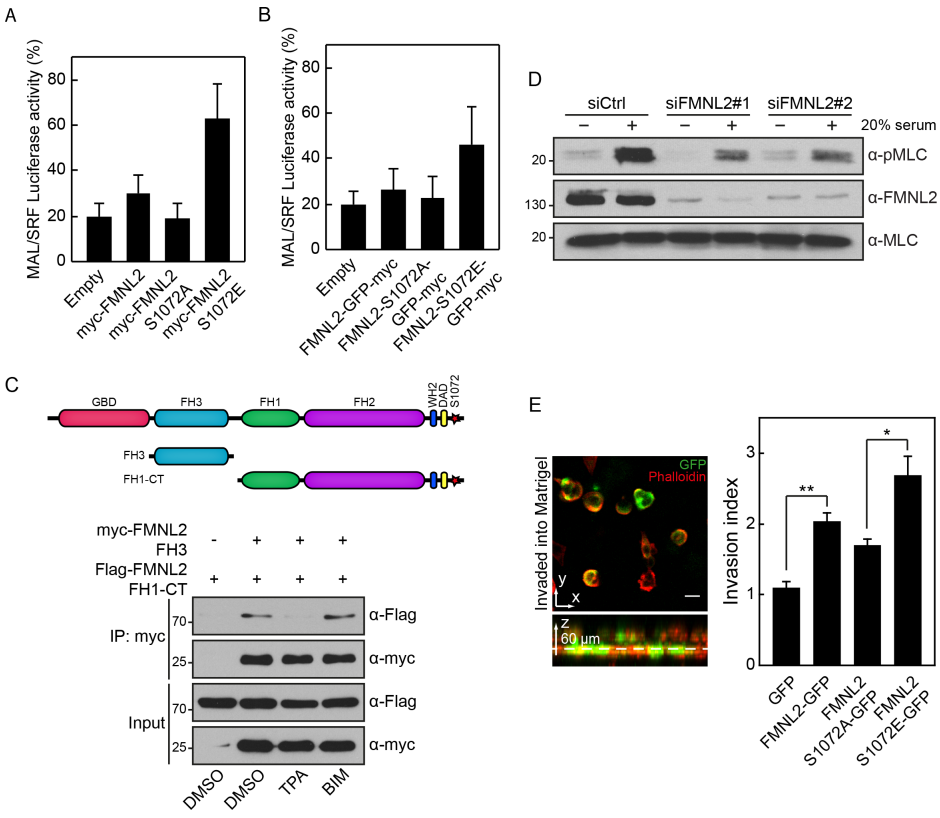

Figure 29. Effects of FMNL2 phosphorylation on rounded cell invasion in 3D. A. HEK293 cells were transfected with myc-FMNL2, FMNL2-S1072A or FMNL2-S1072E, together with MAL/SRF reporter 3DA.Luc and Renilla luciferase pRLTK. SRF activity was measured 24 h after transfection. Error bar: + s.e.m. (n=3). **B.** FMNL2, FMNL2-S1072A or FMNL2-S1072E-GFP-myc was expressed in the same assay as in A. Error bar: + s.e.m. (n=3). **C.** Immunoprecipitations of HEK293 cells expressing Flag-FMNL2-FH1-CT and myc-FMNL2-FH3 after DMSO, 200 nM TPA or 2 μM BIM treatment. **D.** FMNL2 were silenced by two different siRNAs in HeLa cells. After 72 hours, cells were starved for 3 hours and stimulated with 20% fetal bovine serum for 10 min. Phospho-myosin light chain (p-MLC), MLC and FMNL2 were detected in Western blotting. Numbers indicate molecular weight (kD). **E.** Left: Representative images of 3D Matrigel invasion using A375M2 cells stably expressing GFP or GFP-tagged

proteins after doxycycline (dox) induction. Lower panel shows the z-projection. Dashed line indicates the membrane of the insert. Green: GFP; Red: rhodamine-phalloidin. Scale bar: 20 μm. Right: Invasion of A375M2 cells stably expressing GFP, FMNL2-GFP, FMNL2-S1072A-GFP and FMNL2-S1072E-GFP are shown. Percentage of invaded cell over the total cell number was quantified and normalized between dox-induced and non-induced cells. Error bar: + s.e.m. (n=3); two stars: $p < 0.001$; one star: $p < 0.05$.

5 Discussion

Cell motility is mainly driven by the dynamic reorganization of the actin cytoskeleton (Pollard and Borisy, 2003). The nucleation promoting factors of the Arp2/3 complex, and other actin regulating proteins such as Rho GTPases, cofilin, LIM kinase have been extensively studied in cancer models (Bravo-Cordero et al., 2011; Ellenbroek and Collard, 2007; Nürnberg et al., 2011; Olson and Sahai, 2008; Wang et al., 2007). Formins, as the largest family of actin nucleators and the largest group of Rho GTPase effectors, are emerging to be involved in cancer cell adhesion, migration and invasion. FMNL2 is widely expressed in human tissues and is upregulated in colorectal cancer (Zhu et al., 2011, 2008). In addition, it is required for rounded cell invasion in 3D downstream of RhoC (Kitzing et al., 2010). Here, I described a novel regulatory mechanism of FMNL2 through phosphorylation by protein kinase C, which is involved in cancer cell invasion.

5.1 Effects of FMNL2 on actin assembly

Although diverse formins employ a common mechanism to assemble actin filaments, there are substantial differences in the kinetic reaction (Kovar, 2006; Pollard, 2007). In the FMNL subfamily, FMNL1 and FMNL3 show low actin polymerization activity *in vitro* (Harris, 2006; Heimsath and Higgs, 2012). However, FMNL2 inhibits actin polymerization in a concentration-dependent manner. This was confirmed in another study (Block et al., 2012). This inhibitory effect of FMNL2-FH1-CT on actin polymerization also affects the polymerizing ability of mDia1, implicating a strong interaction between FMNL2 and the barbed ends of actin filaments. Thus, FMNL2 may remain binding to the barbed ends replacing mDia1.

Although FMNL2 exhibits an inhibitory effect on actin polymerization *in vitro*, there is no evidence for cellular FMNL2 to inhibit actin assembly. For example, FMNL2-FH1-CT induces stress fiber formation in cells. Thus, it is questionable how useful the *in vitro* assay is to study FMNL2 functions. The *in vitro* assay may lack important factors which are necessary for the proteins to function properly in cells. Thus, the lack of actin

polymerization activity *in vitro* does not exclude that FMNL2 can polymerize actin under physiological conditions. It is possible that FMNL2 needs additional factors to adopt a proper conformation for actin polymerization in cells.

5.2 Nuclear localization of FMNL2 C-terminus

The C-terminus of FMNL2 (FMNL2-FH1-CT) shows accumulation in the cell nucleus. Studies on deletion mutants indicate that a possible nuclear localization sequence (NLS) lies within the WH2 domain of FMNL2. Why should formins be targeted into the nucleus? A recent study showed that serum stimulation could induce nuclear actin polymerization, which depends on the activation of endogenous mDia in the nucleus. The actin assembly activity of mDia in the nucleus also leads to accumulation of MAL in the nucleus (Baarlink et al., 2013). FMNL2 harbors a putative NLS and endogenous FMNL2 seems to have a nuclear distribution in cells (Gardberg et al., 2010). Whether autoinhibition masks the NLS of FMNL2 and whether its activation is related to the nuclear localization need to be studied.

5.3 Membrane localization of FMNL2

Endogenous FMNL2 was reported to localize diffusely in the cytoplasm and the peri-nuclear region (Gardberg et al., 2010). However, these results should be interpreted with caution since the FMNL2 antibody was reported to recognize both FMNL2 and FMNL3 (Block et al., 2012). Here, it is demonstrated that ectopically expressed FMNL2 localizes to the plasma membrane and intracellular membranes. Although Rho GTPases play a central role in recruiting formins to cellular membranes, recent studies suggest that additional factors help to drive membrane localization and activation of certain formins (Brandt et al., 2007; Chhabra et al., 2009; Copeland et al., 2007; Seth et al., 2006). Indeed, RhoC is found to be important for the plasma membrane localization of FMNL2. Moreover, FMNL2 was reported to be N-myristoylated. Mutation of the myristoylation site prevented FMNL2 from localizing to lamellipodia (Block et al., 2012). A similar phenomenon has been observed in this work. Loss of myristoylation leads to the loss of plasma membrane localization of full length FMNL2, whereas the isolated N-terminus

containing the Rho GTPase binding domain of FMNL2 can still localize to the plasma membrane even in the absence of myristoylation (data not shown). Thus, a potential model of FMNL2 subcellular localization could be that myristoylation ensures that FMNL2 is tethered to cellular membranes in its autoinhibited conformation, while RhoC regulates the activity of FMNL2 and modulates the type of membrane to which FMNL2 is bound. It is not clear whether FMNL2 is first released from autoinhibition and recruited to the plasma membrane or it is activated at the plasma membrane after the recruitment. In this regard, the regulation of FMNL2 localization may need additional factors. Although useful information can be obtained by observing the localization behavior of the overexpression of proteins in cells, better antibodies are needed to reliably address the localization and function of endogenous FMNL2 under different conditions.

5.4 Phosphorylation of FMNL2

5.4.1 FMNL2 is post-translationally phosphorylated

Emerging evidences implicate that additional factors, other than Rho GTPases, are involved in the activation of formins. The activity of a number of formins is subject to phosphorylation (Hannemann et al., 2008; Matheos et al., 2004; Takeya et al., 2008; Wang et al., 2009). In a search for additional factors regulating its activity, FMNL2 was found to be phosphorylated by PKC at Ser 1072. Among all the PKC isozymes, FMNL2 could be phosphorylated by several PKCs in the *in vitro* kinase assays, while it appears to be specifically phosphorylated by PKCα in cells. This discrepancy of *in vitro* and *in vivo* results may come from the reduced specificity between the kinases and the substrates *in vitro*, and the lack of regulatory factors in the *in vitro* system. The specificity of FMNL2 phosphorylation by PKCα indicates that there might be a specific function regulated by PKCα activation. In addition, the interaction between FMNL2 and PKCα is stronger in cells treated by BIM I inhibitor. Since the enzymatic reaction between kinases and their substrates are highly transient and dynamic, it is possible that BIM I as an ATP-competitive inhibitor locks the kinase domain of PKCα at a conformation favorable for FMNL2 binding.

Like other prototypic formins, FMNL2 autoinhibition is mediated by DID-DAD interaction (Kitzing et al., 2010; Vaillant et al., 2008). The Ser 1072 is located in close vicinity to the DAD domain, which led to the hypothesis that phosphorylation on this residue might affect the DID-DAD interaction of FMNL2. Indeed, the DID-DAD interaction is weaker when Ser 1072 is phosphorylated. Thus, the phosphorylation of FMNL2 by PKC may substantially contribute to FMNL2 autoinhibition. Moreover, phosphorylation of FMNL2 can be enhanced by RhoC. Thus RhoC releases the autoinhibition of FMNL2 and enhances FMNL2 phosphorylation by PKC, whereas this phosphorylation can also release FMNL2 autoinhibition. How the three events are interconnected and which one is the initiating factor remain elusive. Active PKC localizes to the plasma membrane. It is observed that FMNL2 colocalizes with active RhoC on the plasma membrane and intracellular membrane structures. Hence it is likely that through binding to FMNL2 GBD, RhoC recruits or facilitates FMNL2 localization in a close vicinity to PKC. In addition, RhoC binding can release FMNL2 into a conformation that is favorable for kinase-substrate reaction, which ultimately enhances the phosphorylation of FMNL2. Phosphorylation may further stabilize or reinforce the active conformation of FMNL2.

Taken together, FMNL2 is not restricted to the regulation of Rho GTPase only, but become integrated into a signaling network which also involves PKC regulation and function. How RhoC and PKC coordinate in regulating FMNL2 activity and function opens an interesting field for future studies.

5.4.2 Internalization of FMNL2 upon PKCα activation

Translocation from the cytoplasm to the plasma membrane upon activation is a unique property of the classical and novel PKCs (Sakai et al., 1997). It is intriguing that FMNL2 is gradually internalized upon PKCα translocation and activation. However, the phospho-deficient mutant (S1072A) of FMNL2 is also internalized as the wild type when overexpressed in cells (data not shown). One possible explanation is that overexpressed FMNL2 dimerizes with endogenous FMNL2 so that the mutant can also be internalized upon PKCα activation. Although internalization is not inhibited in an endogenous

FMNL2 reduced background, the phospho-deficient mutant shows a slower internalization rate. Hence, the Ser 1072 residue contributes to the internalization of FMNL2. The internalization might need the phosphorylation of other unknown residues on FMNL2. Although five more residues were tested according to consensus sequence scanning, none were responsible for this process. PKCα may also activate additional signals or factors, which regulate FMNL2 internalization.

Phosphorylation of FMNL2 can release its autoinhibition. It was thus speculated that activated FMNL2 might locally initiate actin polymerization that is required for its internalization. A mutant FMNL2 defective in actin binding (FMNL2-ILI3A) could be internalized similarly as the wild type (data not shown). Thus it is unlikely that the actin assembly activity of FMNL2 is required for this process. Moreover, it has been reported that FMNL2 appears to activate PI3K, PKB/Akt, and MAPK signaling pathways (Liang et al., 2013). It is possible that FMNL2 may change the lipid composition of membranes which might be required for its internalization.

Biochemical studies have shown that both endogenous and overexpressed FMNL2 are anchored to the cell membrane structures. The observation of FMNL2 redistribution from the plasma membrane to the intracellular membrane structures is most likely through membrane internalization. In other words, FMNL2 may follow endocytic route to accomplish internalization. Among the intracellular markers tested, FMNL2 has been found on Rab4, Rab5 or Rab7 positive endosomes pointing towards the fact that FMNL2 may be endocytosed upon activation of PKCα. It remains unclear whether FMNL2 is involved in endosome motility or cargo transport.

The application of the calcium ionophore, A23187, provides the evidence that FMNL2 internalization is reversible as well as PKCα translocation and activation. PKCα is rapidly translocated by calcium that is brought into the cells by A23187. It is known that intracellular calcium concentration is tightly controlled. Thus it is likely that the high calcium concentration is reduced rapidly to a low level by the cells. Accordingly, PKCα is deactivated and translocated back to the cytosol gradually. Following PKCα deactivation, the internalized FMNL2 returns to the plasma membrane. Thus, FMNL2

internalization is reversible. The reversibility of the internalization of FMNL2 can be utilized by the cells to respond to extracellular cues and to rapidly transduce and switch off signals in time.

5.5 The relationship between FMNL2 and β1 integrin

PKCα is known to control the intracellular trafficking of integrin heterodimers via a direct interaction with β1 integrin (Ng et al., 1999; Parsons et al., 2002). FMNL2 was identified to be required for β1 integrin internalization (Arjonen et al., Turku centre for Biotechnology, unpublished data). It is consistent with the finding that FMNL2 appears on the endosome vesicles. Silencing of FMNL2 leads to an increased cell surface α5β1 integrin level most likely due to the reduced internalization of β1 integrin. FMNL2 interacts with the cytoplasmic tail of α5 integrin but not β1, indicating an indirect effect on β1 integrin through α5 integrin binding. Consistent with that, FMNL2 exhibits colocalization with α5 integrin positive vesicles.

How could FMNL2 regulate the internalization of α5β1 integrin? It is known that formins regulate actin dynamics. Actin filament assembly can generate mechanical forces to induce membrane invagination and contraction (Kaksonen et al., 2006). Wild type FMNL2 negatively affects cell surface α5β1 integrin levels, implicating a role in regulating α5β1 integrin turnover. However, the ILI3A mutant defective in actin binding shows no differences on α5β1 integrin surface levels in comparison to the wild type. This mutant also exhibits colocalization with α5 integrin vesicles (data not shown). Thus, the role of FMNL2 in regulating α5β1 integrin internalization appears to be independent on FMNL2-mediated actin polymerization. Additionally, FMNL2 is found to interact with the nucleation promoting factor WASH that promotes Arp2/3 mediated branching (personal communication with Zech, Beatson Institute). WASH mediated actin polymerization is reported to be required for α5β1 integrin recycling (Zech et al., 2011). Hence, it is possible that FMNL2 acts as a bridge between α5β1 integrin and the actin assembly machinery. Another possibility is that the role of FMNL2 in α5β1 integrin internalization is not related to actin assembly at all. It might be that FMNL2 behaves as

a recruiting factor or a scaffolding protein to collect and transduce the signals to downstream factors in the endocytic pathway.

The contribution of PKCα regulated FMNL2 activity to PKCα regulated β1 integrin trafficking is unclear. The internalization of α5β1 integrin mediated by the phospho-mutants in an endogenous FMNL2 reduced background needs to be studied. It may also be necessary to compare the internalization rates of the mutant and the wild type FMNL2. So far, it is known that PKCα regulates β1 integrin trafficking, PKCα phosphorylates FMNL2 and PKCα activation leads to FMNL2 internalization. All the three signals may converge on FMNL2 to regulate α5β1 integrin internalization necessary for related cellular functions.

5.6 FMNL2 in cancer cell invasion

Many actin regulators, including FMNL2, are shown to be upregulated in cancer progression (Nürnberg et al., 2011; Wang et al., 2004; Zhu et al., 2008). Although FMNL2 seems to be a poor actin nucleator *in vitro*, it has a role in actin turnover in cells (Kitzing et al., 2010). FMNL2 activity is regulated by phosphorylation. Consistently, the phospho-mimetic mutant of FMNL2 drives the invasion of A375M2 melanoma cells into 3D Matrigel to a significantly higher degree than the phospho-deficient mutant. Thus, the driving force of promoting invasion in 3D may arise from the actin assembly activity of FMNL2.

Rounded cell invasion requires low surface integrin level and high cortical actomyosin contractility (Hegerfeldt et al., 2002; Sanz-Moreno et al., 2008). FMNL2 negatively regulates β1 integrin surface level. Reduced FMNL2 in cells leads to a reduced level of p-MLC, a marker of actomyosin contractility. Thus, FMNL2 affects three factors: actin polymerization, β1 integrin surface level and actomyosin contractility, which are all crucial for cancer cell invasion. These functions of FMNL2 might be regulated and connected by PKCα. The phosphorylation by PKCα activates FMNL2, which may regulate actin assembly. At the same time, PKCα activation results in FMNL2 internalization which may be needed for β1 integrin turnover. However, the effect of

FMNL2 phosphorylation on p-MLC level remains elusive. How the three functions coordinate with each other and whether one of the functions is more important are unknown. Nevertheless, these functions could all affect the invasiveness of cancer cells.

The important effects of FMNL2 in actin polymerization, β1 integrin surface level and actomyosin contractility make it an interesting candidate for cancer therapy. However, these effects also indicate that there might exist essential cellular functions of FMNL2 which could restrain the effectiveness of anti-cancer drugs.

5.7 Conclusion

The work presented herein focuses on the regulation of FMNL2 and its role in cancer cell invasion. A novel mechanism of FMNL2 regulation was identified, which involves post-translational modification of FMNL2 by PKCα at Ser 1072. Phosphorylation leads to a partial release of FMNL2 autoinhibition and accelerates cancer cell invasion in 3D matrix. Upon PKCα activation, FMNL2 is internalized through endocytosis providing a platform for spatiotemporal regulation of actin assembly. Phosphorylation of Ser 1072 affects the internalization rate of FMNL2. Internalized FMNL2 localizes to the α5 integrin positive vesicles. FMNL2 negatively affects cell surface α5β1 integrin levels (Figure 30). Hence, phosphorylation plays a role in FMNL2 activation and localization, which may exert functions in actin assembly and integrin trafficking. In addition, FMNL2 controls the p-MLC level. Taken together, these factors may act in concert to explain the invasive capacity of the deregulated FMNL2. Through phosphorylation, FMNL2 is integrated into a signaling network which involves not only the regulation of Rho GTPase but also the regulation and function of PKC. This integration may account for the important functions of FMNL2 in regulating cell motility and also make FMNL2 an interesting candidate as an anti-invasive target for cancer therapy.

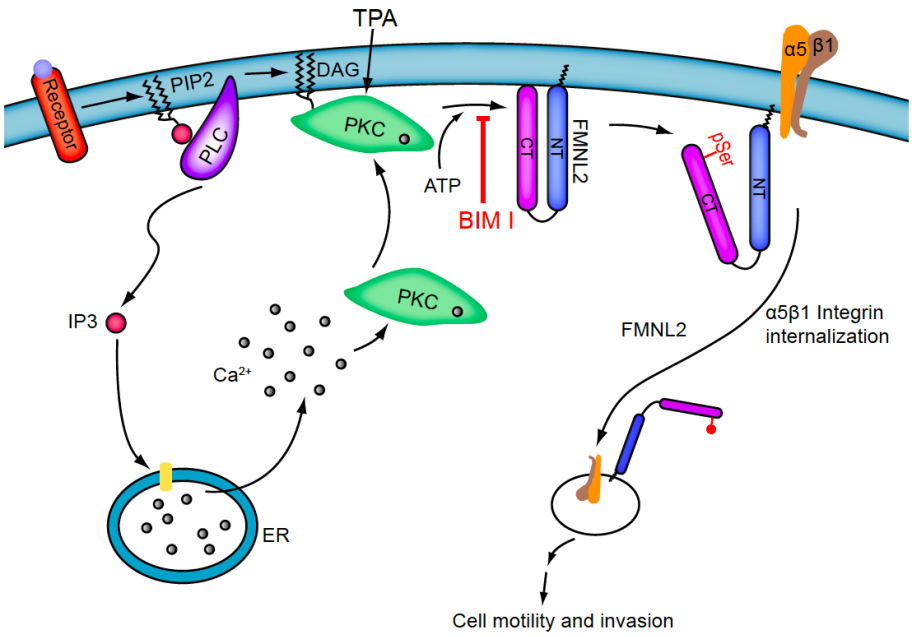

Figure 30. Schematic model of this work. Extracellular signals stimulate receptors which in turn activate phospholipase C (PLC). PLC cleaves phosphatidylinositol-4, 5-biphosphate (PIP_2) into diacylglycerol (DAG) and inositol triphosphate (IP_3). IP_3 releases calcium from endoplasmic reticulum. Calcium binds protein kinase C (PKC) to pre-target PKC to membranes. Upon DAG binding, PKC undergoes a conformational change to be fully activated. FMNL2 is then phosphorylated by PKC and partially releases its autoinhibition. By regulating α5β1 integrin internalization through unknown mechanisms, FMNL2 promotes cancer cell invasion.

6 References

Ahuja, R., Pinyol, R., Reichenbach, N., Custer, L., Klingensmith, J., Kessels, M.M., and Qualmann, B. (2007). Cordon-Bleu Is an Actin Nucleation Factor and Controls Neuronal Morphology. Cell *131*, 337–350.

Albelda, S.M., Mette, S.A., Elder, D.E., Stewart, R., Damjanovich, L., Herlyn, M., and Buck, C.A. (1990). Integrin distribution in malignant melanoma: association of the beta 3 subunit with tumor progression. Cancer Res. *50*, 6757–6764.

Alberts, A.S. (2001). Identification of a Carboxyl-Terminal Diaphanous-Related Formin Homology Protein Autoregulatory Domain. J. Biol. Chem. *276*, 2824–2830.

Alvaro, V., Lévy, L., Dubray, C., Roche, A., Peillon, F., Quérat, B., and Joubert, D. (1993). Invasive human pituitary tumors express a point-mutated alpha-protein kinase-C. J. Clin. Endocrinol. Metab. *77*, 1125–1129.

Arjonen, A., Alanko, J., Veltel, S., and Ivaska, J. (2012). Distinct Recycling of Active and Inactive β1 Integrins. Traffic *13*, 610–625.

Avizienyte, E., Wyke, A.W., Jones, R.J., McLean, G.W., Westhoff, M.A., Brunton, V.G., and Frame, M.C. (2002). Src-induced de-regulation of E-cadherin in colon cancer cells requires integrin signalling. Nat. Cell Biol. *4*, 632–638.

Baarlink, C., Brandt, D., and Grosse, R. (2010). SnapShot: Formins. Cell *142*, 172–172.e1.

Baarlink, C., Wang, H., and Grosse, R. (2013). Nuclear Actin Network Assembly by Formins Regulates the SRF Coactivator MAL. Science *340*, 864–867.

Di Blasio, L., Droetto, S., Norman, J., Bussolino, F., and Primo, L. (2010). Protein Kinase D1 Regulates VEGF-A-Induced αvβ3 Integrin Trafficking and Endothelial Cell Migration. Traffic *11*, 1107–1118.

Block, J., Breitsprecher, D., Kühn, S., Winterhoff, M., Kage, F., Geffers, R., Duwe, P., Rohn, J.L., Baum, B., Brakebusch, C., et al. (2012). FMNL2 Drives Actin-Based Protrusion and Migration Downstream of Cdc42. Curr. Biol. *22*, 1005–1012.

Brandt, D.T., Marion, S., Griffiths, G., Watanabe, T., Kaibuchi, K., and Grosse, R. (2007). Dia1 and IQGAP1 interact in cell migration and phagocytic cup formation. J. Cell Biol. *178*, 193–200.

Brandt, D.T., Baarlink, C., Kitzing, T.M., Kremmer, E., Ivaska, J., Nollau, P., and Grosse, R. (2009). SCAI acts as a suppressor of cancer cell invasion through the transcriptional control of β1-integrin. Nat. Cell Biol. *11*, 557–568.

Bravo-Cordero, J.J., Oser, M., Chen, X., Eddy, R., Hodgson, L., and Condeelis, J. (2011). A Novel Spatiotemporal RhoC Activation Pathway Locally Regulates Cofilin Activity at Invadopodia. Curr. Biol. *21*, 635–644.

Bretscher, M.S. (1992). Circulating integrins: alpha 5 beta 1, alpha 6 beta 4 and Mac-1, but not alpha 3 beta 1, alpha 4 beta 1 or LFA-1. Embo J. *11*, 405–410.

Brooks, P.C., Strömblad, S., Sanders, L.C., von Schalscha, T.L., Aimes, R.T., Stetler-Stevenson, W.G., Quigley, J.P., and Cheresh, D.A. (1996). Localization of matrix metalloproteinase MMP-2 to the surface of invasive cells by interaction with integrin alpha v beta 3. Cell *85*, 683–693.

Brooks, P.C., Silletti, S., von Schalscha, T.L., Friedlander, M., and Cheresh, D.A. (1998). Disruption of angiogenesis by PEX, a noncatalytic metalloproteinase fragment with integrin binding activity. Cell *92*, 391–400.

Campellone, K.G., and Welch, M.D. (2010). A nucleator arms race: cellular control of actin assembly. Nat. Rev. Mol. Cell Biol. *11*, 237–251.

Castagna, M., Takai, Y., Kaibuchi, K., Sano, K., Kikkawa, U., and Nishizuka, Y. (1982). Direct activation of calcium-activated, phospholipid-dependent protein kinase by tumor-promoting phorbol esters. J. Biol. Chem. *257*, 7847–7851.

Caswell, P., and Norman, J. (2008). Endocytic transport of integrins during cell migration and invasion. Trends Cell Biol. *18*, 257–263.

Caswell, P.T., and Norman, J.C. (2006). Integrin Trafficking and the Control of Cell Migration. Traffic *7*, 14–21.

Caswell, P.T., Spence, H.J., Parsons, M., White, D.P., Clark, K., Cheng, K.W., Mills, G.B., Humphries, M.J., Messent, A.J., Anderson, K.I., et al. (2007). Rab25 Associates with α5β1 Integrin to Promote Invasive Migration in 3D Microenvironments. Dev. Cell *13*, 496–510.

Caswell, P.T., Vadrevu, S., and Norman, J.C. (2009). Integrins: masters and slaves of endocytic transport. Nat. Rev. Mol. Cell Biol. *10*, 843–853.

Chan, D.C., and Leder, P. (1996). Genetic Evidence That Formins Function within the Nucleus. J. Biol. Chem. *271*, 23472–23477.

Cheng, K.W., Lahad, J.P., Kuo, W., Lapuk, A., Yamada, K., Auersperg, N., Liu, J., Smith-McCune, K., Lu, K.H., Fishman, D., et al. (2004). The RAB25 small GTPase determines aggressiveness of ovarian and breast cancers. Nat. Med. *10*, 1251–1256.

Chereau, D., Boczkowska, M., Skwarek-Maruszewska, A., Fujiwara, I., Hayes, D.B., Rebowski, G., Lappalainen, P., Pollard, T.D., and Dominguez, R. (2008). Leiomodin Is an Actin Filament Nucleator in Muscle Cells. Science *320*, 239–243.

Chesarone, M.A., and Goode, B.L. (2009). Actin nucleation and elongation factors: mechanisms and interplay. Curr. Opin. Cell Biol. *21*, 28–37.

Chesarone, M.A., DuPage, A.G., and Goode, B.L. (2010). Unleashing formins to remodel the actin and microtubule cytoskeletons. Nat. Rev. Mol. Cell Biol. *11*, 62–74.

Chhabra, E.S., and Higgs, H.N. (2006). INF2 Is a WASP Homology 2 Motif-containing Formin That Severs Actin Filaments and Accelerates Both Polymerization and Depolymerization. J. Biol. Chem. *281*, 26754–26767.

Chhabra, E.S., Ramabhadran, V., Gerber, S.A., and Higgs, H.N. (2009). INF2 is an endoplasmic reticulum-associated formin protein. J. Cell Sci. *122*, 1430–1440.

Clark, E.A., Golub, T.R., Lander, E.S., and Hynes, R.O. (2000). Genomic analysis of metastasis reveals an essential role for RhoC. Nature *406*, 532–535.

Colón-Franco, J.M., Gomez, T.S., and Billadeau, D.D. (2011). Dynamic remodeling of the actin cytoskeleton by FMNL1γ is required for structural maintenance of the Golgi complex. J. Cell Sci. *124*, 3118 –3126.

Copeland, J.W., and Treisman, R. (2002). The Diaphanous-related Formin mDia1 Controls Serum Response Factor Activity through its Effects on Actin Polymerization. Mol. Biol. Cell *13*, 4088–4099.

Copeland, S.J., Green, B.J., Burchat, S., Papalia, G.A., Banner, D., and Copeland, J.W. (2007). The Diaphanous Inhibitory Domain/Diaphanous Autoregulatory Domain Interaction Is Able to Mediate Heterodimerization between mDia1 and mDia2. J. Biol. Chem. *282*, 30120 –30130.

Cox, D., Brennan, M., and Moran, N. (2010). Integrins as therapeutic targets: lessons and opportunities. Nat. Rev. Drug Discov. *9*, 804–820.

DeWard, A.D., Eisenmann, K.M., Matheson, S.F., and Alberts, A.S. (2010). The role of formins in human disease. Biochim. Biophys. Acta Bba - Mol. Cell Res. *1803*, 226–233.

Dominguez, R., and Holmes, K.C. (2011). The Structure of G and F Actin Filaments. Annu. Rev. Biophys. *40*.

Eisenmann, K.M., Harris, E.S., Kitchen, S.M., Holman, H.A., Higgs, H.N., and Alberts, A.S. (2007). Dia-Interacting Protein Modulates Formin-Mediated Actin Assembly at the Cell Cortex. Curr. Biol. *17*, 579–591.

Ellenbroek, S.I.J., and Collard, J.G. (2007). Rho GTPases: functions and association with cancer. Clin. Exp. Metastasis *24*, 657–672.

Faix, J., and Grosse, R. (2006). Staying in Shape with Formins. Dev. Cell *10*, 693–706.

Fernandez-Borja, M., Janssen, L., Verwoerd, D., Hordijk, P., and Neefjes, J. (2005). RhoB regulates endosome transport by promoting actin assembly on endosomal membranes through Dia1. J. Cell Sci. *118*, 2661–2670.

Friedl, P., and Alexander, S. (2011). Cancer Invasion and the Microenvironment: Plasticity and Reciprocity. Cell *147*, 992–1009.

Friedl, P., and Gilmour, D. (2009). Collective cell migration in morphogenesis, regeneration and cancer. Nat. Rev. Mol. Cell Biol. *10*, 445–457.

Friedl, P., and Wolf, K. (2003). Tumour-cell invasion and migration: diversity and escape mechanisms. Nat. Rev. Cancer *3*, 362–374.

Gaggioli, C., Hooper, S., Hidalgo-Carcedo, C., Grosse, R., Marshall, J.F., Harrington, K., and Sahai, E. (2007). Fibroblast-led collective invasion of carcinoma cells with differing roles for RhoGTPases in leading and following cells. Nat. Cell Biol. *9*, 1392–1400.

Garcia-Bermejo, M.L., Leskow, F.C., Fujii, T., Wang, Q., Blumberg, P.M., Ohba, M., Kuroki, T., Han, K.-C., Lee, J., Marquez, V.E., et al. (2002). Diacylglycerol (DAG)-lactones, a New Class of Protein Kinase C (PKC) Agonists, Induce Apoptosis in LNCaP Prostate Cancer Cells by Selective Activation of PKCα. J. Biol. Chem. *277*, 645–655.

Gardberg, M., Talvinen, K., Kaipio, K., Iljin, K., Kampf, C., Uhlen, M., and Carpén, O. (2010). Characterization of Diaphanous-related formin FMNL2 in human tissues. Bmc Cell Biol. *11*, 55.

Geiger, B., Spatz, J.P., and Bershadsky, A.D. (2009). Environmental sensing through focal adhesions. Nat. Rev. Mol. Cell Biol. *10*, 21–33.

Gimond, C., Flier, A. van der, Delft, S. van, Brakebusch, C., Kuikman, I., Collard, J.G., Fässler, R., and Sonnenberg, A. (1999). Induction of Cell Scattering by Expression of β1 Integrins in β1-Deficient Epithelial Cells Requires Activation of Members of the Rho Family of Gtpases and Downregulation of Cadherin and Catenin Function. J. Cell Biol. *147*, 1325–1340.

Gladson, C.L., and Cheresh, D.A. (1991). Glioblastoma expression of vitronectin and the alpha v beta 3 integrin. Adhesion mechanism for transformed glial cells. J. Clin. Invest. *88*, 1924–1932.

Goley, E.D., and Welch, M.D. (2006). The ARP2/3 complex: an actin nucleator comes of age. Nat. Rev. Mol. Cell Biol. *7*, 713–726.

Goodnight, J., Mischak, H., Kolch, W., and Mushinski, J.F. (1995). Immunocytochemical Localization of Eight Protein Kinase C Isozymes Overexpressed in NIH 3T3 Fibroblasts ISOFORM-SPECIFIC ASSOCIATION WITH MICROFILAMENTS, GOLGI, ENDOPLASMIC RETICULUM, AND NUCLEAR AND CELL MEMBRANES. J. Biol. Chem. *270*, 9991–10001.

Gould, C.J., Maiti, S., Michelot, A., Graziano, B.R., Blanchoin, L., and Goode, B.L. (2011). The Formin DAD Domain Plays Dual Roles in Autoinhibition and Actin Nucleation. Curr. Biol. *21*, 384–390.

Griner, E.M., and Kazanietz, M.G. (2007). Protein kinase C and other diacylglycerol effectors in cancer. Nat. Rev. Cancer *7*, 281–294.

Grodsky, N., Li, Y., Bouzida, D., Love, R., Jensen, J., Nodes, B., Nonomiya, J., and Grant, S. (2006). Structure of the Catalytic Domain of Human Protein Kinase C β II Complexed with a Bisindolylmaleimide Inhibitor‡. Biochemistry (Mosc.) *45*, 13970–13981.

Grosse, R., Copeland, J.W., Newsome, T.P., Way, M., and Treisman, R. (2003). A role for VASP in RhoA-Diaphanous signalling to actin dynamics and SRF activity. Embo J. *22*, 3050–3061.

Guo, W., and Giancotti, F.G. (2004). Integrin signalling during tumour progression. Nat. Rev. Mol. Cell Biol. *5*, 816–826.

Hager, M.H., Morley, S., Bielenberg, D.R., Gao, S., Morello, M., Holcomb, I.N., Liu, W., Mouneimne, G., Demichelis, F., Kim, J., et al. (2012). DIAPH3 governs the cellular transition to the amoeboid tumour phenotype. Embo Mol. Med. *4*, 743–760.

Hakem, A., Sanchez-Sweatman, O., You-Ten, A., Duncan, G., Wakeham, A., Khokha, R., and Mak, T.W. (2005). RhoC is dispensable for embryogenesis and tumor initiation but essential for metastasis. Genes Dev. *19*, 1974–1979.

Han, Y., Eppinger, E., Schuster, I.G., Weigand, L.U., Liang, X., Kremmer, E., Peschel, C., and Krackhardt, A.M. (2009). Formin-Like 1 (FMNL1) Is Regulated by N-Terminal Myristoylation and Induces Polarized Membrane Blebbing. J. Biol. Chem. *284*, 33409–33417.

Hannemann, S., Madrid, R., Stastna, J., Kitzing, T., Gasteier, J., Schönichen, A., Bouchet, J., Jimenez, A., Geyer, M., Grosse, R., et al. (2008). The Diaphanous-Related Formin FHOD1 Associates with ROCK1 and Promotes Src-Dependent Plasma Membrane Blebbing. J. Biol. Chem. *283*, 27891–27903.

Harris, E.S. (2006). Mechanistic Differences in Actin Bundling Activity of Two Mammalian Formins, FRL1 and mDia2. J. Biol. Chem. *281*, 14383–14392.

Harris, E.S., Gauvin, T.J., Heimsath, E.G., and Higgs, H.N. (2010). Assembly of filopodia by the formin FRL2 (FMNL3). Cytoskeleton *67*, 755–772.

Hegerfeldt, Y., Tusch, M., Bröcker, E.-B., and Friedl, P. (2002). Collective Cell Movement in Primary Melanoma Explants Plasticity of Cell-Cell Interaction, β1-Integrin Function, and Migration Strategies. Cancer Res. *62*, 2125–2130.

Heimsath, E.G., and Higgs, H.N. (2012). The C Terminus of Formin FMNL3 Accelerates Actin Polymerization and Contains a WH2 Domain-like Sequence That Binds Both Monomers and Filament Barbed Ends. J. Biol. Chem. *287*, 3087–3098.

Higgs, H.N. (2005). Formin proteins: a domain-based approach. Trends Biochem. Sci. *30*, 342–353.

Hill, C.S., Wynne, J., and Treisman, R. (1995). The Rho family GTPases RhoA, Racl , and CDC42Hsregulate transcriptional activation by SRF. Cell *81*, 1159–1170.

Huang, C., Rajfur, Z., Borchers, C., Schaller, M.D., and Jacobson, K. (2003). JNK phosphorylates paxillin and regulates cell migration. Nature *424*, 219–223.

Hynes, R.O. (2002). Integrins: Bidirectional, Allosteric Signaling Machines. Cell *110*, 673–687.

Iiizumi, M., Bandyopadhyay, S., Pai, S.K., Watabe, M., Hirota, S., Hosobe, S., Tsukada, T., Miura, K., Saito, K., Furuta, E., et al. (2008). RhoC Promotes Metastasis via Activation of the Pyk2 Pathway in Prostate Cancer. Cancer Res. *68*, 7613–7620.

Ivaska, J., Whelan, R.D.H., Watson, R., and Parker, P.J. (2002). PKC[epsi] controls the traffic of [beta]1 integrins in motile cells. Embo J *21*, 3608–3619.

Ivaska, J., Vuoriluoto, K., Huovinen, T., Izawa, I., Inagaki, M., and Parker, P.J. (2005). PKC[epsiv]-mediated phosphorylation of vimentin controls integrin recycling and motility. Embo J *24*, 3834–3845.

Jaffe, A.B., and Hall, A. (2005). RHO GTPASES: Biochemistry and Biology. Annu. Rev. Cell Dev. Biol. *21*, 247–269.

Jaken, S., and Parker, P.J. (2000). Protein kinase C binding partners. BioEssays *22*, 245–254.

Johnston, R.J., Copeland, J.W., Fasnacht, M., Etchberger, J.F., Liu, J., Honig, B., and Hobert, O. (2006). An unusual Zn-finger/FH2 domain protein controls a left/right asymmetric neuronal fate decision in C. elegans. Development *133*, 3317–3328.

Jones, S., Zhang, X., Parsons, D.W., Lin, J.C.-H., Leary, R.J., Angenendt, P., Mankoo, P., Carter, H., Kamiyama, H., Jimeno, A., et al. (2008). Core Signaling Pathways in Human Pancreatic Cancers Revealed by Global Genomic Analyses. Science *321*, 1801–1806.

Kaksonen, M., Toret, C.P., and Drubin, D.G. (2006). Harnessing actin dynamics for clathrin-mediated endocytosis. Nat. Rev. Mol. Cell Biol. *7*, 404–414.

Kikkawa, U., Takai, Y., Tanaka, Y., Miyake, R., and Nishizuka, Y. (1983). Protein kinase C as a possible receptor protein of tumor-promoting phorbol esters. J. Biol. Chem. *258*, 11442–11445.

Kitzing, T.M., Sahadevan, A.S., Brandt, D.T., Knieling, H., Hannemann, S., Fackler, O.T., Großhans, J., and Grosse, R. (2007). Positive feedback between Dia1, LARG, and RhoA regulates cell morphology and invasion. Genes Dev. *21*, 1478–1483.

Kitzing, T.M., Wang, Y., Pertz, O., Copeland, J.W., and Grosse, R. (2010). Formin-like 2 drives amoeboid invasive cell motility downstream of RhoC. Oncogene *29*, 2441–2448.

Korobova, F., Ramabhadran, V., and Higgs, H.N. (2013). An Actin-Dependent Step in Mitochondrial Fission Mediated by the ER-Associated Formin INF2. Science *339*, 464–467.

Kovar, D.R. (2006). Molecular details of formin-mediated actin assembly. Curr. Opin. Cell Biol. *18*, 11–17.

Kovar, D.R., Harris, E.S., Mahaffy, R., Higgs, H.N., and Pollard, T.D. (2006). Control of the Assembly of ATP- and ADP-Actin by Formins and Profilin. Cell *124*, 423–435.

Kraft, A.S., Anderson, W.B., Cooper, H.L., and Sando, J.J. (1982). Decrease in cytosolic calcium/phospholipid-dependent protein kinase activity following phorbol ester treatment of EL4 thymoma cells. J. Biol. Chem. *257*, 13193–13196.

Lämmermann, T., and Sixt, M. (2009). Mechanical modes of "amoeboid" cell migration. Curr. Opin. Cell Biol. *21*, 636–644.

Leach, K.L., James, M.L., and Blumberg, P.M. (1983). Characterization of a specific phorbol ester aporeceptor in mouse brain cytosol. Proc. Natl. Acad. Sci. *80*, 4208–4212.

LeClaire, L.L., Baumgartner, M., Iwasa, J.H., Mullins, R.D., and Barber, D.L. (2008). Phosphorylation of the Arp2/3 complex is necessary to nucleate actin filaments. J. Cell Biol. *182*, 647–654.

Li, F., and Higgs, H.N. (2003). The Mouse Formin mDia1 Is a Potent Actin Nucleation Factor Regulated by Autoinhibition. Curr. Biol. *13*, 1335–1340.

Li, F., and Higgs, H.N. (2005). Dissecting Requirements for Auto-inhibition of Actin Nucleation by the Formin, mDia1. J. Biol. Chem. *280*, 6986–6992.

Li, J., Ballif, B.A., Powelka, A.M., Dai, J., Gygi, S.P., and Hsu, V.W. (2005). Phosphorylation of ACAP1 by Akt Regulates the Stimulation-Dependent Recycling of Integrin β1 to Control Cell Migration. Dev. Cell *9*, 663–673.

Li, Y., Zhu, X., Zeng, Y., Wang, J., Zhang, X., Ding, Y., and Liang, L. (2010). FMNL2 Enhances Invasion of Colorectal Carcinoma by Inducing Epithelial-Mesenchymal Transition. Mol. Cancer Res. *8*, 1579 –1590.

Liang, L., Li, X., Zhang, X., Lv, Z., He, G., Zhao, W., Ren, X., Li, Y., Bian, X., Liao, W., et al. (2013). MicroRNA-137, an HMGA1 Target, Suppresses Colorectal Cancer Cell

Invasion and Metastasis in Mice by Directly Targeting FMNL2. Gastroenterology *144*, 624–635.e4.

Liu, J.-F., Crépin, M., Liu, J.-M., Barritault, D., and Ledoux, D. (2002). FGF-2 and TPA induce matrix metalloproteinase-9 secretion in MCF-7 cells through PKC activation of the Ras/ERK pathway. Biochem. Biophys. Res. Commun. *293*, 1174–1182.

Liu, W., Sato, A., Khadka, D., Bharti, R., Diaz, H., Runnels, L.W., and Habas, R. (2008). Mechanism of activation of the Formin protein Daam1. Proc. Natl. Acad. Sci. *105*, 210–215.

Lizárraga, F., Poincloux, R., Romao, M., Montagnac, G., Le Dez, G., Bonne, I., Rigaill, G., Raposo, G., and Chavrier, P. (2009). Diaphanous-Related Formins Are Required for Invadopodia Formation and Invasion of Breast Tumor Cells. Cancer Res. *69*, 2792 – 2800.

Lobert, V.H., Brech, A., Pedersen, N.M., Wesche, J., Oppelt, A., Malerød, L., and Stenmark, H. (2010). Ubiquitination of α5β1 Integrin Controls Fibroblast Migration through Lysosomal Degradation of Fibronectin-Integrin Complexes. Dev. Cell *19*, 148–159.

Lønne, G.K., Cornmark, L., Zahirovic, I.O., Landberg, G., Jirström, K., and Larsson, C. (2010). PKCα expression is a marker for breast cancer aggressiveness. Mol. Cancer *9*, 76.

Lu, J., Meng, W., Poy, F., Maiti, S., Goode, B.L., and Eck, M.J. (2007). Structure of the FH2 Domain of Daam1: Implications for Formin Regulation of Actin Assembly. J. Mol. Biol. *369*, 1258–1269.

Machesky, L.M., Atkinson, S.J., Ampe, C., Vandekerckhove, J., and Pollard, T.D. (1994). Purification of a cortical complex containing two unconventional actins from Acanthamoeba by affinity chromatography on profilin-agarose. J. Cell Biol. *127*, 107–115.

Margadant, C., Monsuur, H.N., Norman, J.C., and Sonnenberg, A. (2011). Mechanisms of integrin activation and trafficking. Curr. Opin. Cell Biol. *23*, 607–614.

Matheos, D., Metodiev, M., Muller, E., Stone, D., and Rose, M.D. (2004). Pheromone-induced polarization is dependent on the Fus3p MAPK acting through the formin Bni1p. J. Cell Biol. *165*, 99–109.

Meerbrey, K.L., Hu, G., Kessler, J.D., Roarty, K., Li, M.Z., Fang, J.E., Herschkowitz, J.I., Burrows, A.E., Ciccia, A., Sun, T., et al. (2011). The pINDUCER lentiviral toolkit for inducible RNA interference in vitro and in vivo. Proc. Natl. Acad. Sci. *108*, 3665–3670.

Miller, A.L., and Bement, W.M. (2009). Regulation of cytokinesis by Rho GTPase flux. Nat. Cell Biol. *11*, 71–77.

Miralles, F., Posern, G., Zaromytidou, A.-I., and Treisman, R. (2003). Actin Dynamics Control SRF Activity by Regulation of Its Coactivator MAL. Cell *113*, 329–342.

Miranti, C.K., and Brugge, J.S. (2002). Sensing the environment: a historical perspective on integrin signal transduction. Nat. Cell Biol. *4*, E83–E90.

Miyagi, Y., Yamashita, T., Fukaya, M., Sonoda, T., Okuno, T., Yamada, K., Watanabe, M., Nagashima, Y., Aoki, I., Okuda, K., et al. (2002). Delphilin: a Novel PDZ and Formin Homology Domain-Containing Protein that Synaptically Colocalizes and Interacts with Glutamate Receptor δ2 Subunit. J. Neurosci. *22*, 803–814.

Mochly-Rosen, D., Das, K., and Grimes, K.V. (2012). Protein kinase C, an elusive therapeutic target? Nat. Rev. Drug Discov. *11*, 937–957.

Moriya, K., Yamamoto, T., Takamitsu, E., Matsunaga, Y., Kimoto, M., Fukushige, D., Kimoto, C., Suzuki, T., and Utsumi, T. (2012). Protein N-Myristoylation Is Required for Cellular Morphological Changes Induced by Two Formin Family Proteins, FMNL2 and FMNL3. Biosci. Biotechnol. Biochem. *76*, 1201–1209.

Moseley, J.B., Sagot, I., Manning, A.L., Xu, Y., Eck, M.J., Pellman, D., and Goode, B.L. (2004). A Conserved Mechanism for Bni1- and mDia1-induced Actin Assembly and Dual Regulation of Bni1 by Bud6 and Profilin. Mol. Biol. Cell *15*, 896–907.

Moseley, J.B., Maiti, S., and Goode, B.L. (2006). Formin Proteins: Purification and Measurement of Effects on Actin Assembly. In Methods in Enzymology, C.J.D. William E. Balch, ed. (Academic Press), pp. 215–234.

Moser, M., Legate, K.R., Zent, R., and Fässler, R. (2009). The Tail of Integrins, Talin, and Kindlins. Science *324*, 895–899.

Mostafavi-Pour, Z., Askari, J.A., Parkinson, S.J., Parker, P.J., Ng, T.T.C., and Humphries, M.J. (2003). Integrin-specific signaling pathways controlling focal adhesion formation and cell migration. J. Cell Biol. *161*, 155–167.

Mu, D., Cambier, S., Fjellbirkeland, L., Baron, J.L., Munger, J.S., Kawakatsu, H., Sheppard, D., Broaddus, V.C., and Nishimura, S.L. (2002). The integrin αvβ8 mediates epithelial homeostasis through MT1-MMP–dependent activation of TGF-β1. J. Cell Biol. *157*, 493–507.

Muller, P.A.J., Caswell, P.T., Doyle, B., Iwanicki, M.P., Tan, E.H., Karim, S., Lukashchuk, N., Gillespie, D.A., Ludwig, R.L., Gosselin, P., et al. (2009). Mutant p53 Drives Invasion by Promoting Integrin Recycling. Cell *139*, 1327–1341.

Munger, J.S., Huang, X., Kawakatsu, H., Griffiths, M.J.., Dalton, S.L., Wu, J., Pittet, J.-F., Kaminski, N., Garat, C., Matthay, M.A., et al. (1999). A Mechanism for Regulating Pulmonary Inflammation and Fibrosis: The Integrin αvβ6 Binds and Activates Latent TGF β1. Cell *96*, 319–328.

Narumiya, S., Tanji, M., and Ishizaki, T. (2009). Rho signaling, ROCK and mDia1, in transformation, metastasis and invasion. Cancer Metastasis Rev. *28*, 65–76.

Ng, T., Shima, D., Squire, A., Bastiaens, P.I.H., Gschmeissner, S., Humphries, M.J., and Parker, P.J. (1999). PKC[alpha] regulates [beta]1 integrin-dependent cell motility through association and control of integrin traffic. Embo J *18*, 3909–3923.

Nishikawa, K., Toker, A., Johannes, F.-J., Songyang, Z., and Cantley, L.C. (1997). Determination of the Specific Substrate Sequence Motifs of Protein Kinase C Isozymes. J. Biol. Chem. *272*, 952–960.

Nishimura, T., and Kaibuchi, K. (2007). Numb Controls Integrin Endocytosis for Directional Cell Migration with aPKC and PAR-3. Dev. Cell *13*, 15–28.

Nürnberg, A., Kitzing, T., and Grosse, R. (2011). Nucleating actin for invasion. Nat. Rev. Cancer *11*, 177–187.

Olson, M.F., and Sahai, E. (2008). The actin cytoskeleton in cancer cell motility. Clin. Exp. Metastasis *26*, 273–287.

Otomo, T., Tomchick, D.R., Otomo, C., Panchal, S.C., Machius, M., and Rosen, M.K. (2005). Structural basis of actin filament nucleation and processive capping by a formin homology 2 domain. Nature *433*, 488–494.

Pan, Q., Bao, L.W., Kleer, C.G., Sabel, M.S., Griffith, K.A., Teknos, T.N., and Merajver, S.D. (2005). Protein Kinase Cε Is a Predictive Biomarker of Aggressive Breast Cancer and a Validated Target for RNA Interference Anticancer Therapy. Cancer Res. *65*, 8366–8371.

Pan, Q., Bao, L.W., Teknos, T.N., and Merajver, S.D. (2006). Targeted Disruption of Protein Kinase Cε Reduces Cell Invasion and Motility through Inactivation of RhoA and RhoC GTPases in Head and Neck Squamous Cell Carcinoma. Cancer Res. *66*, 9379–9384.

Pan, X., Rudolph, J.M., Abraham, L., Habermann, A., Haller, C., Krijnse-Locker, J., and Fackler, O.T. (2012). HIV-1 Nef compensates for disorganization of the immunological synapse by inducing trans-Golgi network–associated Lck signaling. Blood *119*, 786–797.

Pankov, R., Endo, Y., Even-Ram, S., Araki, M., Clark, K., Cukierman, E., Matsumoto, K., and Yamada, K.M. (2005). A Rac switch regulates random versus directionally persistent cell migration. J. Cell Biol. *170*, 793–802.

Parekh, D.B., Ziegler, W., and Parker, P.J. (2000). Multiple pathways control protein kinase C phosphorylation. Embo J. *19*, 496–503.

Parsons, D.W., Jones, S., Zhang, X., Lin, J.C.-H., Leary, R.J., Angenendt, P., Mankoo, P., Carter, H., Siu, I.-M., Gallia, G.L., et al. (2008). An Integrated Genomic Analysis of Human Glioblastoma Multiforme. Science *321*, 1807–1812.

Parsons, M., Keppler, M.D., Kline, A., Messent, A., Humphries, M.J., Gilchrist, R., Hart, I.R., Quittau-Prevostel, C., Hughes, W.E., Parker, P.J., et al. (2002). Site-Directed Perturbation of Protein Kinase C- Integrin Interaction Blocks Carcinoma Cell Chemotaxis. Mol. Cell. Biol. *22*, 5897–5911.

Paul, A., and Pollard, T. (2008). The Role of the FH1 Domain and Profilin in Formin-Mediated Actin-Filament Elongation and Nucleation. Curr. Biol. *18*, 9–19.

Pederson, T., and Aebi, U. (2002). Actin in the nucleus: what form and what for? J. Struct. Biol. *140*, 3–9.

Pellegrin, S., and Mellor, H. (2005). The Rho Family GTPase Rif Induces Filopodia through mDia2. Curr. Biol. *15*, 129–133.

Pellinen, T., Tuomi, S., Arjonen, A., Wolf, M., Edgren, H., Meyer, H., Grosse, R., Kitzing, T., Rantala, J.K., Kallioniemi, O., et al. (2008). Integrin Trafficking Regulated by Rab21 Is Necessary for Cytokinesis. Dev. Cell *15*, 371–385.

Peng, J., Wallar, B.J., Flanders, A., Swiatek, P.J., and Alberts, A.S. (2003). Disruption of the Diaphanous-Related Formin Drf1 Gene Encoding mDia1 Reveals a Role for Drf3 as an Effector for Cdc42. Curr. Biol. *13*, 534–545.

Perl, A.-K., Wilgenbus, P., Dahl, U., Semb, H., and Christofori, G. (1998). A causal role for E-cadherin in the transition from adenoma to carcinoma. Nature *392*, 190–193.

Pillé, J.-Y., Denoyelle, C., Varet, J., Bertrand, J.-R., Soria, J., Opolon, P., Lu, H., Pritchard, L.-L., Vannier, J.-P., Malvy, C., et al. (2005). Anti-RhoA and Anti-RhoC siRNAs Inhibit the Proliferation and Invasiveness of MDA-MB-231 Breast Cancer Cells in Vitro and in Vivo. Mol. Ther. *11*, 267–274.

Pollard, T.D. (2007). Regulation of Actin Filament Assembly by Arp2/3 Complex and Formins. Annu. Rev. Biophys. Biomol. Struct. *36*, 451–477.

Pollard, T.D., and Borisy, G.G. (2003). Cellular Motility Driven by Assembly and Disassembly of Actin Filaments. Cell *112*, 453–465.

Pollard, T.D., and Cooper, J.A. (2009). Actin, a Central Player in Cell Shape and Movement. Science *326*, 1208–1212.

Prévostel, C., Martin, A., Alvaro, V., Jaffiol, C., and Joubert, D. (1997). Protein kinase C alpha and tumorigenesis of the endocrine gland. Horm. Res. *47*, 140–144.

Pring, M., Evangelista, M., Boone, C., Yang, C., and Zigmond, S.H. (2003). Mechanism of Formin-Induced Nucleation of Actin Filaments. Biochemistry (Mosc.) *42*, 486–496.

Quinlan, M.E., Heuser, J.E., Kerkhoff, E., and Dyche Mullins, R. (2005). Drosophila Spire is an actin nucleation factor. Nature *433*, 382–388.

Quinlan, M.E., Hilgert, S., Bedrossian, A., Mullins, R.D., and Kerkhoff, E. (2007). Regulatory interactions between two actin nucleators, Spire and Cappuccino. J. Cell Biol. *179*, 117–128.

Rantala, J.K., Mäkelä, R., Aaltola, A.-R., Laasola, P., Mpindi, J.-P., Nees, M., Saviranta, P., and Kallioniemi, O. (2011). A cell spot microarray method for production of high density siRNA transfection microarrays. Bmc Genomics *12*, 162.

Ridley, A.J., Schwartz, M.A., Burridge, K., Firtel, R.A., Ginsberg, M.H., Borisy, G., Parsons, J.T., and Horwitz, A.R. (2003). Cell Migration: Integrating Signals from Front to Back. Science *302*, 1704–1709.

Romero, S., Le Clainche, C., Didry, D., Egile, C., Pantaloni, D., and Carlier, M.-F. (2004). Formin Is a Processive Motor that Requires Profilin to Accelerate Actin Assembly and Associated ATP Hydrolysis. Cell *119*, 419–429.

Rose, R., Weyand, M., Lammers, M., Ishizaki, T., Ahmadian, M.R., and Wittinghofer, A. (2005). Structural and mechanistic insights into the interaction between Rho and mammalian Dia. Nature *435*, 513–518.

Rotty, J.D., Wu, C., and Bear, J.E. (2013). New insights into the regulation and cellular functions of the ARP2/3 complex. Nat. Rev. Mol. Cell Biol. *14*, 7–12.

Sabeh, F., Shimizu-Hirota, R., and Weiss, S.J. (2009). Protease-dependent versus -independent cancer cell invasion programs: three-dimensional amoeboid movement revisited. J. Cell Biol. *185*, 11–19.

Sahai, E. (2005). Mechanisms of cancer cell invasion. Curr. Opin. Genet. Dev. *15*, 87–96.

Sahai, E. (2007). Illuminating the metastatic process. Nat. Rev. Cancer *7*, 737–749.

Sahai, E., and Marshall, C.J. (2003). Differing modes of tumour cell invasion have distinct requirements for Rho/ROCK signalling and extracellular proteolysis. Nat. Cell Biol. *5*, 711–719.

Sakai, N., Sasaki, K., Ikegaki, N., Shirai, Y., Ono, Y., and Saito, N. (1997). Direct Visualization of the Translocation of the Γ-Subspecies of Protein Kinase C in Living Cells Using Fusion Proteins with Green Fluorescent Protein. J. Cell Biol. *139*, 1465–1476.

Sanz-Moreno, V., Gadea, G., Ahn, J., Paterson, H., Marra, P., Pinner, S., Sahai, E., and Marshall, C.J. (2008). Rac Activation and Inactivation Control Plasticity of Tumor Cell Movement. Cell *135*, 510–523.

Sanz-Moreno, V., Gaggioli, C., Yeo, M., Albrengues, J., Wallberg, F., Viros, A., Hooper, S., Mitter, R., FÃ©ral, C.C., Cook, M., et al. (2011). ROCK and JAK1 Signaling Cooperate to Control Actomyosin Contractility in Tumor Cells and Stroma. Cancer Cell *20*, 229–245.

Sarmiento, C., Wang, W., Dovas, A., Yamaguchi, H., Sidani, M., El-Sibai, M., DesMarais, V., Holman, H.A., Kitchen, S., Backer, J.M., et al. (2008). WASP family members and formin proteins coordinate regulation of cell protrusions in carcinoma cells. J. Cell Biol. *180*, 1245–1260.

Schönichen, A., Alexander, M., Gasteier, J.E., Cuesta, F.E., Fackler, O.T., and Geyer, M. (2006). Biochemical Characterization of the Diaphanous Autoregulatory Interaction in the Formin Homology Protein FHOD1. J. Biol. Chem. *281*, 5084–5093.

Seth, A., Otomo, C., and Rosen, M.K. (2006). Autoinhibition regulates cellular localization and actin assembly activity of the diaphanous-related formins FRLα and mDia1. J. Cell Biol. *174*, 701–713.

Shi, Y., Zhang, J., Mullin, M., Dong, B., Alberts, A.S., and Siminovitch, K.A. (2009). The mDial Formin Is Required for Neutrophil Polarization, Migration, and Activation of the LARG/RhoA/ROCK Signaling Axis during Chemotaxis. J. Immunol. *182*, 3837–3845.

Somlyo, A.P., and Somlyo, A.V. (2000). Signal transduction by G-proteins, Rho-kinase and protein phosphatase to smooth muscle and non-muscle myosin II. J. Physiol. *522*, 177–185.

Sotiropoulos, A., Gineitis, D., Copeland, J., and Treisman, R. (1999). Signal-Regulated Activation of Serum Response Factor Is Mediated by Changes in Actin Dynamics. Cell *98*, 159–169.

Steinberg, S.F. (2008). Structural Basis of Protein Kinase C Isoform Function. Physiol. Rev. *88*, 1341–1378.

Stoletov, K., Kato, H., Zardouzian, E., Kelber, J., Yang, J., Shattil, S., and Klemke, R. (2010). Visualizing extravasation dynamics of metastatic tumor cells. J. Cell Sci. *123*, 2332–2341.

Takai, Y., Kishimoto, A., Inoue, M., and Nishizuka, Y. (1977). Studies on a cyclic nucleotide-independent protein kinase and its proenzyme in mammalian tissues. I. Purification and characterization of an active enzyme from bovine cerebellum. J. Biol. Chem. *252*, 7603–7609.

Takai, Y., Kishimoto, A., Kikkawa, U., Mori, T., and Nishizuka, Y. (1979). Unsaturated diacylglycerol as a possible messenger for the activation of calcium-activated, phospholipid-dependent protein kinase system. Biochem. Biophys. Res. Commun. *91*, 1218–1224.

Takeya, R., Taniguchi, K., Narumiya, S., and Sumimoto, H. (2008). The mammalian formin FHOD1 is activated through phosphorylation by ROCK and mediates thrombin-induced stress fibre formation in endothelial cells. Embo J *27*, 618–628.

Tan, C., Costello, P., Sanghera, J., Dominguez, D., Baulida, J., de Herreros, A.G., and Dedhar, S. (2001). Inhibition of integrin linked kinase (ILK) suppresses beta-catenin-Lef/Tcf-dependent transcription and expression of the E-cadherin repressor, snail, in APC-/- human colon carcinoma cells. Oncogene *20*, 133–140.

Tanji, M., Ishizaki, T., Ebrahimi, S., Tsuboguchi, Y., Sukezane, T., Akagi, T., Frame, M.C., Hashimoto, N., Miyamoto, S., and Narumiya, S. (2010). mDia1 Targets v-Src to the Cell Periphery and Facilitates Cell Transformation, Tumorigenesis, and Invasion. Mol. Cell. Biol. *30*, 4604–4615.

Thiery, J.P. (2002). Epithelial–mesenchymal transitions in tumour progression. Nat. Rev. Cancer *2*, 442–454.

Thompson, M.E., Heimsath, E.G., Gauvin, T.J., Higgs, H.N., and Kull, F.J. (2013). FMNL3 FH2–actin structure gives insight into formin-mediated actin nucleation and elongation. Nat. Struct. Mol. Biol. *20*, 111–118.

Tuomi, S., Mai, A., Nevo, J., Laine, J.O., Vilkki, V., Ohman, T.J., Gahmberg, C.G., Parker, P.J., and Ivaska, J. (2009). PKC{varepsilon} Regulation of an {alpha}5 Integrin-ZO-1 Complex Controls Lamellae Formation in Migrating Cancer Cells. Sci. Signal. *2*, ra32.

Upla, P., Marjomäki, V., Kankaanpää, P., Ivaska, J., Hyypiä, T., Van Der Goot, F.G., and Heino, J. (2004). Clustering Induces a Lateral Redistribution of A2β1 Integrin from Membrane Rafts to Caveolae and Subsequent Protein Kinase C-Dependent Internalization. Mol. Biol. Cell *15*, 625–636.

Urtreger, A.J., Grossoni, V.C., Falbo, K.B., Kazanietz, M.G., and Bal de Kier Joffé, E.D. (2005). Atypical protein kinase C-ζ modulates clonogenicity, motility, and secretion of proteolytic enzymes in murine mammary cells. Mol. Carcinog. *42*, 29–39.

Vaillant, D.C., Copeland, S.J., Davis, C., Thurston, S.F., Abdennur, N., and Copeland, J.W. (2008). Interaction of the N- and C-terminal Autoregulatory Domains of FRL2 Does Not Inhibit FRL2 Activity. J. Biol. Chem. *283*, 33750 –33762.

Valdembri, D., Caswell, P.T., Anderson, K.I., Schwarz, J.P., König, I., Astanina, E., Caccavari, F., Norman, J.C., Humphries, M.J., Bussolino, F., et al. (2009). Neuropilin-1/GIPC1 Signaling Regulates α5β1 Integrin Traffic and Function in Endothelial Cells. Plos Biol. *7*, e25.

Vavylonis, D., Kovar, D.R., O'Shaughnessy, B., and Pollard, T.D. (2006). Model of Formin-Associated Actin Filament Elongation. Mol. Cell *21*, 455–466.

Vavylonis, D., Wu, J.-Q., Hao, S., O'Shaughnessy, B., and Pollard, T.D. (2008). Assembly Mechanism of the Contractile Ring for Cytokinesis by Fission Yeast. Science *319*, 97–100.

Vial, E., Sahai, E., and Marshall, C.J. (2003). ERK-MAPK signaling coordinately regulates activity of Rac1 and RhoA for tumor cell motility. Cancer Cell *4*, 67–79.

Vizio, D.D., Kim, J., Hager, M.H., Morello, M., Yang, W., Lafargue, C.J., True, L.D., Rubin, M.A., Adam, R.M., Beroukhim, R., et al. (2009). Oncosome Formation in Prostate Cancer: Association with a Region of Frequent Chromosomal Deletion in Metastatic Disease. Cancer Res. *69*, 5601–5609.

Vleminckx, K., Vakaet Jr, L., Mareel, M., Fiers, W., and Van Roy, F. (1991). Genetic manipulation of E-cadherin expression by epithelial tumor cells reveals an invasion suppressor role. Cell *66*, 107–119.

Wallar, B.J., Stropich, B.N., Schoenherr, J.A., Holman, H.A., Kitchen, S.M., and Alberts, A.S. (2006). The Basic Region of the Diaphanous-autoregulatory Domain (DAD) Is Required for Autoregulatory Interactions with the Diaphanous-related Formin Inhibitory Domain. J. Biol. Chem. *281*, 4300–4307.

Wallar, B.J., DeWard, A.D., Resau, J.H., and Alberts, A.S. (2007). RhoB and the mammalian Diaphanous-related formin mDia2 in endosome trafficking. Exp. Cell Res. *313*, 560–571.

Wang, J., Neo, S.P., and Cai, M. (2009). Regulation of the Yeast Formin Bni1p by the Actin-Regulating Kinase Prk1p. Traffic *10*, 528–535.

Wang, Q.J., Bhattacharyya, D., Garfield, S., Nacro, K., Marquez, V.E., and Blumberg, P.M. (1999). Differential Localization of Protein Kinase C δ by Phorbol Esters and Related Compounds Using a Fusion Protein with Green Fluorescent Protein. J. Biol. Chem. *274*, 37233–37239.

Wang, W., Goswami, S., Lapidus, K., Wells, A.L., Wyckoff, J.B., Sahai, E., Singer, R.H., Segall, J.E., and Condeelis, J.S. (2004). Identification and Testing of a Gene Expression Signature of Invasive Carcinoma Cells within Primary Mammary Tumors. Cancer Res. *64*, 8585–8594.

Wang, W., Eddy, R., and Condeelis, J. (2007). The cofilin pathway in breast cancer invasion and metastasis. Nat. Rev. Cancer *7*, 429–440.

Watanabe, N., Kato, T., Fujita, A., Ishizaki, T., and Narumiya, S. (1999). Cooperation between mDia1 and ROCK in Rho-induced actin reorganization. Nat. Cell Biol. *1*, 136–143.

Watanabe, S., Ando, Y., Yasuda, S., Hosoya, H., Watanabe, N., Ishizaki, T., and Narumiya, S. (2008). mDia2 Induces the Actin Scaffold for the Contractile Ring and Stabilizes Its Position during Cytokinesis in NIH 3T3 Cells. Mol. Biol. Cell *19*, 2328–2338.

Ways, D.K., Kukoly, C.A., deVente, J., Hooker, J.L., Bryant, W.O., Posekany, K.J., Fletcher, D.J., Cook, P.P., and Parker, P.J. (1995). MCF-7 breast cancer cells transfected

with protein kinase C-alpha exhibit altered expression of other protein kinase C isoforms and display a more aggressive neoplastic phenotype. J. Clin. Invest. *95*, 1906–1915.

White, D.P., Caswell, P.T., and Norman, J.C. (2007). αvβ3 and α5β1 integrin recycling pathways dictate downstream Rho kinase signaling to regulate persistent cell migration. J. Cell Biol. *177*, 515–525.

Wickström, S.A., and Fässler, R. (2011). Regulation of membrane traffic by integrin signaling. Trends Cell Biol. *21*, 266–273.

Wipff, P.-J., Rifkin, D.B., Meister, J.-J., and Hinz, B. (2007). Myofibroblast contraction activates latent TGF-β1 from the extracellular matrix. J. Cell Biol. *179*, 1311–1323.

Wolf, K., Mazo, I., Leung, H., Engelke, K., Andrian, U.H. von, Deryugina, E.I., Strongin, A.Y., Bröcker, E.-B., and Friedl, P. (2003). Compensation mechanism in tumor cell migration mesenchymal–amoeboid transition after blocking of pericellular proteolysis. J. Cell Biol. *160*, 267–277.

Wolf, K., Wu, Y.I., Liu, Y., Geiger, J., Tam, E., Overall, C., Stack, M.S., and Friedl, P. (2007). Multi-step pericellular proteolysis controls the transition from individual to collective cancer cell invasion. Nat. Cell Biol. *9*, 893–904.

Woychik, R.P., Maas, R.L., Zeller, R., Vogt, T.F., and Leder, P. (1990). "Formins": proteins deduced from the alternative transcripts of the limb deformity gene. Nature *346*, 850–853.

Wyckoff, J.B., Pinner, S.E., Gschmeissner, S., Condeelis, J.S., and Sahai, E. (2006). ROCK- and Myosin-Dependent Matrix Deformation Enables Protease-Independent Tumor-Cell Invasion In Vivo. Curr. Biol. *16*, 1515–1523.

Xu, Y., Moseley, J.B., Sagot, I., Poy, F., Pellman, D., Goode, B.L., and Eck, M.J. (2004). Crystal Structures of a Formin Homology-2 Domain Reveal a Tethered Dimer Architecture. Cell *116*, 711–723.

Yamashita, M., Higashi, T., Suetsugu, S., Sato, Y., Ikeda, T., Shirakawa, R., Kita, T., Takenawa, T., Horiuchi, H., Fukai, S., et al. (2007). Crystal structure of human DAAM1 formin homology 2 domain. Genes Cells *12*, 1255–1265.

Yang, C., Czech, L., Gerboth, S., Kojima, S., Scita, G., and Svitkina, T. (2007). Novel Roles of Formin mDia2 in Lamellipodia and Filopodia Formation in Motile Cells. Plos Biol. *5*, e317.

Yang, J., Mani, S.A., Donaher, J.L., Ramaswamy, S., Itzykson, R.A., Come, C., Savagner, P., Gitelman, I., Richardson, A., and Weinberg, R.A. (2004). Twist, a Master Regulator of Morphogenesis, Plays an Essential Role in Tumor Metastasis. Cell *117*, 927–939.

Yoon, S.-O., Shin, S., and Mercurio, A.M. (2005). Hypoxia Stimulates Carcinoma Invasion by Stabilizing Microtubules and Promoting the Rab11 Trafficking of the α6β4 Integrin. Cancer Res. *65*, 2761–2769.

Young, K.G., and Copeland, J.W. (2010). Formins in cell signaling. Biochim. Biophys. Acta Bba-Mol. Cell Res. *1803*, 183–190.

Zech, T., Calaminus, S.D.J., Caswell, P., Spence, H.J., Carnell, M., Insall, R.H., Norman, J., and Machesky, L.M. (2011). The Arp2/3 activator WASH regulates α5β1-integrin-mediated invasive migration. J. Cell Sci. *124*, 3753 –3759.

Zhang, J., Anastasiadis, P.Z., Liu, Y., Thompson, E.A., and Fields, A.P. (2004). Protein Kinase C (PKC) βII Induces Cell Invasion through a Ras/Mek-, PKCι/Rac 1-dependent Signaling Pathway. J. Biol. Chem. *279*, 22118–22123.

Zhu, X., Zeng, Y., Guan, J., Li, Y., Deng, Y., Bian, X., Ding, Y., and Liang, L. (2011). FMNL2 is a positive regulator of cell motility and metastasis in colorectal carcinoma. J. Pathol. *224*, 377–388.

Zhu, X.-L., Liang, L., and Ding, Y.-Q. (2008). Overexpression of FMNL2 is closely related to metastasis of colorectal cancer. Int. J. Colorectal Dis. *23*, 1041–1047.

Zigmond, S.H., Evangelista, M., Boone, C., Yang, C., Dar, A.C., Sicheri, F., Forkey, J., and Pring, M. (2003). Formin Leaky Cap Allows Elongation in the Presence of Tight Capping Proteins. Curr. Biol. *13*, 1820–1823.

7 Abbreviations

2D	2-dimensional
3D	3-dimensional
ADP	Adenosine diphosphate
Arp2/3	actin-related proteins 2/3
ATP	Adenosine-5´-triphosphate
BIM I	Bisindolylmaleimide I
Cobl	Cordon-bleu
DAAM1	Disheveled-associated activator of morphogenesis 1
DAAM2	Disheveled-associated activator of morphogenesis 2
DAD	Diaphanous autoregulatory domain
DAG	diacylglycerol
Dia1	Diaphanous 1
Dia2	Diaphanous 2
Dia3	Diaphanous 3
DID	Diaphanous inhibitory domain
DRF	Diaphanous-related formin
ECM	Extracellular matrix
EMT	Epithelial to mesenchymal transition
F-actin	filamentous actin
FH1/2/3	Formin homology 1/2/3 domain
FHOD1	Formin homology domain-containing protein 1
FHOD3	Formin homology domain-containing protein 3
FMN1	Formin 1
FMN2	Formin 2
FMNL1	Formin-like 1
FMNL2	Formin-like 2
FMNL3	Formin-like 3
G-actin	globular actin

GBD	GTPase-binding domain
INF1	Inverted formin 1
INF2	Inverted formin 2
IP_3	inositol triphosphate
JMY	junction-mediating regulatory protein
kD	kilo Dalton
Lmod	Leiomodin
mDia1	mouse Diaphanous 1
MAL	Megakaryocytic acute leukemia
MLC	myosin light chain
MMP	Matrix metalloproteinase
NPF	Nucleation promoting factor
N-WASP	neuronal-WASP
PIP_2	phosphatidylinositol-4, 5-biphosphate
PIP_3	phosphatidylinositol-3, 4, 5-triphosphate
PKC	Protein kinase C
ROCK	Rho-associated coiled-coil protein kinase
SRF	Serum response factor
TPA	12-O-tetradecanoylphorbol-13-acetate
WASH	WASP and SCAR homologue
WASP	Wiskott-Aldrich syndrome protein
WAVE	WASP-family verprolin homologue
WH2 domain	WASP homology domain-2
WHAMM	WASP homologue associated with actin, membranes and microtubules

8 Acknowledgements

I am indebted to many people who have supported, motivated, encouraged, and inspired me and without whom I would not have finished this thesis.

I would like to thank Prof. Dr. Robert Grosse for guiding me from my master thesis through my PhD work, for teaching me not only about science research but also a way of thinking.

Thanks to the distinguished HBIGS PhD program of Heidelberg University, I have acquired not only knowledges from the courses and seminars, but also friendships and networks.

I am grateful to Prof. Dr. Herbert Steinbeisser who has always supported and helped me during the whole PhD period. I am also indebted to Prof. Dr. Oliver Fackler for being always active in giving me advices and practical helps in my experiments.

I would like to thank Prof. Dr. Johanna Ivaska, Jeroen Pouwels and Antti Arjonen from Turku Centre for Biotechnology for their excellent scientific collaboration and help with my project. I am grateful to Prof. Dr. Anne Ridley from King's College London for insightful discussions and suggestions in my project. Thank Tobias Zech from Beatson Institute for stimulating discussions and help. I would also thank Dr. Thomas Hofmann in helping with live imaging.

Thanks a lot to all the current and former members of the laboratory, especially Christian, Thomas, Dominique, Daria, and so on, for their friendship, help, support, motivation, time to share and to chat with me and all the other things. It was really a nice time working with you and getting to know all of you.

Finally, I wish to thank particularly my parents for their unconditional love and continuous support. I also thank all my friends, who mostly do not understand my work but have always believed in me and encouraged me. And thank you, Haisen, for always being there for me.